Characterization of Extracellular Zinc-mediated Inhibition of Human HRVs

Ashlee Bennett

Submitted in partial fulfillment of the requirements for the degree of Doctor of Philosophy in the

Graduate

School of Arts and Sciences

Columbia University

2016

Abstract

Characterization of Extracellular Zinc-mediated Inhibition of Human Rhinoviruses

Ashlee Bennett

As the predominant etiological agent of the "common cold," human rhinoviruses (HRVs) have a substantial economic impact and contribute to severe respiratory complications in immune compromised and asthmatic individuals. While zinc (Zn) ions have been previously shown to have an inhibitory effect upon HRVs, clinical trials using Zn products have produced conflicting results, and the lack of a known mechanism of Zn inhibition has stymied therapeutic development. Previous research on the potential anti-rhinoviral mechanism of Zn compounds focused upon intracellular processes. My research has demonstrated that extracellular exposure of both major and minor group HRVs to Zn chloride (ZnCl) and Zn gluconate (ZnG) is sufficient to profoundly decrease the infectivity of the viral population. The infectivity of other representatives of the picornavirus family is not decreased in the presence of Zn compounds, suggesting that Zn-mediated virus inhibition is HRV specific. Other metal cations similar to Zn have not demonstrated HRV inhibition. Zn-based inhibition of HRVs is independent of pH, is effected within minutes and is dampened at lower temperatures. Furthermore, whereas EDTA can chelate Zn to prevent inhibition of HRVs, it cannot reverse the Zn-based inhibition after it has occurred. In addition, infectious center plaque assay (ICPA) and competition assay data suggest that this mechanism is not related to the virus-cellular receptor interaction, and that Zn-treated viral capsids are still able to interact with receptor binding sites. Moreover, cultivation

and analysis of Zn-resistant HRV1A isolates suggests that genomic discrepancies in the VP1 capsid protein play a role in the mechanism of Zn inhibition. 3 distinct point mutations that conferred amino acid substitutions were found in multiple Zn-resistant isolates. Located in the exterior B-C loop and the interior viral-genome neighboring region of VP1, 2 out of the 3 mutations resulted in a dramatic amino-acid polarity change which likely has the chemical consequence of effectively repelling 2+ cations such as Zn. Furthermore, northern blot analysis reveals that Zn-treated HRVs exhibit an increased susceptibility to genomic RNA degradation, a phenomena that may be facilitated by a Zn-mediated cleavage of viral RNA within the viral capsid. Zn complexed to cheLating compounds Hinokital (HK), Pyrithione (PT) and Pyrrolidine Dithiocarbamate (PDTC) also demonstrated extracellular HRV inhibition, with the sequence and ratio of exposure, or precipitate formation, modulating the outcome. It is not clear if these compounds augment the antiviral mechanism of Zn alone, or initiate a distinct antiviral mechanism unrelated to that performed by Zn in isolation. Based upon the data presented here, Zn mediated inhibition of HRVs can occur in a cell-independent, extracellular manner to degrade viral RNA and thereby abrogate viral infectivity. This mechanism may provide novel insight into further therapeutic development of these compounds or template the design of future small molecule therapeutics against these and similar viruses.

Table of Contents

List of Diagrams

List of Figures

Acknowledgements

Dr. Racaniello
I would like to acknowledge Dr. Racaniello for his mentorship as my advisor who has provided unfailing support to me for the past 5 years. Both his guidance and the intellectual freedom he advocated inspired me to pursue a project that I was passionate about. With his dedication to teaching and passion for virology research, he cultivated an environment that fostered my intellectual curiosity and made my experience as a graduate student one I will look back fondly upon.

Dr. Rafal Tokarz, Dr. Brent Williams, Dr. Omar Jabado and Vishal Kapoor

The camaraderie fostered by Dr. Rafal Tokarz, Dr. Brent Williams, Dr. Omar Jabado and Vishal Kapoor made me excited to wake up everyday and participate in exciting projects at the Center for Infection and Immunity. From paper airplane competitions, soccer games and pub nights, to serious discussions about how to develop better diagnostic technology, these guys provided me unparalleled support and inspiration, even though I ultimately failed to heed their warnings to not go to graduate school.

Dr. Jeremy Lee

As a professor for undergraduates at Drexel University, Dr. Jeremy Lee encouraged me to pursue my passion for biomedical research. Even as a student, he treated me as colleague and our intellectual discussions fostered my confidence to pursue a career as a research scientist. Also, thanks for adopting my surfboard "Al" the Al Merrick when I found out I would be on at least 6 yeasrs of shore-duty.

Dr. Olga Amosova and Dr. Jacques Fresco

Through the Howard Hughes Undergraduate Research Fellowship, I had the privilege of spending the summer at Princeton University where I participated in biochemistry researh lead by Dr. Olga Amosova and Dr. Jacques Fresco. In a project involved in the creation and manipulation of triplex forming oligonucleotides conjugated to intercalating compounds, I got my first taste of real biochemisty lab science techniques and never looked back, and still display my 3-D chemical model of psoralen to remind me of one of the best summers of my life.

Dr. Broitman

As a student at West Chester University my first real scientific discussion and dissection of primary research manuscripts occurred under the tutelage of Dr. Broitman, who bolstered my confidence and encouraged me to pursue laboratory science.

Lindsie Goss, Holly Wolcott, Kate Stafford, Pat Gordon and Maria Sallee (ie "the gang")

I don't think I would have survived the stresses and challenges of the past 6 years without the unfailing support and friendship of Lindsie, Holly, Kate, Pat, and Maria. From group runs, to happy hours to experimental advice, they are all a part of the fondest moments of my graduate career.

Dr. Amy Rosenfeld

With decades of experience, Dr. Amy Rosenfeld is nothing short of a "Lab Ninja" whose advice, insight and expertise helped me get through the final challenging experiments of my project. I owe her eternal gratitude for refraining from tossing me out the window when I wouldn't stop ranting and whining about Northern Blots.

12, 546.8 cups of coffee

I'd like to thank caffeine, my lifes-blood, for sustaining me through early-morning classes, late afternoon plaque assays and 3am time-points. If ever there was a chemical equivalent of a well-meaning cross between an Army drill-sergeant and motivation speaker, you've been it.

CHAPTER 1: INTRODUCTION

Picornavirus overview & taxonomy

As obligate intracellular parasites, viruses require the faculties of a living host to replicate. While their range of dependencies on the living host vary, all viruses fundamentally lack the full complement of necessary enzymes for translation, the creation of an amino acid polypeptide from an mRNA transcript. Outside of a permissive host which possesses the metabolic utilities needed for viral replication, viruses essentially exist as inert chemical structures composed of genomic material surrounded by a proteinaceous shell, and in some species, a host-derived membrane. Their extreme dependency upon host organisms, minimal structure, and uniquely "pseudo-living" nature, has necessitated a divergent classification system, pared down from that seen with living organisms throughout biology. In addition to the Baltimore Scheme (Diagram 1.1) used to classify viruses based upon the nature of their genome and enzymatic requirements to generate mRNA, virus species are taxonomically delineated by Order, Family, Subfamily, Genus & Species (1).

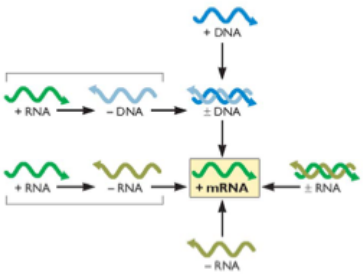

Diagram 1.1 The Baltimore Scheme
The steps necessary to obtain mRNA that can be interpreted by the host cell translation machinery can be schematically derived based upon the virus genome type.

The Picornavirus family, of the order *Picornavirales*, currently contains 18 different genera, all characterized as having a genome consisting of single-stranded RNA of positive polarity, allowing immediate recognition by host cell ribosomes, as well as sharing other structural and replicative similarities (2). Currently, preliminary guidelines for membership into the Picornaviridae family necessitates the identification of 3 key characteristics: (i) functionally homologous 2A, 2B and 3A polypeptides, and leader polypeptides; (ii) a structurally similar Internal Ribosome Entry Site (IRES) ; and (iii) the P1 and P2 genomic regions sharing greater than 40% identity, and the P3 region sharing at least 50% or greater identity (3). The importance and details of the aforementioned structures will be discussed in a following section.

Due to their rapid evolution, picornaviral species posses a great deal of genetic variability, leading them to be often described as "quasi-species"(4). These quasi-species are defined as a polythetic class of similar strains that share a limited range of hosts, significant similarities in their replication cycle, and genetic compatibility (5). Genetic compatibility is defined as being able to undergo homologous recombination and having virtually identical genome maps. These characteristics do not preclude the possibility that picornaviral species may vary significantly in gene sequence, host range, and antigenicity. However, species which fit the aforementioned criteria are typically found to possess amino acid sequence identity of 70% or greater (4). Despite their similar structure, picornaviruses can cause a range of pathologies that vary in viral tropism and clinical severity (6).

General Genomic Structure of Picornaviruses

Consisting of an individual, unimolecular single-stranded unit of RNA of positive polarity, picornaviral protein synthesis can be initiated immediately upon release into the host

cell cytoplasm, with the viral genome capable of acting in a manner analogous to mRNA (7). Directed by an Internal Ribosome Entry Site (IRES), picornaviral translation is cap-independent, a feature which facilitates viral exploitation of the host cell's protein machinery (8). While a variety of post-translational viral protease activities unique to each genus lend diversity to the end product, the picornaviral genome is recognized for its highly-conserved, economical structure (4). Variations characteristic of each genus and species are primarily found within a limited region of the genomic blueprint, lending a plethora of genetic and phenotypic variation to a wide population of viruses, while maintaining their distinct genealogical identity. Averaging just 7 - 8 kb in length, the compact picornaviral genome contains a single Open Reading Frame (ORF) which effectively occupies 85-90% of the available coding region of the RNA (9). An indispensable 40-80 bp 3' poly-A tail, whose length varies by viral species, is genetically encoded and extended during genome production (10). The 50-500 bp 5' terminal region of the genome is believed to be unique to each species, and sports a small virus-encoded protein, VPg, linked to the 5' most nucleotide which is always a "UU" sequence (11). This species-specific region takes on a cloverleaf, or unbranched terminal stem structure, which in combination with the VPg protein, is believed to facilitate the priming of minus-strand RNA synthesis for the production of progeny virus genomes (12). The polyprotein open reading frame of picornaviruses consists of genes encoding viral capsid proteins, followed by genes which encode non-structural viral proteins necessary for genome replication, including the VPg protein (13). After translation initiation facilitated by the IRES, multiple self-cleavage events produce the distinct polypeptides which form viral proteins from this single open reading frame (14).

While significant variation is described among phylogenetic subtypes, the picornaviral genome is principally composed of a sequential cascade of structural and enzymatic proteins,

flanked by 5' and 3' untranslated regions, and characterized by a series of self-cleavage events carried out by embedded proteinase domains that catalyze the production of functional viral proteins (15).

The 5'UTR of picornaviruses

Covalently attached to a 5' terminal uridine of viral RNA by a ubiquitously conserved tyrosine residue, the picornaviral VPg protein is immediately followed by a terminal secondary structural element that predominately consists of low free-energy, unbranched-stems or cloverleaf structures (16). Variable in length and sequence, these 5' terminal domain structures have been documented to bind multiple cellular and viral proteins to facilitate interaction between the 5' and 3' ends of viral RNA which is vital for the template-switching and negative strand synthesis steps of genome replication (2). In HRVs, this cloverleaf structure and downstream pyrimidine-rich tract are universally found to be vital for the conversion of viral RNA from a translation to replication template, despite the observation that the downstream pyrimidine tract varies dramatically, even among isolates of the same serotype (17). Immediately upstream of the polyprotein Open Reading Frame (ORF), one of 4 characteristic Internal Ribosome Entry Site (IRES) structures can be found which are responsible for the cap-independent translation of picornaviral proteins (18). Utilizing a highly-conserved type 1 IRES structure, HRV protein translation is initiated after IRES-mediated binding of the 40s ribosomal subunit, and facilitates scanning to the proper ORF AUG codon, a process which subverts canonical cellular translation initiation and facilitates the preferential production of viral proteins (9). Highly variable among all picornaviruses, an additional spacer sequence ranging from 18-40 bps is found 3' of the IRES in HRVs, and forms a stem structure whose AUG start codon

arrangement is believed to be responsible for the "bait and switch" strategy of competitive ribosomal initiation that has been postulated (5). Furthermore, extreme variability documented in this isolate-unique, 5' region suggests that it may play a role in evasion of host recognition, and avoidance of innate immunity processes (4).

The ORF of picornaviruses

The single ORF of picornaviruses begins with the genetic encryption of the viral capsid proteins. The 5' region of the ORF contains the genes for the 4 principal viral capsid proteins, VP4, VP2, VP3 and VP1, whose numeric designation is representative of their discovery, rather than their position within the genome, or size and structural importance (19). The smallest and characteristically interior capsid protein, VP4, is the first to be translated and is not found in all picornaviruses (4). VP4 is followed by VP2, VP3 and VP1, whose trimeric interaction forms the symmetrical repeating pattern and exterior surface area of the viral capsid (4). However in a process unique to different viral species, proteolytic cleavage of longer polypeptide precursors yields these individual protein products at different stages of viral translation. The first co-translational proteolytic cleavage event in the picornaviral replication cycle separates the viral capsid protein polypeptide, "P1" from the growing amino acid chain (4). Following synthesis of the downstream viral 3C protease which catalyzes further cleavages, P1 yields VP1 and VP3, and also generates a precursor, VP0, which contains proteins VP4 and VP2 (20). Cleavage of VP0 to yield VP4 & VP2 is the final stage in polyprotein cleavage and is observed only in those picornaviruses which contain a VP4 coding region (4) .

Universal picornavirus structure and proteins

Averaging at just 30 nm in diameter, all picornaviruses share an approximately spherical appearance that is the result of icosahedral symmetry achieved by repeating units of just 4 distinct viral capsid proteins (21). This metastable structure is described as having a pseudo-triangulation number of 3, due to the chemical inequivalence of capsid proteins creating quasi-equivalent interactions which distort what is theoretically a mathematically T-1 icosahedron (22). Consequently, each of the 60 triangle-like structures which compose the capsid can be divided into 3 smaller triangles, each with a smaller triangle being representative of a single polypeptide chain that is derived from one of the three major structural proteins (23). The largest of these structural proteins, VP1, is located around the five-fold axis of symmetry while VP2 and VP3 alternately flank the two and three fold axes. VP4 remains within the interior of the capsid and may play a stabilizing role in capsid structure, or viral genomic RNA encapsidation (24). While picornaviruses share general topographic similarities, unique structures on the capsid surface such as protruding loops, canyons, pores and hydrophobic pockets lend huge variation in receptor affinity across the picornavirus family. These structural entities dictate the method of interaction with the cellular receptor the virion will used to gain entry, as well as playing a role in antigenic determination. Furthermore, these structural differences are believed to be responsible for the great degree of variation in physicochemical properties like buoyant density and pH lability observed from species to species (25).

The metastability necessary to allow extracellular stability and transmission from host to host, as well as disassembly to allow for replication, necessitates a set of carefully orchestrated structural changes as the virion attaches and enters the cell. While nuances exist from species to species, two primary approaches of receptor interaction are prevalent among picornaviruses. One

mechanism leads to the formation of a reshaped capsid by a quasi-mechanical interaction with the receptor that is believed to commit the virion to subsequent un-coating. Another approach involves a more straight forward surface-oriented attachment to the receptor which does not alter overall capsid structure (26). While research on the precise cellular entry mechanisms for different picornaviruses is on-going, it is generally accepted that receptor-mediated-endocytosis, wherein the virion is exposed to a low pH environment, is essential to ultimately deliver infectious RNA into the host-cell cytoplasm (27) .

The variety and minutiae of proteins and catalytic activity necessary to execute a picornavirus infectious cycle is highly variegated from species to species. However, there exists a central line-up whose presence and activity are conserved across the picornavirus family. In addition to the 4 canonical viral capsid proteins, proteins 2B, 2C, 3A, 3B, 3C and 3CD are universally found to play an integral role in the infectious cycle of all picornaviruses (4).

Protein 2B and its precursor 2BC are involved in the construction of membranous vesicles on which viral RNA replication is localized. Furthermore, an NH2 terminal amphiphatic helix seen in the 2B proteins of some species is thought to impede golgi trafficking and lower Ca2+ levels, thereby hindering apoptosis of the infected cell (28).

The picornaviral 2C protein is also implicated in the construction of membranous vesicles for RNA replication, however, its exact mechanistic role is unclear. While some studies have observed ATPase and RNA-binding abilities, a lack of structural data has left even its potential oligomerization in doubt (29).

Varying widely in length from species to species, the picornaviral protein 3A, and its precursor 3AB, have been shown to play a role in virulence and host range, in addition to a probable role as a co-factor during RNA replication in some species (30). Interception of protein

traffic between the cellular endoplasmic reticulum and golgi apparatus has also been reported for some enterovirus species (4).

Noted for it's small size and hydrophobic patches, protein 3B -VPg is found covalently attached to the 5' end of picornaviral RNA. While the structure has been determined for the VPg of poliovirus, the precise purpose for multiple copies of this protein found in some picornaviruses is unknown (4). Connected to the 5' terminus of the viral genome via a phosphodiester bond with the hydroxyl of a tyrosine residue, these proteins play a priming role during the virus replication cycle and can be found within the viral capsid after having been encapsidated along with the viral genome during assembly (31).

Coined the "workhorses of the proteolytic cascade" protein 3C is responsible for the vast majority of secondary proteolytic cleavage steps in the picronaviral polyprotein processing necessary to create discrete viral proteins. After initial monomolecular cleavage which separates the P2/P3 junction, this cis-reactive enzyme catalyzes numerous polyprotein cleavage events as well as being postulated to play a role in inhibition of a variety of host cell processes, such as transcription, cap-dependent translation and cytoskeleton remodeling (32).

In many picornaviruses the 3CD precursor protein is also believed to be an active proteinase, acting on both the P1 and P3 cleavage sites (68). In addition, important regulatory functions have been observed such as binding to the 5' cloverleaf structure of viral RNA and CRE RNA binding that is believed to help template the minus strand synthesis necessary for genome production. The solved structure of this protein from poliovirus bolsters its proposed RNA -binding ability (33).

Acting as the RNA-dependent - RNA polymerase, protein 3D and its derivatives are indispensable for picornaviral genome replication (33). This 460-470 amino acid protein plays a

paramount role in the replication complexes that facilitate the production of both plus strand and minus strand genomic RNA (34).

Additional proteins, such as the Leader (L) protein and the 2A protease, are unique to specific genera in the picornavirus family (35). The precise and perhaps varied functions of these proteins differ from species to species, with preliminary research indicating a thematic role in restriction of host cell factors that would be a disadvantage to viral occupation of the translation machinery. In particular, the Enterovirus 2A protease interaction with the cellular translation factor eIF-4G, is believed to give advantage to the IRES-dependent translation of viral proteins during infection (35).

Picornavirus cell entry

Without a host derived lipid envelope, picornaviruses cannot gain entry by fusion with the cellular plasma membrane. Consequently, qualities intrinsic to their capsid structure must provide a mechanism for translocation of nucleoprotein complexes into the cell. Unfortunately, several factors have stymied research progress into the precise mechanism of entry for most picornaviral species, such as the typically high particle to PFU ratio, general complexity and dearth of knowledge of endocytic pathways, and the potential for utilization of multiple routes of entry. One of the only firmly established facts regarding cell entry is that it seems to vary from genus to genus and even species to species, with even structural characteristics of the capsid often unable to accurately predict the route of entry. The majority of picornaviruses are believed to use some form of the clathrin-mediated endocytic pathway, but it is known that many picornaviruses utilize other less-characterized endocytic pathways (36).

Picornavirus translation

With an RNA genome that can serve as the equivalent of mRNA due to its positive polarity, production of viral proteins can occur immediately upon genome release into the cytosol. Furthermore, with an IRES, this translation is not dependent upon availability and assemblage of a multitude of initiation factors to get started. This ease of translation initiation, in combination with proteins that directly inhibit 5' cap assembly, rapidly leads to viral translation dominating host cell resources (37). Exact IRES topography varies from species to species, but picornaviruses can be divided into four principle groups based upon general IRES structure and the cellular factors required to initiate translation. Characteristic of Enteroviruses and Cardioviruses, respectively, type I and type II IRESes require just 4 cellular initiation factors in addition to the 40s ribosomal subunit and ATP to initiate translation (38). Type IV IRESes, seen in hepatitis C virus and porcine teschovirus, are distinguished for their independence from eIF4G to function (4). Type III IRESes have not been extensively characterized and their initiation requirements are unknown. In addition, IRESes often require a number of specific RNA binding proteins known as IRES Trans-Activating Factors (ITAFs) which may provide a stabilizing or ribosomal requirement role to optimize translation (39). Comprehensive characterization of these factors for each viral species is on going. In addition to the IRES and its associating factors, research supports the possibility that interaction between the 5' and 3' ends of the viral RNA genome may play a role in initiating gene expression, modulating gene expression, or both (4). Ribosomal identification of the inaugural AUG codon has been postulated to possibly require both ribosomal scanning and melting of RNA structures for different picornaviral species (40). However, the notable conservation of a polypyrimidine tract downstream of the IRES, but

located a precise distance upstream of the initiating AUG codon, implicates this motif as playing an important role in AUG selection (41).

After successful initiation, translation of the viral RNA genome's single ORF occurs in conjunction with a series of characteristic cleavage events. While the mechanism varies among picornaviruses, the first primary cleavage event occurs co-translationally, separating the viral capsid polypeptides (P1) from downstream replication polypeptides (P2). A second primary cleavage event, more universal in mechanism among picornaviruses, is the intramolecular, cis-cleavage between the 2C and 3A regions mediated by an iteration of the 3C proteinase whose degree of maturation necessary to carry-out the catalytic event varies by species (42). Following these two primary cleavage events, a series of secondary cleavage events mediated by the 3C or 3CD protease produce precursors of the capsid and replication proteins (33). Additional secondary cleavage events are necessary in some picornaviruses, including the processing of the C terminus of an L protein, and alteration of the C-terminal 2A region (43). A final maturation cleavage during the final stages of virion production separates the VP4 and VP2 polypeptides concomitantly as RNA is inserted into the developing capsid structure (44).

Picornavirus RNA genome replication

Most, if not all, non-structural proteins found in the P2 and P3 regions of the picornaviral genome play some role in RNA replication. The members of the P3 region play a more direct role in RNA synthesis, while many of the proteins of the P2 region have been shown to play a more peripheral, but nonetheless important role in the production of viral RNA by catalyzing structural rearrangements on the membranes where RNA replication is localized (28). Coding the viral capsid proteins, the P1 region of the picornavirus genome does not play a role in RNA

replication aside from the potential role of CRE elements within the P1 region which may interact with the VPg protein and assist in its priming functionality (45).

With a genome that can also serve as a template for translation, a picornaviral infectious cycle necessitates a mechanism to alternate the role of viral RNA between these two utilities so that viral proteins and progeny genomes can be produced in appropriate quantities (Diagram 1.2). This process requires the rearrangement of host membranes to form supramolecular structures to act as a scaffold for RNA replication and capsid assembly, in addition to certain cellular and viral protein entities (1). In the immediate aftermath of infection, production of a sufficient quantity of viral capsid proteins, and proteins required for RNA synthesis, necessitates the predomination of viral RNA serving as a translation template. However, a mechanism must be in place to catalyze the shift from translation to RNA replication for a sufficient number of viral genomes to be produced for progeny virions, and it has been demonstrated that viral RNA cannot serve as a translation and genomic template simultaneously (37). It is believed that a negative-feedback loop predicated upon the accumulation of one or more viral proteins produced during translation must be responsible for this transition. However, the proteins or protein precursors which assume this responsibility is still debated. The most characterized mechanism involves cleavage of the cellular protein PCBP2, by viral protein 3C, or its precursor 3CD, which effectively inhibits or disfavors its involvement in translation, but does not preclude its ability to play a role in RNA replication. Additional research has also implicated a role for the host polypyrimidine tract-binding protein (PTB), which cannot continue to stimulate IRES-mediated translation if cleaved or removed by the activity of a viral protein (7).

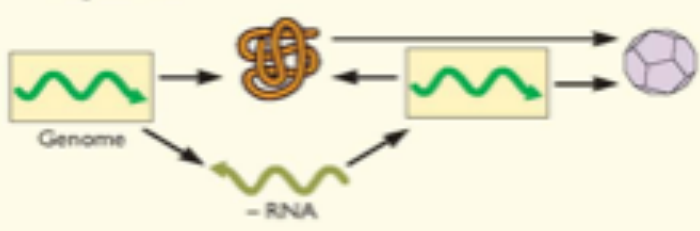

Diagram 1.2 Picornavirus replication strategy
With a positive-sense, single-stranded RNA genome, picornavirus genomes can act as mRNA when they first enter the cell cytoplasm and be translated by host cell machinery to make viral proteins, some of which are necessary to execute RNA genome production. A negative-sense full-length, single-stranded RNA is made to template the synthesis of more positive stranded RNA genomes for progeny virions.

Picornaviral RNA replication occurs on a vesicular, two-dimensional cytosolic-facing membrane surfaces (28). Only the membrane binding abilities of 2B, 2C and 3A that form the foundation of these replication "factories" have been extensively characterized. However, all of the proteins known to be involved in RNA synthesis can be found localized to the surface of these vesicles averaging 300 to 400 nm in diameter. Localization of viral RNA replication to these vesicles is thought to facilitate viral protein concentration dependent assembly of capsids, as well as well as sequestering of the viral RNA replication machinery from cellular mRNAs that it might otherwise copy (4). While numerous tethering and rearranging functionalities have purportedly been observed in various viral proteins in some picornaviral species, the presence of viral protein precursor 3AB alone has been shown to be sufficient to recruit the viral 3D polymerase to the replication sites on these vesicular membranes (46). For all picornaviruses, it is universally accepted that the viral VPg protein plays a central role as a primer for both negative and positive RNA strand synthesis. However, in many picornaviral species, the cis-acting replication elements (CREs) located within the P1 region of the viral genome have also been reported to provide a priming functionality by acting as template for the advantageous uridylylation of VPg (30). Both the 5' non coding region and the 3' noncoding region of the viral genome have also been shown to play a role in the promotion of RNA synthesis, most likely

through the formation of secondary stem-loop and cloverleaf structures that might stabilize the picornaviral replisome. Furthermore, multiple studies support the notion that viral-genome specific elements in the 5' non-coding region allows the viral 3D polymerase to identify and copy only viral RNAs, despite the preponderance of cellular mRNAs (47). Underscoring this point is the experimental observation that the homopolymeric tract in the 3' non-coding region is required for RNA synthesis, despite the fact that its length varies from species to species (4). In some picornaviruses, ubiquitination of the viral 3D polymerase is also believed to play an important role in promotion of RNA synthesis (4). While full length, negative-sense viral RNA is necessary to template the formation of additional positive-sense genomes, the two breeds of RNA are found in vastly different quantities during viral infection, with positive-sense RNA predominating in ratios ranging from 30:1 to 70:1 (48).

Picornaviral interference with host cell processes

A successful viral infection relies upon the consumption of cellular resources in the form of enzymes, energy and other proteins and intermediates such as tRNA. Consequently, nearly all-viral species have evolved mechanisms to aid in commandeering host resources for viral benefit. Picornaviruses have evolved several strategies to inhibit the expression of host genes and protein production to tip the metabolic balance in their favor during infection. Acting on four general levels: transcription, translation initiation, nuclei-cytoplasmic trafficking and disruption of structures that aid in mRNA processing, these inhibitory mechanisms produce profound alterations in the host cell which can be observed as Cytotoxic Effect (CPE) during in vitro infections (4). The precise mechanisms used to achieve manipulation of cellular resources varies by species, but virtually all picornaviruses studied have been documented to employ at least one

or more of these tactics, with evolution having selected for many picornaviral proteins which appear to have dual functions that involve promoting viral replication, while impeding host cell functions that would be detrimental to progeny virion production (49).

The 3C polymerase and 3CD precursors of enteroviruses such as PV, have been shown to act on transcription factors that affect Pol I, Pol II, and Pol III function (4). Numerous picornaviruses have been shown to possess viral proteins such as 2A and L with the ability to directly inhibit the cap-dependent translation initiation on which host cells rely via cleavage of cap recognition proteins such as eIF4G and eIF4E (50). Cleavage of PABP by the picornaviral 3C protease plays a role in inhibition of cellular translation and in the transition from viral RNA replication to translation (4). Additional inhibition of cellular translation is achieved through direct interaction with ribosomes and control of eIF2alpha phosphorylation through modulation of the critical protein kinase R (PKR) (51). Disruption of essential nucleo-cytoplamic transport has been documented in Enteroviruses and Cardioviruses where the 2A and L proteinase have been observed to catalyze the destruction of key nuclear pore complex proteins like Nup 98 and Nup 62 (52). Picornaviral induction of cellular mRNA silence and decay is seen in the modulation of stress granules (SGs) and disruption of mRNA processing bodies (PBs) (53).

Picornavirus assembly

Picornaviral particle morphogenesis and cellular egress are the least characterized stages of the infectious cycle, and most investigations into these processes have focused upon PV. In these studies, initial myristolization of the viral polypeptide P1 segment, and association with cellular heat-shock protein Hsp90, is shown to be important for initial steps in P1 organization, but 5s pentamer formation after P1 cleavage into VP0, VP1 and VP3 does not appear to require

chaperones (4). This 5s pentamer is considered to be the fundamental building block of the picornaviral capsid. The subsequent 14s pentamer is composed of 5, 5s pentamers, the formation of which is thought to be aided by the presence of the myristic acid association on the N terminus of P1 (4). Incorporation of the viral RNA genome has been hypothesized to occur via condensation of the 14s pentamers around the viral RNA, or by RNA insertion into an already virtually complete capsid structure. Currently, there is no strong evidence for the existence of "packing signals" within the viral RNA to guide selective viral genome incorporation for most picornaviruses (4). However, interaction between the non-structural 2C-ATPase and capsid proteins in Enteroviruses has garnered experimental support as a mechanism that provides morphogenesis specificity in this species. Complete capsid formation with failure to insert an RNA genome is also believed to occur frequently for some picornaviruses, possibly accounting for the large particle-to-PFU ratio seen in many species (4).

Human Rhinoviruses (HRVs)

While having previously been defined as its own genus, advances in genome analysis combined with new taxonomic requirements delimiting genus characteristics, HRVs have been reassigned to the Enterovirus genus of the Picornaviradae family (4). While transmission of most Enterovirus genus members is characterized by feco-oral or respiratory routes, HRVs are distinguished by their tropic restriction to the respiratory mucosa, a characteristic which is likely a result of the receptor distribution within the tissues of the host, and documented acid lability which does not make them amenable to gastric environments (54). Transmission and tropism aside, HRVs share the same predominant picornaviral and enteroviral molecular features previously described. Their designation as HRVs is due to the etymology of the root "rhino" and

their association with disease affecting the nasal passageways; it is not to be confused with viral infections afflicting the mammalian rhinoceros species or the potential zoonotic transmission of a rhinoceros-endemic virus to humans.

HRV classification and taxonomy

With well over a hundred different serotypes, the genetic diversity found within the HRV family is staggering. While HRVs have been historically delineated by receptor affiliation, advances in sequencing technology have allowed HRVs to be further classified based upon genomic phylogeny. Phylogenic analysis has been especially helpful in understanding the newly characterized HRV-C, whose association with more severe cases of respiratory distress underlies the clinical importance of understanding HRV evolution (55) . Interestingly, receptor preference is not exclusive to each genetic clade, with the ICAM-1 receptor being the most proliferatively represented. The minor group HRVs which utilize the LDLR receptor are not as well represented as their major group counterparts, however, the still have a strong clinical presence (4). Distinctions among the 3 different phylogenetic clades are featured prominently in the 5' UTR whose secondary structures play a role in modulation of both translation and transcription. In particular, the spacer region immediately 3' to the cloverleaf structure in the 5' UTR is found to vary in length significantly between the different clades, and also considerably within them. In addition, key features of the IRES, whose presence is responsible for recruitment of the 40s subunit and initiation of translation, is found to vary considerably among the three clades. The amount of HRV type A representatives has led to the further categorization into small groups or "clades" which share genetic similarity. One such clade, know as "clade D", has demonstrated a significant amount of clustering and divergence that its possible designation as a new species,

"HRV-D", is being debated (56). Amino acid comparison matrices have also identified clusters within the HRV-C and HRV-B species who most likely share a common ancestor. Phylogenetic analysis has revealed that HRV-A shares a common ancestor with HRV-C, which is considered a sister group to the HRV-B clade (4). The clinical severity of HRV-C makes the intersection of HRVA and HRVB, and the resulting phenotype, an important and on-going area of study (Diagram 1.3). While the immunological pressure for evolution and variation on exposed antigenic regions is expected and observed among these species and clusters, it is also important to note that much sequence variability can be seen in non-antigenic regions as well (57). The source of this genotype variation among HRVs can be largely attributed to the HRV polymerase whose lack of a proofreading mechanism has been cited to result in base-pair mis-incorporations with an approximate frequency of once every 10^3 or 10^4 basepairs. This variability has led many to use the term "quasi-species" to address the genetic variability inherent in any HRV population (58). In addition to constitutive genetic diversity created by the RdRp, additional diversity is produced via recombination between different species, mostly likely during instances of co-infection. One such HRV that is believed to have evolved via a recombination event is hrv-46, whose genome has been shown to be largely comprised of hrv-53 and hrv-80 genetic material (4) .

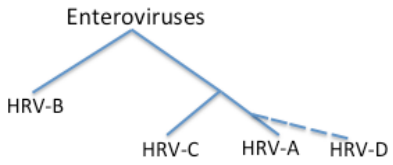

Diagram 1.3 The phylogeny of HRVs
The three key species of HRV are shown, and their relationship to their parent class, the Enteroviruses. The dashed line indicates that HRV-D is not officially distinguished as a species despite the strong genetic identity of this cluster.

Despite their genetic similarity, HRVs can be further classified into three serotypes based upon the cellular receptor used to gain entry into susceptible cells. Endocytic uptake of the virus particle is dependent upon successful interaction with the appropriate receptor and ultimately results in release into the host cell cytosol by an incompletely described process so that an infectious cycle can begin (59).

Receptor classification

Comprising approximately 90% of HRV serotypes, major group HRVs interact with the Intracellular Adhesion Molecule 1 (ICAM1) through a depression or "canyon" around the five fold axis of the icosahedron (4). In contrast, minor group HRVs interact with members of the Low Density Lipoprotein Receptor (LDL-R), which includes the LDL-R and the LDL-R - related protein (60). In addition, while major group HRVs are found to bind within the canyon at the 5-fold axis of symmetry, minor group HRVs are found to interact with their receptor around the 5-fold axis of symmetry and may not bind within the canyon itself (4). First described in 2006, Rhinovirus C (HRV-C) has been documented to gain cellular entry using the Cadherin Related Family Member 3 (CDHR3) receptor (4). While research on this new HRV is ongoing, the clinically severe infections in the lower respiratory tract attributed to this serotype may or may not be due to receptor tropism and potential preference for the lower respiratory tract (61). Despite variation in receptor usage, airway epithelial cells are currently found to be the primary targets of HRV infection in clinical investigations, with possible infection of airway macrophages that might play a role in inflammation, possible asthma aggravation, and allergen sensitization (Diagram 1.4) (62).

Diagram 1.4 Receptors used by viruses.
A range of receptors used by viruses demonstrates the degree of conformational variability

In addition to receptor-based classification, there has also been an attempt to classify HRVs based upon drug susceptibility (4). The delineation into group HRV-A or HRV-B is based upon sensitivity to a panel of compounds, with minor group HRVs found to exclusively be members of HRV-B, the group which has been shown to result in more than twice as many severe clinical infections per serotype (63). Studies into the possible structural reasons for these phenomena are ongoing.

HRV structure

Elegant in it's simplicity, the rhino viral capsid consists of just 4 distinct proteins whose non-covalent and repetitive interaction facilitates the graceful assemblage of a classic icosahedron with a triangulation number of 3 (64). Common to all picornaviruses, 60 copies of 4 proteins: VP1, VP2, VP3 & VP4, form the repeating promoter whose 5-fold axis contains a canyon for receptor binding (65). While the comparably small VP4 remains concealed within the

capsid structure, VP1, VP2 & VP3 can be seen as three smaller triangle-like structures on the surface of each face (26). A final cleavage event where the precursor VP0 undergoes cleavage to produce VP4 and VP2 is the final step to producing a mature infectious virion (4). The complete icosahedron is composed of 12 pentamers, which are the aggregate of 5 protomers. A single protomer consists of 1 copy of each HRV capsid protein (Diagram 1.5). Contributing most of the visible surface area, VP1 is located around the five fold axis and contains a wedge-shaped eight-stranded Beta barrel, known as a "jelly roll", that is largely responsible for the bulk of the viral capsid (66). Additionally, surface loops on this protein contain the principal antigenic sites, which can vary considerably. In some HRVS the exact structure of the "canyon" found on the VP1 surface is cited to control capsid flexibility and un-coating and assembly constraints (4). Interaction of drugs like Win compounds with the canyon can have a locking effect on the capsid structure, preventing un-coating (67). Many HRVs also contain a "pocket-factor" a natural fatty acid ligand which imbeds in the hydrophobic canyon on the viral capsid surface, a small lipid whose association with the viral capsid might play a stabilizing role, however the exact function is unknown (68). Described as having "open" and "closed" conformations, this hydrophobic canyon formed by the beta barrels of VP1 has been most noted for it's interaction with the antiviral compound pleconaril, whose displacement of the pocket factor and canyon occupation is associated with inhibition of capsid functions (69) . Changes in the structure of this canyons is believed to be responsible for the Win-drug resistance observed in the recently discovered, and markedly more virulent, HRV-C (70).

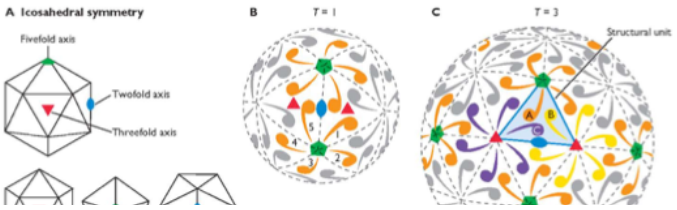

Diagram 1.5 Triangulation of the icosahedral capsid.
The five-fold, three-fold and two-fold axis of the icosahedron are illustrated. The increase in triangulation number on the geography of the structural unit illustrated between the T-1 and T-3 capsid.

Several loops protruding off of the HRV capsid surface are associated with antigenicity and drug susceptibility. Known for its flexibility, the B-C loop is believed to modulate virus-receptor interactions, especially that of the major group HRV interaction with ICAM-1, and is located around the 5 fold axis of the icosahedron near an ostensible pore structure (4) . Mutations within this loop region are thought to modulate host immune system detection and have been shown to be involved in the generation of F-12 antibody Fab fragment escape mutants (4). Studies where the B-C loops from different strains of PV and coxsackie viruses were swapped lead to differential susceptibility of these viruses to neutralizing antibodies, without a dramatic effect on the rest of the viral replication cycle. Key differences in the B-C and H1-loops has also been cited to play a role in the receptor preference difference between major and minor group HRVs (16) . In studies on HRV14 susceptibility to Win compounds, movement of the B-C loop, as well as other loops structures on the capsid surface, was shown to occur with Win compound binding, despite the distance from the Win compound canyon site (26). Furthermore, mutations in the B-C loop have been shown to alter the susceptibility of HRV14 to damage due to proteases such as trypsin (71). These observations underscore the importance of the B-C loop in critical capsid dynamics.

Genomic structure

Characteristic of all picornaviruses, HRVs posses a single-stranded RNA genome of positive polarity containing the general features present among all Enteroviruses. Translation of the uncapped rhinoviral genome occurs upon release into the host-cell cytosol and interaction of host ribosomes with the IRES within the long 5' untranslated region(4). This IRES is followed by a long open reading frame (ORF) which codes for a self-cleaving polyprotein (Diagram 1.6). Cleavage activity of the 2A and 3C proteases result in the production of the P1 polypeptide which contains the rhinoviral capsid & enzymatic proteins (4). Like other picornaviruses, HRVs are found to have an accompanying VPg protein, whose presence is necessary to template and prime the production of viral genome replication. Structurally, the VPg protein of HRVs is found to be structurally analogous to that of picornaviruses generally (72).

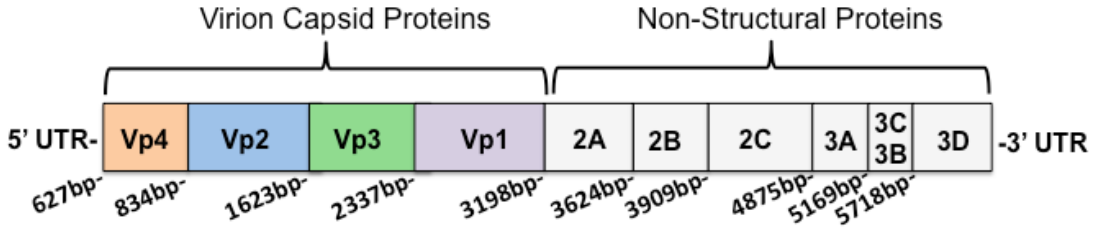

Diagram 1.6 HRV genome structure
The general structure of the HRV ORF is shown. Delineations are representative of the distinct proteins post cleavage cascade

Rhinovirus receptor binding and cell - entry

Composed of just nucleic acid and protein with no metabolic source of energy, HRVs do not posses the energetic potential to forcibly enter a host cell, and must rely on cell-mediated

endocytotic processes to gain entry into their host. Virus interaction with the cellular receptor that will trigger its membrane fusion or endocytosis is essential to gain cell entry. These receptors used by the virus have other functions relevant to the cell that viruses exploit through natural selection. A cell that sports a receptor that has been co-opted by a virus for cell entry is described as being "susceptible" to viral infection. The ability of the host cell to provide resources that enable the successful completion of the viral infectious cycle is known as "permissivity". Only a permissive and susceptible cell can support natural viral uptake and replication (59). For HRVs, susceptible and permissive cells are found in the nasopharyngeal tract which the virus gains access to via a respiratory-based transmission process (4). The rhinoviral capsid has been documented to "breathe", a structural distinction that separates it from poliovirus. This "breathing" is the mechanistic transition into a 135S particle that involves the transient externalization of internal sequences, including the myristolated VP4 and the N terminus of VP1. The stable formation of this 135S particle is thought to occur upon major group rhinovirus ICAM-1 receptor contact, while minor group rhinovirus transition into a 135S particle does not occur until exposure to the lowered pH of the endosome after internalization (73). The reasons for this distinction is likely due to the structural differences in the viral capsid that are also responsible for the choice in receptor for each group. The details of the receptor-mediated endocytic process and genome release of HRVs is not known, but it has been determined that both major and minor group HRVs utilize clathrin-mediated endocytosis (Diagram 1.7).

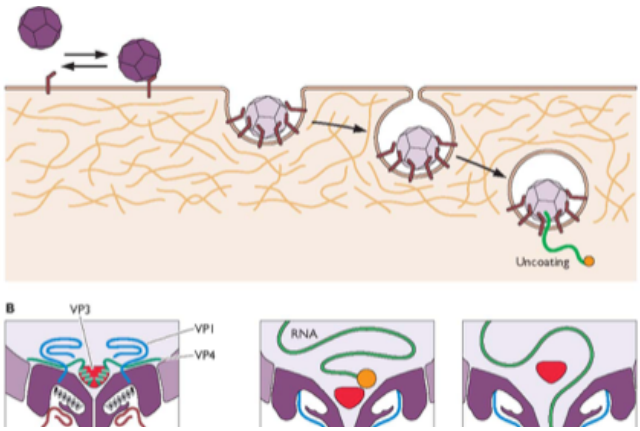

Diagram 1.7 Viral Endocytosis.
The un-enveloped or naked icosahedron is internalized by receptor-mediated endocytosis. Interaction with the virus receptor might alter the viral capsid (B: 1-3) and lead to genome release as the endosome acidifies.

The cell entry process for HRVs has been characterized in terms of centrifugation of HRV particles whose differential sedimentation is indicative of HRV structural changes. As they travel towards the interior of the cell, endosomes experience gradual acidification of their interior, a process which is believed to facilitate the "hair-pinning"- like conformational changes that allow fusion and release of the endosomal contents into the cytosol (Diagram 1.7) (4). It is believed that both major and minor group HRVs primarily exist as 135S particles while contained within the endosome, with minor group HRVs only stably taking on this conformation as the endosome acidifies (4). Once released into the cytosol, the HRV particles are observed to transition into 80S particles, which no longer contain the viral RNA. The noted interaction of 135S particles with liposomes in the cell cytosol may play a role in triggering the conformational transition to the 80S particle (4). The insertion of viral capsid proteins of the extruded 135S particle into the liposomes is thought to create, or expand, a pore structure in the capsid which is responsible for genome release (74).

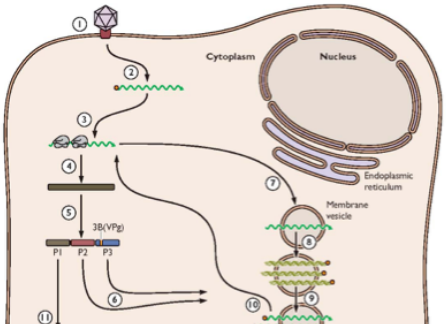

Diagram 1.8 Picornaviruses replication
The stages of the picornavirus replication cycle are shown as (1) attachment, (2) genome release, (3) translation of viral genome, (4) viral polypeptide production, (5) initial polypeptide cleavage, (6) use of viral enzymes to facilitate genome replication, (7) use of viral genomic RNA to template more RNA replication, (8) creation of -stranded viral RNA to use as templates for + stranded RNA, (9) creation of + stranded RNA viral genomes, (10) use of viral + stranded RNA as mRNA, (11) secondary cleavage to make viral capsid proteins, (12) capsid assembly, (13) cellular egress

HRV translation

As a single-stranded RNA of positive polarity, the HRV genome can act as mRNA and be immediately translated by host ribosomes. In this way, HRVs are not required to come equipped with the RNA-dependent RNA polymerase essential for their genome replication; this and other necessary proteins are created during the first cycle of translation of viral RNA (75). Interaction of the HRV IRES with the host ribosome results in the initiation of HRV translation. In addition to being able to operate independently of the cap-binding proteins seen in cellular mRNA translation, HRVs also come equipped with proteins capable of interference with host cell cap factors, resulting in a predomination of viral RNA synthesis as the infection proceeds (4). Having a type 1 IRES, the HRV principally requires just the 40s ribosomal subunit, eIF2-GTP-met-tRNA, eIFI, or eIF1A for translation initiation. Polypyrimidine-tract Binding protein (PTB)- based modulation of HRV translation occurs via the RRM motif, resulting in stimulation of HRV translation (76). In HRVs, polyprotein cleavage is primarily mediated by the 2A and 3C

proteases in the P1, P2 and P3 segments. Interestingly, some HRV 2A and 3C proteases are thought to experience both active and passive nucleo-cytoplasmic transport (4) .

HRV genome replication

The transition to use viral RNA to template genome synthesis, rather than translation, is believed to be mediated by PCBP2 whose increasing numbers as HRV infection progresses are due to the production of proteinases 3C and 3CD, whose cleavage of PCBP2 results in its preferential interaction with RNA-synthesis initiation factors (77). Characteristic of picornaviruses, the amphipathic N-terminal helices of HRV 2B, 2C and 3A proteins are responsible for localization of HRV RNA synthesis factories to membranous vesicles within the host cells (Diagram 1.8) (28). The structure of the RNA dependent RNA polymerase (RDRP), known as 3CDpol for HRV1B, 16 and 14, has been solved via x-ray crystallography. Typical of nucleotide polymerases, it is composed of a "right hand" structure with thumb, finger and palm domains, with the order of the "finger" regions being the most prominent distinction seen between it and that of the PV RDRP (34). The VPg protein plays the role of primer for both positive and negative strand RNA synthesis and requires uridylation to form the VPg-pUpU complex, a process which is mitigated by the Cis-Acting Replication Elements (CRE) (4). While CREs are not unique to HRVs, HRV2A has been documented to posses a novel CRE element located within the VP2 region of the ORF, which has not been documented in all picornaviruses (78). Elongation of the oligonucleotide involves both double and single stranded intermediates on immobilized replication complexes. The debate over the movement of double-strand templates over immobilized single stranded templates, or vice-versa, is ongoing (4).

HRV assembly and cell egress

Studies investigating the process of HRV assembly have produced 80S and 135S particles, similar to those seen during cellular entry and capsid un-coating of other picornaviruses. Concentration of viral genome replication and production of proteins on liposomes is believed to facilitate the formation of the non-ionic repeating interactions of viral capsid proteins. During HRV1A assembly within infected HeLa cells 6s, 13s and 14s sub-particles have been documented, similar to that seen in Enteroviruses (66). The 150S particle is believed to contain viral RNA, however, the virion is not considered to be mature until cleavage of VP0 to form VP1 and VP4 has occurred. Association of the viral RNA with VP4 or the genome-attached VPg protein with VP4 is believed to promote viral genomic RNA entry into the capsid (4). The possibility of RNA insertion into a mostly-complete HRV capsid, or HRV capsid construction condensing around viral RNA in a concerted manner, is still debated (79).

Immune system detection and antagonism

While HRV Infection of the nasal-pharyngeal tract results in shedding of the infected ciliated epithelial cells, the degree of cytopathic destruction caused by HRVs does not correlate to the severity of clinical symptoms documented, especially in the lower airways (80). This observation suggests that immunopathologies may play a significant role in the duration and severity of HRV infection. To that effect, studies in cultured airway epithelial cells, and other cells types, have revealed that each step in the HRV replication cycle is capable of triggering various entry-points into the pro-inflammatory pathway whose activity may be responsible for

exacerbation of HRV infection symptoms in the upper and lower airway. Unfortunately, distinction between major and minor HRVs in their ability to induce various actors in the pro-inflammatory pathway has not been holistically determined, and at the current date we only possess a piece-meal story of pro-inflammatory activity for each HRV type (4) .

Through studies with major group HRVs, viral interaction with the ICAM receptor alone, has been shown to induce downstream Jun animo-terminal kinase (JNK) and extracellular signal-regulated kinase (ERK) activity which can modulate interleukin-8, neutrophil chemoattractants and other pro-inflammatory cytokines (81). In addition to receptor binding, viral activity within the endosome during cellular uptake has been shown to induce NF-kB activity after ICAM receptor engagement (82). Furthermore, studies with UV-irradiated HRVs, whose UV-damaged genome cannot initiate a replication cycle, only resulted in dampening, rather than abolishment, of the HRV-induced IL-8 production in a cultured epithelial cell model (83) . These studies demonstrate that viral replication, or generation of replication intermediates, may not be necessary for some pathways of innate immune system induction, at least in the HRV subtypes studied.

As HRV replication commences in the cytoplasm, the double-stranded RNA (dsRNA) intermediate necessary for viral genome replication can trigger the host innate response through detection by multiple receptors. RIG-I and MDA5, both found throughout the cytoplasm, can bind viral dsRNA through carboxy-terminal RNA DExD/H-box domains and interact with beta interferon protein simulator 1 through amino terminal caspase activation (84). This activity ultimately leads to the activation of IFN-regulated factor 3 (IRF3) and NF-kB transcription factors, and lead to downstream induction of interferons and pro-inflammatory cytokines with the potential to stem the progression of viral spread. Viral dsRNA binding of Toll-Like Receptor

3 (TLR3) is shown to play an analogous role, however it remains localized to endosomal and plasma membranes (85). These pattern recognition receptors do not act exclusively on HRVs, but TLR3 and MDA5, but not RIG-I, have been found to maximize the innate immune response activity against HRVs (4).

The presence of an active HRV infection can result in the up-regulation of expression of numerous genes that govern the antiviral innate immune response. While an increase in IL-8 production and an array of neutrophils are the predominant findings of clinical studies using nasal secretions and sputum from HRV-infected patients, in vitro studies have revealed the up-regulation of numerous chemokines, including ENA-78, GRO-alpha, IP-10 and RANTES (86). Furthermore, in vitro studies have documented HRV induction of the IFN-beta and -y, 2', 5' -oligoadenylate synthetases, Mx-1, Mx-2 and viperin antiviral proteins (87).

As a microcosm of evolutionary biology, it is not surprising that HRVs have developed strategies to mitigate the antiviral defenses of infected cells and prevent their detection in the host cytosol (Diagram 1.9). To that effect, IPS-1 and RIG-I have been shown to be cleaved by HRV proteases 2A and 3C in a HeLa cell model of infection, and proteolytic cleavage of the p65-RelA NF-kB subunit by HRV14 has been documented as well (88). Some reports have also suggested that HRVs may have a mechanism of degrading MDA-5 and preventing IRF3 dimerization, however these studies are less conclusive (89).

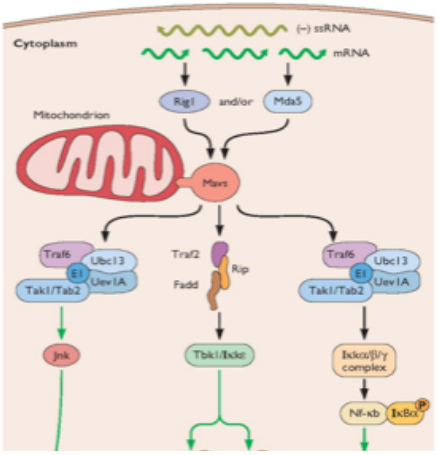

Diagram 1.9 Viral interactions with cellular immunity mediators
The interaction of viral replication components with cellular immunity mediators such as Rig-I, MDA-5 and Nf-kb, which leads to up-regulation of antiviral genes and the production of an anti-viral state unless precluded by viral proteins.

The consistent reoccurrence of HRV infections into late stages of life is testament to their ability to evade the production of a sufficient adaptive immune response. While adaptive immune responses are mounted during HRV infection, the sheer number of HRVs in circulation and the antigenic variability of these highly-mutagenic RNA viruses render adaptive immune system defenses non-effective in most cases. Though cross-reactivity has been shown to occur in some cases, a high amount of variation in antigenic regions prevents the production of efficacious antibodies, and has also stymied attempts to make an HRV vaccine (16).

HRV infection of the upper respiratory tract is associated with congestion, excess mucus production, sore throat, rhinorrhea, sneezing, general malaise and often fever for a period of 5-10 days (4). Taken together, these symptoms of acute viral rhinophayngitis are colloquially known as “the common cold”. While acute viral rhinopharyngitis of numerous etiologies may produce the aforementioned symptoms, HRVs have been documented to cause up to 50% of all adult cases year-round, with greater predominance in the spring and autumn, in the later of which HRVs have been cited to cause up to 90% of cases (4). The exact reasons behind this seasonal

pattern are not known, but both ambient air humidity, temperature and social activities, such as the return to school in younger populations, has been postulated to play a role (4). While adults suffer from 2-3 occurrences of the common cold on average per year, young children and infants can experience up to 7-10 episodes per year (4). This discrepancy is believed to be due to interaction with fomites or other infected individuals, age-related immune system differences, or both (4).

Clinical importance and economic implications

While generally not of grievous consequence for healthy adult individuals, HRV infections have been implicated in the morbidity and mortality of the very young, geriatric, immune compromised, or those suffering form other respiratory ailments (4).

Infants and young children are known to experience up to 10 episodes of viral-based upper respiratory tract infections per year, with HRV being indicted as the most common culprit (90). Some studies have cited that up to 26% of children hospitalized with fever and respiratory symptoms were HRV positive, a higher percentage of than that of RSV and other respiratory viruses that are often considered to be more severe (4). Furthermore, HRV has been found in the nasopharynx of up to 40% of acute otitis media cases, an inflammatory disease affecting the middle ear that commonly afflicts infants and young children (4). While exacerbation of asthma is a frequently cited consequence of HRV infection, this exacerbation is believed to precipitate the long-term alteration of airway passages that favor the development of asthma when reoccurring episodes of HRV-infection occur early in life (91). In some studies, this correlation between recurrent wheeze-inducing HRV infections and acute asthma episodes latter in life was stronger than the correlation between aero-allergen sensitization and asthma development (92).

The increased morbidity with HRV infection seen in geriatric patients is believed to be a result of general immune-system decline and a decrease in alveolar elasticity and elastic lung recoil with age. A similar mechanism is believed to account for exacerbations of HRV seen in patients with COPD (93).

Genetically inherited in an autosomal dominant fashion, Cystic Fibrosis (CF) results in mutations that lead to the loss of function of a key transmembrane regulator, leading to the production and build-up of thick, detrimental mucus in the respiratory tract. Consequently, viral, allergic or bacterial - induced respiratory stress are a leading cause of morbidity and mortality for these patients (94). The presence of HRV has been detected in up to 46% of CF patients with severe pulmonary exacerbations, and up to 58% of cases of aggravation of airway function, often in conjunction with a secondary bacterial infection (95).

Allergic inflammation poses a great threat to respiratory function, and the incidences of allergy development has experienced a marked increase in developed nations over the past 3 decades. Recent studies have shown that HRV-induced airway inflammation and sensitization of the epithelial tissue layer may promote the formation of respiratory allergies (96).

Clinical experimentation detects the presence of HRV 10 hours post-infection with the first “burst” of viral release occurring at approximately 48 hours post infection. Under experimental conditions with a low MOI, multiple bursts can be observed (4). In addition, laboratory experimentation has revealed that HRVs replicate better at a 33C, rather than the canonical 37C used in most virology studies (4). This observation supported the theory that HRV replication is restricted to tissues of the upper airway, a notion bolstered by the absence of HRV in lower airway tissue secretions from clinical isolates (4). However, more recent studies using immuno-histochemistry, and in situ hybridization on lower airway bronchial epithelium, have

detected HRV16 proteins and RNA in these regions (97). Travel to the lower airways is thought to be a possible consequence of the recruitment of inflammatory cells and immune responders after chemokine production in upper airways and resulting airway responsiveness, but this hypothesis has not been proven (98)

Chemical properties of Zn

Characteristic of a transition metal, Zn can be found in multiple oxidation states, with 2+ being the most prevalent in biological systems. In addition to readily forming compounds and ligand binding, Zn has been shown to exhibit a hexagonal close-packed crystal structure and is diamagnetic (4). As the first member of group 12 on the periodic table, the volatile metals, Zn can form alloys readily, the most famous being brass, an alloy of Copper and Zn. In additional to its pronounced role in biological systems, Zn is of strong commercial value and is found in everything from batteries and shampoos, to paints and electronic components (4). The cultivation of this 24th most abundant element on earth for commercial use is believed to have occurred as early as the 7th century BC (4). Zn is described as being the most chemically similar to Magnesium (Mg) as it is an ion of similar size, also commonly found with a 2+ charge. However, despite their chemical similarity, Zn and Mg are very divergent in their degree of participation in biological processes, including inhibition of HRVS (99).

The role of Zn in biological processes and enzymatic function

As a transition metal, Zn is distinguished for the essential role it has been shown to play in many biological processes. Crucial for prenatal and post-natal development, Zn is regarded as an essential mineral whose deficiency is associated with many diseases. From growth retardation

and developmental delays, to increased susceptibility to infections and immune dysfunction, the probable role of Zn in vital biological process was long expected before advances in molecular biology techniques were available to study its role in detail (99). Zn is now known to play a crucial role in the reactive center of over 100 different enzymes, whose catalytic activity depends on its availability (4). Stored and transferred as metallothioneins, Zn has been shown to play a critical role in the activity of transcription factors, which play a direct role in modulation of gene expression. In proteins, Zn is often found to associate with the side chains of amino acids like glutamic acid, aspartic acid, histidine and cysteine which may promote its catalytic role (4). The presence of a total of 2-4 grams of Zn throughout the average adult human body underscores this element's ubiquitous role in biological processes (4). While research on the many roles of Zn is on-going, it is currently believed that at least 10% of all human proteins are capable of interacting with the flexible coordination geometry of this lewis - acid (4). However, despite its biological necessity, an excess of Zn can result in detrimental physiological outcomes such as ataxia and copper deficiency (100). The availability of Zn is strongly linked to the integrity of the immune system. Zn deficiency has been shown to dampen both antibody and innate immune system responses across the animal kingdom, leading to susceptibility to opportunistic infections (4). Zn deficiency mediated T and B cell loss in the bone marrow can result in lymphopenia and thymic atrophy, and directly impede the development of immature lymphocytes (101).

The zinc proteome comprises an ever-growing database of metalloproteins who rely on precise "coordination environments" to effect catalytic activity. The characterization of genetic "signatures" in these coordination environments has precipitated the rapid discovery of additional Zn binding proteins through high throughput sequencing analysis (276). Zn catalysis sites within proteins are generally characterized by three ligands in addition to one water molecule, with

additional ligands playing stabilizing roles in some enzymatic species (276). While extensive classification of Zn-binding proteins has become a distinct field of study, most binding regions can be characterized by the presence of an array of histidines, cysteines and glutamate residues, with their arrangement in space playing a deterministic factor rather than one specific sequence motif (276). At present, the four principle classes of metalloprotein catalytic sites are the Class I oxidoreductases, Class II transferases, Class III hydrolases and Class IV lyases. Zinc Finger Proteins (ZFP), who have been shown to play a nearly ubiquitous role in DNA binding and modulation of gene expression, are principally identified by their Class II cysteine and histadine-rich repeats that form a three dimensional structure that can "grip" DNA (102). Conserved from higher lever vertebrates, to prokaryotes, yeast and plants, ZFPs can have one or two binding sites comprised of runs of cysteines, histidines, or cysteine alone, of 4 residues or more. The actual dissociation constant (Kd) of Zn in ZFP coordination complexes is unknown due to physiological complications that are mitigated by variable intracellular environments. However, in vitro studies predicated on a single ZFP motif has indicated that the motif might range from 10^-9 to 10^-11 concentrations (103). The physiological importance and ubiquity of ZFPs in biological systems underscores the potential detrimental consequence of deregulation of Zn homeostasis within the cell.

In contrast to ZBPs, EDTA, a common buffering agent in biological assays, has been found to have a Zn Kd is the range of 10^-16. While EDTA is also a chelator of other 2+ cations like Mg and Ca, it has been found to selectively deplete solutions of Zn, vastly favoring it over other divalent cations. Consequently, EDTA has been found to strip Zn cations from biological proteins even under conditions of limited exposure. Furthermore, the dramatic and rapid removal of Zn cations from the histidine-rich active sites of some ZBP leads to irreparable damage when

the true native structure of these enzymes cannot be re-formed (104). Consequently, EDTA has extensively been used to experimentally modulate the bioavailability of Zn in vitro, with high enough concentrations able to remove even trace amounts of this metal (104).

Prior research on HRVs and Zn

In 1974, a general study examining the effect of various metal compounds on viral production in tissue culture noted a sharp decrease in HRV infection after HRV infected cells were exposed to Zn (105). This observation led to a follow-up study which characterized the accumulation of a large picornaviral polypeptides in the presence of Zn ions (106). This observation suggested that intracellular Zn ions might play a role in the disruption of the polypeptide cleavage events characteristic of picornaviruses. An additional study by Koran and Butterworth confirmed this hypothesis, demonstrating inhibition of viral polypeptide cleavage during HRV replication when intracellular Zn levels were raised (107). However, it is important to note that this polyprotein processing failure in the presence of Zn was not found to be unique to HRVs. Butterworth and Koran made these observations in multiple picornaviruses such as PV and coxsackie B3 virus (CBV3). Therefore, this mechanism is unlikely to account for the HRV-specific inhibition initially documented. Fueled by these experimental insights, a group lead by Eby et al, conducted the first Zn lozenge clinical trial that demonstrated reduction in the duration of the common cold in individuals enrolled in the study (108). However, in this study, the etiology of the infectious agent eliciting the “common cold” symptoms was not determined prior to enrollment. Therefore, the decrease in duration of the symptoms experienced by lozenge users cannot be directly attributable to HRV inhibition.

In 1987, work performed by Geist et al. discounted the research of Eby and Butterworth by demonstrating that the levels of intracellular Zn necessary to observe HRV inhibition were cytotoxic to the HeLa and WI -38 cells infected. Furthermore, they determined that the level of Zn needed to see viral inhibition greatly exceeded that seen in normal human serum after lozenge administration (109). However, additional work investigating the potency of a number of different Zn compound demonstrated that the amount of free Zn+ in solution and HRV2 inhibition held a linear relationship, with no reported cytotoxicity (110). Around the same time, immunological studies reporting the potentiation of interferons by Zn offered a different explanation for success seen in some clinical trials (101) .

Clinical trials aside, no in vitro experimental investigation into the potential inhibitory properties of Zn alone on HRVs has been reported in over two decades. However, studies using Zn in conjunction with chelating and ionophoric agents has been conducted (4). In all of these studies, one of the salient findings has been the dependency on Zn availability within the cell to observe antiviral activity. Intracellular inhibition of HRVs and other picornaviruses was seen with pyrithione (PT) and hinokitiol (HK) only when sufficient Zn was present, and the inhibitory potential of pyrrolidine dithiocarbamate (PDTC) was only observed when Zn+ or Cu+ was present (4). In both of these studies inhibition of polyprotein processing was cited as a key mechanism of viral inhibition (111). However, the unnatural amount of Zn+ and ionophore concentrations needed within an infected cell to witness inhibition of viral replication makes the relevancy of these mechanisms doubtful. Furthermore, the additional observations of multiple viral protease failure and truncation of RNA synthesis, suggests that this decrease in virion production may be due to the generalized effect of cell distress due to detrimentally elevated cation levels. Finally, in the two studies which present association with and disruption of

polyprotein processing as the possible mechanism of Zn inhibition, other picornaviruses were either not tested, or shown to experience the same type of inhibition when exposed to unnaturally high levels of intracellular Zn, or Zn in conjunction with ionophores. Therefore, even if abnormally high intracellular Zn levels can disrupt polyprotein processing, this mechanism is unlikely to account for the very HRV-specific inhibition documented in prior studies, and investigated in this body of research.

Despite discrepancies in experimental findings, numerous clinical trials using a variety of Zn lozenge formulations were conducted over the next two decades with disparate outcomes. However, attempts to perform meta-analyses on clinical trial outcomes from different studies also resulted in divergent outcomes, presumably due to the parameters used to determine the studies included, and the statistical models used to model the data (112). The most recent and comprehensive meta-analysis conducted in 2015, concluded that Zn gluconate lozenges are effective if use commences within 24 hours of the onset of symptoms (113).

Despite the lack of a descriptive mechanism of Zn antiviral activity or consistently decisive clinical trials, numerous entities have seized upon the commercial opportunity to bring various Zn-based products to market, claiming that they have the potency to relieve the common-cold sufferer. As a testament for the demand for common-cold therapeutics, the profitability of these products have experienced undisputed growth (114). Even with the negative publicity garnered by the makers of Zicam, with patient claims of permanent nasal sensory damage, the demand for Zn-based products has not diminished, even after studies carried out in rats revealed that excess Zn exposure could have a detrimental impact on the olfactory neuroepithelium (115). The resounding financial success of these controversial products can most likely be attributed to the large population of common-cold sufferers with discretionary income whose desperation for

symptom relief supersedes the lack of medical consensus as to their viability. It follows then, that the development of a scientifically substantiated treatment for the common cold would garner even greater public appreciation and commercial success.

Summary and scope of research

In this study I have examined the role of Zn in antiviral inhibition when applied to HRVs in isolation. In prior studies, the application of Zn to HRV-infected cells yielded inhibitory results, but the experimental design used did not allow for the examination of HRVs and Zn in isolation. The dampened HRV production could not be directly attributed to Zn due to the potential cellular stress, or alteration of normal innate immune functions, that could have also played a role in the abrogation of HRV production. Furthermore, many of these studies were not HRV-specific. Given the physiological constraints of nasal spray or lozenge use, I hypothesized that the majority of any Zn-based inhibition attributable to these products was likely to occur through extracellular contact of these therapeutics with HRVs. To test this conjecture, I designed a series of experiments that examined the effect of Zn on HRVs in isolation and demonstrated that extracellular exposure to Zn alone is sufficient to decrease the infectivity of an HRV population. I then demonstrated the specificity of this mechanism for HRVs and Zn, and characterized the mechanism behind this profound abrogation of HRV infectivity after Zn exposure. Through the cultivation of Zn-resistant mutants, I was able to characterize topographical areas of the viral capsid that might lend Zn susceptibility and prevent the Zn-mediated damage to HRV RNA observed. Furthermore, I also demonstrated the ability of Zn-ionophore complexes to facilitate extracellular inhibition of HRVs using lower Zn concentrations than that required in Zn-based inhibition alone.

Since it was first described in 1974, the potential of Zn to inhibit HRVs has inspired numerous clinical trials and the production of Zn-based products with dubious efficiency. Here I have attempted to demonstrate and describe a mechanism of Zn inhibition of HRVs that is viable in the context of Zn lozenge or nasal spray use and might explain the successes seen in some clinical trials. It is my hope that the results of these studies might template the design of more efficacious Zn-based therapeutics.

CHAPTER 2: MATERIALS AND METHODS

Cells, viruses and plasmids

The HeLa S3 and H1 (human cervical carcinoma) cell lines were maintained in Dulbecco's modified essential medium (DMEM; Life Technologies, Carlsbad, CA) supplemented with a 1% penicillin-streptomycin solution (Invitrogen, Carlsbad, CA) and 10% bovine calf serum (HyClone, Logan, UT). Cells were maintained at 33-37C and split using trypsin (Gibco) regularly (70-90% confluence). The pACYC177-Xmal-T7-WT-RV1A-Xho1 plasmid was harvested from One Shot® TOP10 Chemically Competent E. coli (Life Technologies/Invitrogen cat# C4040-10) using a QIAGEN Plasmid Midi Kit (cat# 12143), following the manufacturer's protocol after transformation using the manufacturer's protocol and incubation at 37C overnight with constant agitation in standard LB broth (10g Bacto-tryptone, 5g yeast extract,10g NaCl (pH 7.5 in 1000ml) supplemented with 1000 mg/ml ampicillin.

Poliovirus was isolated from HeLa cells transfected with in vitro synthesized RNA using lipofectamine (Invitrogen) (32, 33). These stocks were fractionated into aliquots to minimize the number freeze-thaw cycles and kept at -80C

HRV16, HRV39, HRV1A, and Coxsackievirus B3

HRV16, HRV39, HRV1A, and Coxsackievirus B3 were isolated from HeLa cells transfected with in vitro-synthesized RNA (34-36). All in vitro- synthesized RNAs were transcribed from linearized templates using T7 RNA polymerase and following the manufacturer's protocol (Promega, Madison, WI). These stocks were aliquoted to minimize the number freeze-thaw cycles and kept at -80C.

Cation, EDTA Ionophore solutions.

Stock solutions of 0.1M EDTA, pH 8.0 (Sigma), 0.1M $ZnCl_2$ (Sigma), 0.1M Zn aspartate (Sigma), 0.1M Zn gluconate (MP Biomedicals, Santa Ana, CA), 0.1M $MgCl_2$ (Sigma), 0.1M $MnCl_2$ (Sigma), 0.1M $CaCl_2$ (Sigma), 100mM -.1uM Pyrithionine (Sigma), 100um-.1M Hinokitiol (Sigma) and 100um -.1M PDTC (Sima) were prepared in 1X phosphate buffered saline (PBS) pH 7.4 or double distilled water pH 7.4 (Millipore, Billerica, MA). All solutions were filtered through a 2⌠M filter (Millipore) before use in cell culture. All ionophores and Zinc salts were purchased from Sigma Aldrich. Solutions were kept at 4C.

Zn Treatment

Zn solution was added to viral sera to achieve the concentration desired. PBS (Life Technologies cat# 21600-010) was used to control for volume in untreated samples. After addition of Zn, the samples were inverted 2-5 times and then placed on nutator at 37C, or 4C in the case of temperature based studies.

Plaque assays.

To determine the titer of PV and EV68, virus dilutions were prepared in virus binding buffer (VBS, 1X PBS supplemented with 0.01% bovine serum albumin). 100ul of each dilution was used to infect the confluent monolayer on a 6-well flat bottomed plate where each well contained 9.5cm^2 surface area (Falcon). The plates were incubated with periodically agitation at 37C for 45 minutes. After incubation, HeLa cells were covered with 2ml of an overlay consisting of DMEM (Millipore 122 Fisher, Billerica, MA), 0.2% $NaHCO_3$ (Sigma, St. Louis, MO), 5% bovine calf serum, 1% penicillin-streptomycin and 0.9% bacto-agar (Fisher Scientific, Carlsbad, CA). Cells were incubated for 48h and developed using 10% trichloroacetic acid and crystal violet.

To determine the titer of HRV16, HRV39, EMCV, and Coxsackievirus, virus dilutions were prepared in virus binding buffer (VBS, 1X PBS supplemented with 0.01% bovine serum albumin). 100ul of each dilution was used to infect the confluent monolayer on a 6-well flat bottomed plate where each well contained 9.5cm^2 surface area (Falcon). The plates were incubated with periodically agitation at 37C for 45 minutes. HeLa cells were covered with 2ml of an overlay of DMEM, 0.2% $NaHCO_3$, 1% bovine calf serum, 1% penicillin- streptomycin, 0.1M $MgCl_2$ (Sigma) and 0.8% Noble agar. After the overlay solidified, it was covered with 2ml liquid medium consisting of DMEM, 0.04 M $MgCl_2$, 0.002% glucose (Sigma), 0.1% bovine serum albumin (Sigma), 2 mM sodium pyruvate (Invitrogen), 4mM glutamine (Invitrogen), 4mM oxaloacetic acid (Sigma), 0.2% $NaHCO_3$ and 1% penicillin-streptomycin. Cells were incubated for 72-96h and developed using 10% trichloroacetic acid and crystal violet.

To determine the titer of HRV1A and HRV2, virus dilutions were prepared in virus binding buffer (VBS, 1X PBS supplemented with 0.01% bovine serum albumin). 100ul of each dilution was used to infect the confluent monolayer on a 6-well flat bottomed plate where each well contained 9.5cm^2 surface area (Falcon). The plates were incubated with periodically agitation at 37C for 45 minutes. 2ml of the HRV1A plating medium composed of DMEM supplemented with 2% bovine calf serum, 40mM $MgCl_2$, 0.01% $NaHCO_3$, 1% penicillin-streptomycin and 1% low-gelling type VII agarose (Sigma) was applied after incubation. Cells were incubated for 96-120h and developed using 10% trichloroacetic acid and crystal violet.

ICPA Assays

Infectious Center plaque assays were performed using the same HeLa cells and HRV1A and PV stocks previously described. 100 ul of HRV1A and PV stocks were used to infect a monolayer of

HeLa cells which were held at 4C for 20 -45min by keeping the HeLa dishes on ice and monitoring the temperature using a thermometer. The plates were cooled to 4C prior to infection and kept at 4C through the viral infection, centrifugation and washes. After the incubation period, the remaining viral inoculate was removed and the plates were washed 3 times with PBS that had been cooled to 4C. Following the washes, these cells were harvested mechanically using a cell scraper and gently pipetted into a centrifuge tube and spun at 200 rpm for 5 min at 4C. Excess supernatant was removed and the cells were gently resuspended in cooled 4C PBS, underwent serial dilutions, also in PBS, and 100 ul of each dilution were plated on a second mono-layer of HeLa cells. Following a 30 min incubation period at 37C, 2ml of a semi-solid agarose overlay was applied that was identical in composition as that used for traditional HRV1A or PV plaque assays. After a 96 -144 hr incubation period (HRV1A) or 72-96hr incubation period (PV), the 10% trichloroacetic acid was applied to the ICPA for at least 20 minutes to fixate the HeLa monolayer and followed by staining with crystal violet solution and subsequent washing in the same manner as a traditional plaque assay.

Competition Assays

Confluent monolayers of HeLa cells in 60mm dishes were infected with a mixture of untreated and Zn-treated HRVIA with the amount of untreated HRV1A held constant. The approximate PFU per 50ul aliquot of untreated HRV1A was determined. This amount of untreated HRV1A was held constant while increasing amounts of Zn-treated HRV1A was added to the inoculate mixture. The 100ul volume of each inoculate was kept equal by using DMEM to make up the difference when the maximum amount of Zn-treated HRV1A was not used. These 100ul inoculate mixes were used to infect each well of HeLa cells and held at incubation at 37C for

45min with intermittent agitation. An identical procedure was used for competition between untreated HRV1A and UV-inactivated HRV1A

.

UV-inactivated HRV1A

500ul aliquots of untreated HRV1A was applied to 10cm dishes and spread into a thin layer. These dishes were then subjected to UV irradiation for 7 minutes in a Stratalinker 2400 (Stratagene, LaJolla, CA). Confirmation of complete inactivation of the HRV1A population using this method was achieved by performing a traditional plaque assay using 100ul of each 500ul treatment group.

Northern Blot Hybridization Analysis

Viral RNA was fractionated in 1% agarose containing 6% formaldehyde in 1X MOPs buffer. After electrophoresis at approximately 85-95 volts for 1.5-2 hours, lanes containing RNA markers were excised and viewed on a UV transilluminator to confirm the presence of RNA, the remainder of the gel was moved to a capillary transfer apparatus and RNAs were transferred to a positively charged nylon membrane (Roche) in 2x SSC buffer overnight. Following transfer to the membrane, RNA was cross-linked to the membrane in a Stratalinker 2400 (Stratagene, LaJolla, CA) for 25-50 sec and then the membrane was baked at approximately 80°C under vacuum for 2-3 hours, pre- hybridized, and then hybridized with a digoxigenin-labeled DNA probe according to the manufacturer's protocol (Roche, Indianapolis, IN).

Digoxigenin DNA probe synthesis and preparation

A digoxigenin DNA probe for HRV1A RNA was synthesized using a DIG labeling and detection (Roche, Indianapolis, IN) with custom HRV1A primer sets to produce a 500 bp-800bp DNA. Prior to addition to hybridization solution, the DIG probe was boiled for 10 minutes and then immediately chilled on ice to promote double stranded DNA separation. A random-hexamer primed Digoxigenin probe was also made using randem hexamers Life Technologies (cat # N8080127) and the PyACY-HRV1A plasmid.

Isolation of viral RNA

Virion RNA was isolated from virus particles produced by ultracentrifugation of infected cell supernatants in an SW28 rotor at 28,000 rpm for 3h at 4°C. Supernatants were discarded, and pellets were pooled and suspended in 500ul of DMEM or PBS An equal volume of TRIzol LS reagent (Ambion/RNA, Life Technologies) and RNA was extracted according to the manufacturers' protocol, and RNA pellets were resuspended using 12-20ul of DepC (Sigma Aldrich)-treated water.

Sucrose gradient HRV1A purification

HRV was fractionated on sucrose (Sigma Aldrich) gradients (5% to 45% w/v) at 40,000 rpm for 2 hr after application of 500ul of .2uM viral Sera was carefully added to the top of the column . Fractions of 0.5 ml were collected from the top down and stored at - 80°C before assaying for viral infectivity and viral RNA.

Native Gel Analysis

Aliquots of sucrose gradient fractions were applied to an 8-12% native gel matrix and subjected

to electrophoresis at 40-90V at 4C for 3-6 hours. Following transfer to a an Amersham hypofilm (GE Healthcare) membrane using a Bio-Rad vertical transfer apparatus overnight, the membrane was probed using a Coomassie Blue (Sigma Aldrich) procedure or silver-stain procedure (Ambion) using the manufacturer's protocol.

Denaturing SDS-PAGE Gel Analysis

Aliquots of sucrose gradient fractions were applied to an 10-12% SDS PAGE gel matrix and subjected to electrophoresis at 60-90V at 4C for 1.5-2.5 hours. Following transfer to a membrane using a Bio-Rad vertical transfer apparatus overnight, the membrane was probed using a Coomassie Blue procedure or Silver-stain procedure (Ambion).

Reverse Transcription of viral RNA and DNA

RNA isolated by Trizol was resuspended in DepC-treated water. Approximately 10 µl or 2 µg of RNA was used to template DNA synthesis by SuperScript III reverse transcriptase and was primed with random hexamers according to the manufacturer's directions (Invitrogen, Carlsbad, CA).

Primer design, sequencing and sequencing analysis

HRV1A primers for genome synthesis were designed using APE (A Plasmid Editor) open-source software. Fifteen primer pairs were designed to produce overlapping amplicons of approximately 500 bp, and these primer pairs were optimized for similar Tm values, enabling the production of longer amplicons if used together (Figure 2.1). A list of primers used can be found in Supplementary Table 1. PCR was performed with Herculase polymerase (Agilent Technologies, Santa Clara, CA) using the manufacturers' standard protocol aside a lower binding temperature to accommodate the Tm of the primers used.

HRV1A bp	Orientation	Sequence 5'-3'
1-510	Forward	TTAAAACTGGGTGTGGGTTGTTC
1-510	Reverse	AAACTCATTGGCTTATGAGCCAT
404 -1013	Forward	AAAGATCGGACAGGGTGTGAAG
404-1013	Reverse	TGATGATGTATCAGGTTGTGTTGGT
939 -1475	Forward	GGGGTCTGGCCGCATTACTTA
939-1475	Reverse	CATTGAATCCATTGGCACAGCA
1479 -1943	Forward	CGACATAATAACTGGAGCCTGGT
1479-1943	Reverse	GGTGTAATAGCTTGCAATCTCCC
1879-2588	Forward	AAGTAGACATTACATCACAGCCTTTG
1879-2588	Reverse	AACCTTTATTCTTGAGATGTGGACA
2406-2975	Forward	CATCACACTACATCAAACTCTGCC
2406 -2975	Reverse	AACTACGCTACCATACTTGGAAGAAG
2927- 3536	Forward	TGATGGATATGATGGAGACAACAC
2927- 3536	Reverse	TCTACAAAGAAGTTTTCCACCACA
3504- 4026	Forward	CCTGGTGATTGTGGTGGAAAAC
3504- 4026	Reverse	GGGCCTGGGGTAGCATAGATT
3952-4526	Forward	CACGTGGTCTTGAATGGATTGG
3952-4526	Reverse	AAATGGTTTACCCTTGTCAGGCA
4459-5000	Forward	GCCAAATGGTTTCAAGTGTTACAT
4459-5000	Reverse	CACTTGGCACTCTGCTGGAAT
4891-5578	Forward	ACGCTCCACCACCACCAG
4891-5578	Reverse	TTAAGCATTCTGGCTGTTTGATTT
5473- 6030	Forward	TGGCACTTTCAGCTAATCAAGA
5473- 6030	Reverse	CCTTCTATCCCAAACACGCTAT
5974-6548	Forward	TGACACTAGATATTGATTCCAGGC
5974-6548	Reverse	TGTTGATTTAAACAAGTGCTTGGA
6443-7068	Forward	ACACCCTGTCTGGTTTCAAGC
6443-7068	Reverse	GATCATAAGGTGGGATATACAGTGC
6973- 7137	Forward	TGATGTGGCACAATGGACG
6973- 7137	Reverse	ATAGAATTAAAGAATCATTCATTCATTATT

Figure 2.1 Primers used to sequence the full-length HRV1A genome.
Using A Plasmid Editor (APE) software, 15 pairs of over-lapping primers were designed whose compatible Tms allow for flexible targeting of any region of the HRV1A genome as any Forward primer can be used with any Reverse primer. Each pair was tested and yields an approximately 500-600 bp product when used with Herculase Taq polymerase with the PCR protocol described in Materials and Methods pg

Creation of mutant clones

The following procedure outlines the steps taken to make the mutant clones of HRV1A by

introducing the mutations found in Zn-resistant isolates. The initial template was the

pACYC177-Xmal-T7-WT-RV1A-Xho1 plasmid.

1. PCR using mutagenesis primers over mutation site “a1” & “B2” and “A2” & “b1”.
   - yields two linear amplicons each containing the mutagenesis site with overlapping mutagenesis regions
   - Final product needs to be inserted back into plasmid so the “A” & “D” primers were be designed to end at or near a restriction site/ contain the restriction site
   1a) Confirm amplicon presence and size on gel
   1b) Harvest, Purify & Quantify (Zymogen gel purification kit, Nanodrop)
   1c) Confirm mutagenesis site was successful via sanger sequencing (Genewiz)

2. PCR using amplicons from round 1 as template using primer pair A/D
   - the complimentary ends of the first round of PCR amplicons hybridize and the final product with the desired mutation was created

2a) Amplicon was check on gel for presence and size
2b) Harvest, Purify & Quantify (Zymogen gel purification kit, Nanodrop)
2c) Confirm mutagenesis site was successful via sanger sequencing (Genewiz)

3. Digestion of amplicon from step 2 and the destination vector (pACYC177-Xmal-T7-WT-RV1A-Xho1) using restriction endonucleases Sac1 HF & Sfo1.

4. Purification of digested vector and amplicon from step 3 (phenol-choroform or Zymogen DNA clean-up kit)

5. Ligation of digested vector and amplicon from step 4 using T4 DNA ligase at 4C overnight (New England Biolabs)

6. Confirmation of successful ligation and site directed mutagenesis by gel visualization and followed by sanger sequencing (Genewiz,) .

The primers designed for site-directed mutagenesis are shown below.

Pair 1
Forward: 5' CATCACACTACATCAAAATCTGCCCCACTTTTAG 3'
Reverse: 5' CTAAAAGTGGGGCAGATTTTGATGTAGTGTGATG 3'

Pair 2
Forward: 5' GTCATCACACTACATCAAAATCTGCCCCACTTTTAGATG 3'
Reverse: 5' CATCTAAAAGTGGGGCAGATTTTGATGTAGTGTGATGAC 3'

Pair 3
Forward: 5' GTCATCACACTACATCAAAATCTGCCCCACTTTTAGATGC 3'
Reverse: 5' GCATCTAAAAGTGGGGCAGATTTTGATGTAGTGTGATGAC 3'

PCR

PCR was performed using Herculase (Ambion) and the accompanying recommended protocol with the adjustment of a lower binding temperature (51-54C) to accommodate the Tm of the HRV1A primers in a ThermoCycler (Fischer Model number)

DNA Electrophoresis & Amplicon Purification

PCR amplicons were visualized and isolated on 10% agarose gels (Sigma Aldrich) supplemented with Ethidium Bromide (Sigma Alderich). After subjected to electrophoresis for 5-1.25 hrs, the amplicons were visualized on a UV-transilluminator . A 500bp ladder was used to confirm the size of the amplicons (Fermantos O' Gene Ruler) When purification was necessary prior to sequencing, the gel slices corresponding to the amplicon were excised using sterile razorblades. The DNA from these gel slices were then extracted from the gel using a Zymogen Gel Extraction kit columns, following the manufacturers protocol. The final elution was performed with 12-20ul of sterilized H20 or TE buffer (1M Tris-HCl, pH 7.5 or 8.0,10 mM2 ml0.5M EDTA, pH 8, in 988 ml ddH2O).

Sequencing

Sanger sequencing of samples was performed by Genewiz (South Plainfield, NJ). Both consensus sequence text files and raw data files were returned for analysis. The samples were prepared with 2uM of each primer according the Genewiz protocol.

Transfection of mutant clones

A TransIT-HeLaMonster Transfection Kit (Mirus Fisher) was used to with viral RNA synthesized using T7 High Yield RNA Synth Kit (New England Biolabs) with H1 HeLa cells.

Analysis of Results

A Bash shell scripting pipeline was written to uniformly extract, process and format each sequencing output using the consensus sequence supplied by Genewiz. This text-file output was then aligned using APE (A Plasmid Editor) open-source software. The sequences were aligned to both the HRV1A plasmid on which which the primers were templated and to the official NCBI

sequence. When discrepancies were found in mutant strains, the raw data file from Genewiz was consulted to confirm that the base-pair in the consensus sequence was soundly chosen. The resulting polypeptide sequence for each region containing deviations from the wild type sequence was generated using the following code. Wild-type sequences and control sequenced Genewiz isolates were used for comparison. Additional exploration into the potential impact of alterations in amino acid sequence was performed through assignment of each amino acid to it's integer corresponding the biochemical Janin, Kyte-Dolittle or E.Weis value that is a quantitative expression of hydrophobicity, size and chemical reactivity. Alignment and plotting of this string of integers revealed the potential severity biochemical change at certain amino acid sites within the VP1 polypeptide.

```
gencode = {

    'ATA':'I', 'ATC':'I', 'ATT':'I', 'ATG':'M','ACA':'T', 'ACC':'T', 'ACG':'T', 'ACT':'T', 'AAC':'N', 'AAT':'N', 'AAA':'K',
'AAG':'K', 'AGC':'S', 'AGT':'S', 'AGA':'R', 'AGG':'R', 'CTA':'L', 'CTC':'L', 'CTG':'L', 'CTT':'L', 'CCA':'P', 'CCC':'P',
'CCG':'P', 'CCT':'P','CAC':'H', 'CAT':'H', 'CAA':'Q', 'CAG':'Q', 'CGA':'R', 'CGC':'R', 'CGG':'R', 'CGT':'R','GTA':'V',
'GTC':'V', 'GTG':'V', 'GTT':'V','GCA':'A', 'GCC':'A', 'GCG':'A', 'GCT':'A', 'GAC':'D', 'GAT':'D', 'GAA':'E',
'GAG':'E','GGA':'G', 'GGC':'G', 'GGG':'G', 'GGT':'G','TCA':'S', 'TCC':'S', 'TCG':'S', 'TCT':'S','TTC':'F', 'TTT':'F',
'TTA':'L', 'TTG':'L','TAC':'Y', 'TAT':'Y', 'TAA':'_', 'TAG':'_', 'TGC':'C', 'TGT':'C', 'TGA':'_', 'TGG':'W'}

janin_code = {

    'I': 0.7, 'F': 0.5, 'V': 0.6, 'L': 0.5, 'W': 0.3, 'M': 0.4, 'A': 0.3, 'G': 0.3, 'C': 0.9, 'Y': -0.4, 'P': -0.3, 'T': -0.2, 'S': -0.1, 'H':
-0.1, 'E': -0.7, 'N': -0.5, 'Q': -0.7, 'D': -0.6, 'K': -1.8, 'R': -1.4}

kd_code = {

    'I': 4.5, 'F': 2.8, 'V': 4.2, 'L': 3.8, 'W': -0.9, 'M': 1.9, 'A': 1.8, 'G': -0.4, 'C': 2.5, 'Y': -1.3, 'P': -1.6, 'T': -0.7, 'S': -0.8,
'H': -3.2, 'E': -3.5, 'N': -3.5, 'Q': -3.5,'D': -3.5, 'K': -3.9, 'R': -4.5}

ew_code = {

    'I' : 0.73, "F" : 0.61, 'V': 0.54, 'L': 0.53, 'W': 0.37, 'M': 0.26, 'A': 0.25, 'G': 0.16, 'C': 0.04, 'Y': 0.02, 'P': -0.07, 'T': -
0.18, 'S': -0.26, 'H': -0.40, 'E': -0.62, 'N': -0.64, 'Q': -0.69, 'D': -0.72, 'K': -1.10, 'R': -1.8}

def translate_dna(dna):

    last=len(dna)-2

    print(last)
```

```
    polypep=""
    for base in range(0,last,3):
        codon=dna[base:base+3]
        print("Codon:",codon)
        amino=gencode.get(codon.upper(), 'X')
        print(amino)
        polypep+=amino
    print(polypep)
    return(polypep)


def janin_scale(polypep):
    janin_points = []
    for aa in polypep:
        janin = janin_code.get(aa)
        print(janin)
        janin_points.append(janin)
    print("\n Janin_points:", janin_points )
    return [janin_points]


def kd_scale(polypep):
    kd_points = []
    for aa in polypep:
        kd = kd_code.get(aa)
        print(kd)
        kd_points.append(kd)
    print("\n Kyte and Doolittle points:", kd_points)
    return [kd_points]
```

```
def ew_scale(polypep):
    ew_points = []
    for aa in polypep:
        ew = ew_code.get(aa)
        print(ew)
        ew_points.append(ew)
    print("\n Eisenberg Weis points:", ew_points)
    return [ew_points]


dna=input("Paste Sequence for Translation Here:")
dna=dna.upper()
translate_dna(dna)
pp = translate_dna(dna)
janin_scale(pp)
kd_scale(pp)
ew_scale(pp)
```

Pymol 3-dimensional Molecular Imaging

Images produced using MacPymol with PDB file 1r1a.pdb. Full and half capsid coordinates are from VIPERdb (viperdb.scripps.edu).

Hinokitiol Treatment

HK in solution was added to viral sera to result in the concentration desired or mixed with Zn via inversion and vortexing. PBS was used to control for volume in untreated samples. After addition of HK, the samples were inverted 2-5 times and then placed on nutator at 37C, or 4C in the case of temperature based studies.

Pyrithione Treatment

PT in solution was added to viral sera to result in the concentration desired or mixed with Zn via inversion and vortexing. PBS was used to control for volume in untreated samples. After addition of PT, the samples were inverted 2-5 times and then placed on nutator at 37C, or 4C in the case of temperature based studies.

PDTC Treatment

PDTC in solution was added to viral sera to result in the concentration desired or mixed with Zn via inversion and vortexing. PBS was used to control for volume in untreated samples. After addition of PDTC the samples were inverted 2-5 times and then placed on nutator at 37C, or 4C in the case of temperature based studies.

PDTC- Zn Compound Synthesis

30uM or 60uM PDTC and 30uM Zn were mixed, vortexed and left at room temperature or heated up to 60C for 20-60min. The precipitate was spun down on a table-top centrifuge and the supernatant was removed. The precipitate then underwent 1-3 additional washes involving re-suspension in distilled water and centrifugation.

Rnase Inhibtion

10 units of Rnase 1 (Thermo Tcientific) per 50 ul of HRV was incubate at 37C for 45 min

CHAPTER 3: ZN-BASED INHIBITION OF HRVs

Exposure to Zn+ salts inhibits HRV infectivity

Previous studies on the inhibition of HRV replication by Zn+ examined the effect of adding the cation to infected cells (106). However, when I attempted to replicate the conditions seen in some of these studies, I observed that Zn+ exposure was toxic to HeLa and TE cells at the amounts necessary to achieve high intracellular concentrations. This cytotoxicity of intracellular Zn was also noted in prior studies (109). Consequently, I chose to take an alternative approach, and postulated that any physiologically relevant mechanism of Zn-based inhibition relying on lozenge or spray use as a vehicle of delivery was most likely to be successful during the extracellular stage of the viral replication cycle, before virions had attached and entered a susceptible and permissive cell. Therefore, I hypothesized that there might possibly be an extracellular mechanism of Zn-mediated HRV inhibition that might account for the successes seen in some clinical trials. I chose to test this hypothesis by exposing HRVs to Zn+ compounds prior to their exposure to susceptible and permissive cells using the general experimental work-flow shown below, which involved treating HRVs in isolation with Zn compounds, prior to serial dilution and inoculation of a confluent monolayer of susceptible and permissive HeLa cells. To assay for infectivity of the treated virus particles, a plaque assay was performed, wherein a semi-solid agarose overlay is applied to the infected monolayer that effectively restricts diffusion of the progeny virions after the lysis of infected cells. This results in punctate regions of cell death, or "plaques", that can be observed after fixation and staining of the remaining monolayer, after an appropriate incubation period that is predicated upon virus type. Due to serial dilution of the initial inoculate, ultimately, distinct, countable plaques can be observed and used to calculate the original titer of infectious virus in the untreated and Zn-treated samples (Diagram 3.1).

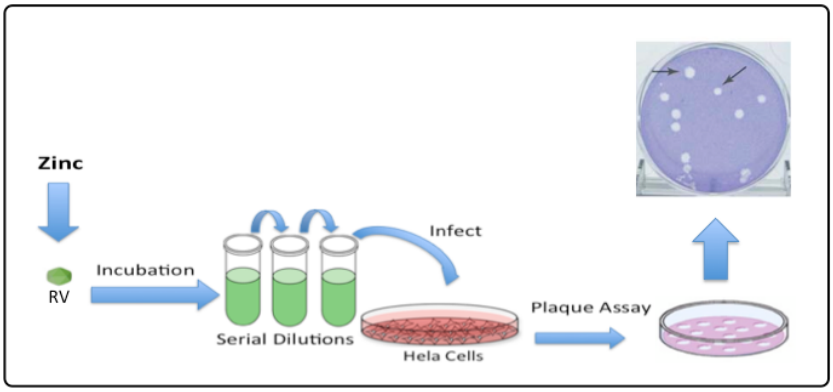

Diagram 3.1 Experimental work-flow for Zn sensitivity
Aliquots of virus were exposed to varying quantities of different Zn+ compounds (Zn-Gluconate, Zn-Chloride & Zn-Aspartate), subjected to a period of incubation, and then aliquots of each dilution were used to infect HeLa cells. Viral titer was ultimately visualized using the appropriate plaque assay protocol for each virus type after fixation and crystal violet staining.

The resulting cytotoxicity from prolonged exposure to high Zn concentrations was observed via fixation of HeLa cell monolayers and crystal violet staining, after which both a decrease in cell number and the preponderance of inclusion bodies and other signs of a moribund cellular state could be readily observed under a standard tissue-microscope (data not shown). As obligate intracellular parasites, viruses require the resources provided by an active cellular metabolism to complete infectious cycles that result in the production of infectious progeny virions. Consequently, perishing cells are unable to support a normal level of viral replication, and can therefore lead to a decrease in total viral yield if infected, which might generate a "false-positive" result when comparing viral titers. Therefore, it was important to confirm that the dilution process inherent in the plaque assay procedure successfully diluted the Zn concentration in the treated viral samples to a degree that was no longer detrimental to the HeLa cell monolayer. To establish that the titers observed from Zn-treated HRVs were not attributable to a decrease in HeLa cell metabolism due to any residual Zn present after dilution, identical Zn

dilutions, sans virus, were applied to previously infected HeLa monolayers. With no comparable decrease in titer seen at even the lowest Zn dilution compared to the Zn-free control infection, I was able to conclude that the dilution of the original Zn-treated sample effectively eliminated any significant detrimental impact on the cells which might lead to a misleading decrease in viral titer in Zn treated groups (Figure 3.1). In addition, HeLa cells were subjected to virus-free incubation in Zn-spiked PBS under identical inoculation conditions and then observed for morbidity under a standard tissue-culture microscope over a period of 5 days while being compared to their untreated counterparts at each time point (data not shown).

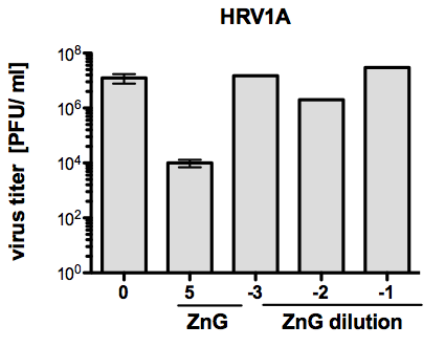

Figure 3.1 Effect of Residual Zn after dilution
Untreated HRV1A (0) was compared to HRV1A subjected to 5 mM ZnG (ZnG), and to the titer of untreated HRV1A wherein dilutions of 10mM ZnG were added post-infection to the agarose overlay for long-term exposure (ZnG dilutions). Virus titers were determined by a plaque assay on a monolayer of HeLa cells.

Using the procedure outlined in Diagram 3.1, I demonstrated that the addition of Zn gluconate (ZnG) or Zn chloride (ZnCl) to stocks of HRVs prior to infection of HeLa cells leads to a decrease in the virus titer as determined by plaque assay, that cannot be attributed to cell death due residual Zn (Figure 3.2). Viral infectivity was reduced greater than 90% by incubation with 2-10 mM ZnCl or ZnG, with 10mM ZnG consistently

rendering almost complete abrogation of viral infectivity (Figure 3.3). While both major and minor group HRVs were shown to experience inhibition with Zn treatment, I found that HRV1A demonstrated the most susceptibility. HRV16 required the greatest amount of Zn exposure to experience inhibition of all the HRVs tested. The reason for this discrepancy is unclear, but believed to be unrelated to the difference in cellular receptor used to gain entry, given that other major group HRVs demonstrated Zn sensitivity similar to that of HRV1A. After initial experimentation with ZnCl, Zn Aspartate and Zn Gluconate, I chose to focus on Zn gluconate (ZnG) due to its relationship with clinical studies (116) .

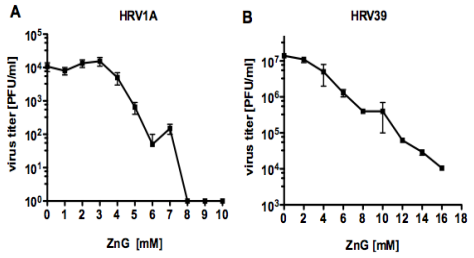

Figure 3.2 HRV1A and HRV39 ZnG dose-response curves
Stocks of HRV1A (A) or HRV39 (B) were incubated with increasing amounts of ZnG as indicated in the figure. Virus titers were determined by plaque assay on monolayers of HeLa cells.

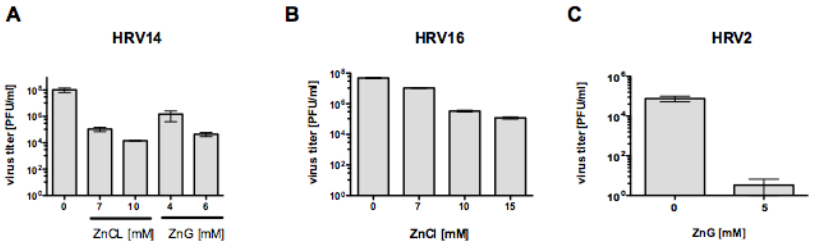

Figure 3.3 Effect of Zn 2+ on infectivity of HRVs 14, 16 & 2.
Stocks of HRV14 (A), HRV16 (B), and HRV2 (C) were incubated with different concentrations of ZnCl or ZnG [mM] as shown in the figures. Virus titers were determined by plaque assay on monolayers of HeLa cells.

Zn-based inhibition is not universal to picornaviruses

Given the conservation of both genome and capsid structure among picornavirses, I next sought to determine if this inhibition might be a universal, or a more broad characteristic of picornaviruses, especially given the previously cited mechanism of Zn-inhibition due to disruption of polyprotein processing which was not established to be specific to HRVs (4). Experimentation with Poliovirus, Coxsackie B3 virus (CVB3), Endomyocarditis virus (EMCV) and Enterovirus 68 (EV68), under identical circumstances with similar and greater quantities of ZnG and ZnCl, did not result in a significant decrease in viral titer (Figure 3.4, Figure 3.5 & Figure 3.6). While the limited scope of other picornaviruses tested does not lend the ability to conclusively determine that this inhibition is exclusive HRVs, it does imply that HRVS possess an attribute, not conserved across the picornavirus family, that makes them susceptible to damage by Zn+ cations. Given that multiple variations in capsid and genome structure exist among the picornaviruses tested, investigation into the possible discrepancy lending Zn+ resistance to each was beyond the scope of this work.

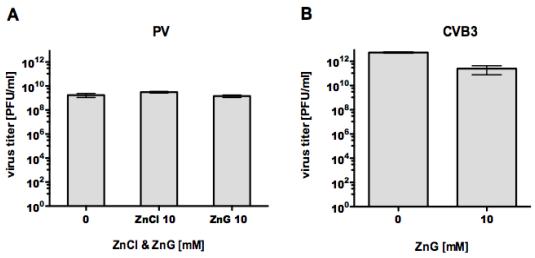

Figure 3.4 Effect of ZnG on poliovirus and coxsackievirus (CVB3)
Stocks of poliovirus (A) and Coxsackievirus B3 (B) were incubated with different concentrations of ZnCl or ZnG prior to infection of HeLa cells. Virus titers were determined by plaque assay on monolayers of HeLa cells.

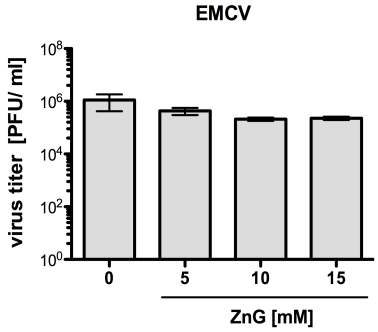

Figure 3.5 Effect of ZnG on the infectivity of EMCV
Stocks of EMCV were exposed to ZnG [mM] or left untreated (0) prior to infection of a HeLa cells. Virus titers were determined by plaque assay on monolayers of HeLa cells.

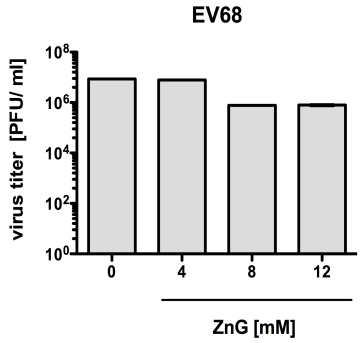

Figure 3.6 Effect of ZnG on the infectivity of EV68
Stocks of EV68 were exposed to ZnG [mM] or left untreated (0) prior to inoculation of a HeLa cells. Virus titers were determined by plaque assay on monolayers of HeLa cells

Zn-based inhibition of HRVs is not pH dependent

Given that HRVs hold the distinction of being one of the few acid-labile members of the picornavirus family, I next sought to investigate the possible relationship of this inhibition to that seen in low pH conditions, and to determine if this Zn-based inhibition of HRVs is pH-independent. Initial investigation into the pH lability of our HRV1A stocks revealed that a significant decrease in titer did not occur until the HRVs were exposed to a pH of 5 or lower, despite previous documentation which suggested that a pH of 6.2 or less is capable of rendering HRVs non-infectious (4). I then determined that the pH of ZnG-infused viral sera never breached a pH level lower than 6.4, even at ZnG concentrations nearly double of what was used to see complete HRV1A inhibition (Figure 3.7). Furthermore, even after a decrease in HRV1A titer is

seen after exposure to a pH of 5, an additional decline in viral titer is observed after ZnG exposure. To determine what, if any, of the inhibition seen with ZnG treatment was attributable to aberrations in the ph of the solution, I used zwitterionic (4-(2-hydroxyethly)-1-piperazineethanesulfonic acid) (HEPES)-buffered ZnG solutions which were confirmed to prevent even the slightest fluctuation of pH at the time of viral treatment (Figure 3.8). These experiments revealed that no appreciable portion of the inhibition seen is simply a consequence of the pH-lability of HRVs.

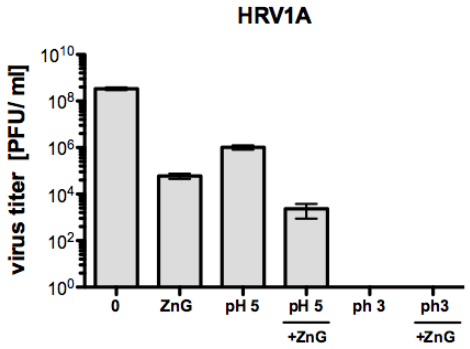

Figure 3.7 Effect of pH on HRV1A titer.
The titer of Untreated HRV1A (0) was compared to that of 8 mM ZnG treated HRV1A and HRV1A exposed to a pH of 5 or 3 with and without ZnG. Virus titers were determined by a plaque assay on a monolayer of HeLa cells.

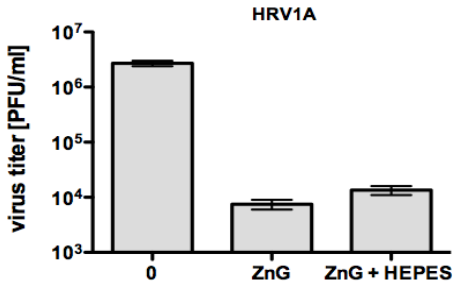

Figure 3.8 Effect of HEPES buffer on ZnG mediated inhibition
Stock of HRV1A were untreated, or incubated with 10 mM ZnG, or 10 mM ZnG plus an equimolar concentration of HEPES. Virus titers were determined by plaque assay on monolayers of HeLa cells.

Zn-based inhibition of HRVs occurs rapidly

Initial experimentation using the work-flow show in Diagram 3.1 involved incubation of HRVs with ZnG for periods of time in excess of 60 minutes as the possible parameters of Zn-based incubation were uncharacterized, and I had not yet deductively honed in on the optimal parameters necessary to observe this inhibition. Having determined the basal quantities and conditions necessary to see extracellular Zn-based inhibition of HRVs, I next sought to determine if the length of exposure had a significant impact on viral inhibition. Examining the results of viral incubation with ZnG for time periods of 5 minutes and 25 minutes revealed that the vast majority of viral inhibition occurs in 5 minutes or less, making longer incubation times unnecessary (Figure 3.9). While exploration of the degree of inhibition seen at even shorter time periods was technically difficult to perform, the profoundly non-linear relationship of duration of ZnG exposure and HRV inhibition seen in this assay suggests that inhibition of HRVs occurs very rapidly upon Zn+ exposure, a finding that is encouraging for therapeutic development.

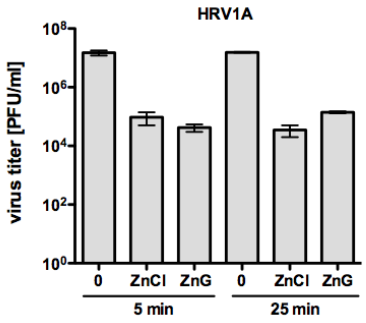

Figure 3.9 Effect of time on ZnG mediated inhibition
HRV1A was exposed to 4mM ZnG and 4mM ZnCl for two discrete time periods of 5 min and 25 min at 37C before infection of HeLa cells. Virus titers were determined by plaque assay on monolayers of HeLa cells.

Effect of temperature on Zn inhibition

37C represents the average ambient temperature in most regions of the human body, and is therefore physiologically relevant in the context of therapeutic pharmacokinetics. Furthermore, this temperature is amenable to HeLa cell growth and survival, and viral infections with picornaviruses are traditionally performed at this temperature. Consequently, 37C was chosen as the initial temperature parameter when exploring Zn-based HRV inhibition. However, it is noted that HRV incubation in plaque assays is optimized at 33-34 C. To determine if temperature played any significant role in Zn-based HRV inhibition, identical assays were performed (as in Diagram 3.1) with HRV incubation at 4C. While a slight decrease is observed in the 4C incubation group compared to the 37C incubation group, this effect is likely due to the well-established kinetic relationship of molecular movement and Brownian motion in aqueous solutions, and allowed me to conclude that Zn-based inhibition of HRVs was not significantly dependent upon temperature beyond what would normally be expected due to the universal laws of thermodynamics (Figure 3.10). The inability of 4C to substantially dampen this inhibition made further testing with at 33C or 34C unnecessary.

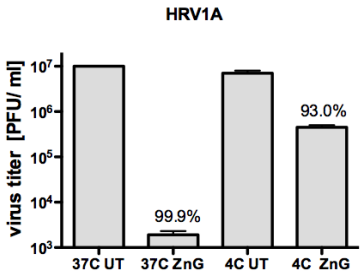

Figure 3.10 Effect of temperature on Zn inhibition
HRV1A was treated with 4mM ZnG and subjected to 30 min of incubation at 25C and 4C and the titers compared to that of untreated (UT) HRV1A. Virus titers were determined by plaque assays on monolayers of HeLa cells

2+ cations do not universally inhibit HRVs

With similar chemical reactivity, 2+ cations often behave analogously in biological systems. In some studies, substitution of a Cu ion for a Zn ion has no discernible effect on enzymatic function (111). Consequently, I sought to determine if the inhibition I was observing was a property exclusive to Zn+, or an effect that can be seen when HRVS are exposed to any 2+ cation in abundance. Mg+, Mn+ and Ca+ were investigated for possible Zn-inhibition given their favorable biochemical profile for low cytotoxicity in tissue culture cells and ready availability. Experiments using Mg2+, Mn2+ and Ca2+ in an experimental workflow identical to that seen with Zn inhibition (Diagram 3.1), and at similar and greater concentrations, resulted in no discernible inhibition of HRV1A. While issues of cytotoxicity and commercial availability prevented a more comprehensive investigation into the effects of all 2+ cations in nature, this result implies that a property characteristic, but perhaps not exclusive to Zn2+, is responsible for HRV inhibition, and that this inhibition is not due to the general presence of any 2+ cation in solution (Figure 3.11)

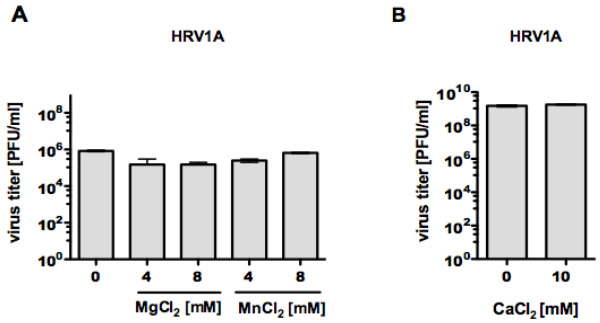

Figure 3.11 Effect of Mg2+, Mn2+, and Ca2+ on HRV
Stocks of HRV1A were incubated with different concentrations of MgCl2, MnCl2, or CaCl2 [mM] as shown in the figure before infection of HeLa cells. Virus titers were determined by plaque assay on monolayers of HeLa cells.

EDTA Chelation of Zinc

EDTA (Ethylenediaminetetraacetic acid) has a chemical profile that makes it a well-established Chelator of metal cations like Zn. Given this Zn-chelating property of EDTA and it's amenability to use in tissue culture, I sought to determine if EDTA chelation of Zn could prevent or reverse the Zn-based inhibition of HRV1A. Using both equimolar, 1:2 and 2:1 ratios of ZnG to EDTA, I found that exposure of Zn to EDTA could prevent downstream inhibition of HRV1A, presumably by chelating Zn out of solution, and thereby prevent its interaction with HRV1A (Diagram 3.2, Figure 3.12). However, addition of EDTA at identical and greater ratios to Zn-treated HRVs could not reverse the HRV1A inhibition that had already occurred. This finding demonstrates that either the Zn mediated damage to HRV1A particles is irreversible, or that the Zn - HRV1A interaction is stronger than the chemical pull of Zn - EDTA chelation (Diagram 3.3, Figure 3.13.). Identical results were also seen with HRV2 (Figure 3.14).

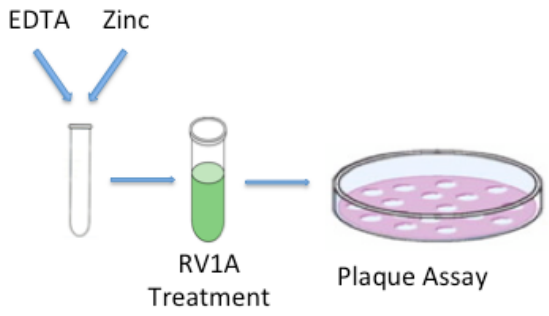

Diagram 3.2 EDTA mixed with Zinc
EDTA is mixed with Zn prior to treatment of an HRV in isolation. Virus titer is then determined by plaque assays on monolayers of HeLa cells

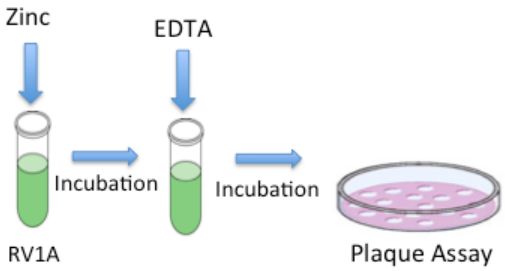

Diagram 3.3 Adding EDTA after Zn treatment
The HRV aliquot is treated sequentially with Zn and EDTA, with EDTA being added only after HRV incubation with Zn. After EDTA incubation, virus titer is determined by plaque assays on monolayers of HeLa cells

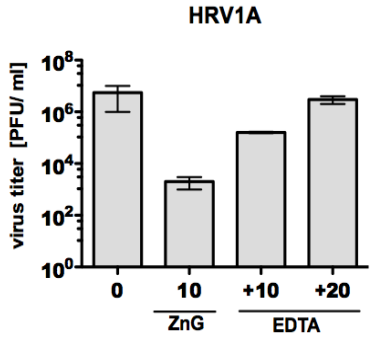

Figure 3.12 EDTA can prevent ZnG inhibition of HRV1A
Compared to the untreated control (0), the addition of 10 and 20 mM EDTA to 10mM ZnG solutions, prior to HRV treatment, can prevent the degree of inhibition seen with ZnG alone. Virus titers were determined by plaque assays on monolayers of HeLa cells

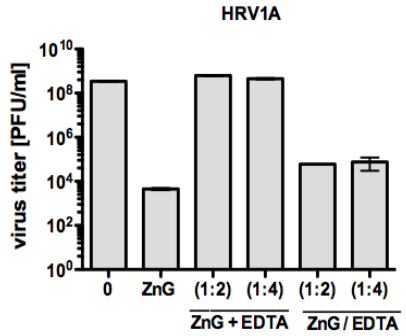

Figure 3.13 Effect of EDTA on inhibition of HRV1A infectivity by ZnG
Stocks of HRV1A were incubated with Zn, ZnG plus EDTA (ZnG + EDTA), or ZnG followed by EDTA (ZnG/EDTA) with ratios of 1:2 and 1:4 yielding nearly identical results. Virus titers were determined by plaque assay on monolayers of HeLa cells.

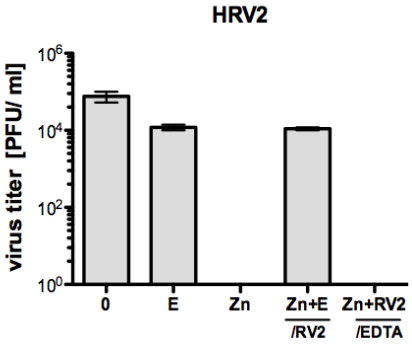

Figure 3.14 Effect of EDTA on inhibition of HRV2 infectivity by ZnG
Stocks of HRV2 were incubated with (20mM) EDTA alone (E), (10mM) ZnG alone (Zn), or a mixture of (1:2) ZnG and EDTA (Zn+E) before HRV2 infection (/RV2), and compared to an untreated HRV2 control (0), and the result of Zn exposure to HRV2 in isolation (Zn+RV2) followed by EDTA addition (/EDTA) at a ratio of 1:2. Virus titers were determined by plaque assays on monolayers of HeLa cells.

Zn-based inhibition does not involve the cell receptor interface

The virus-cell receptor interaction necessary to trigger endocytosis of virions is a crucial step in the viral infectious cycle, and impeding this interaction has been the goal of many antiviral therapeutics. To determine if Zn -based inhibition of HRV1A is dependent upon Zn activity at the virus-receptor interface, Infectious Center Plaque Assays (ICPAs) were designed. In the canonical ICPA assay, virus-infected cells are seeded upon an uninfected cell monolayer, leading to the formation of plaques after viral replication and consequential cell lysis of the initial virus-infected seed cell and infection of surrounding cells on the monolayer. Therefore, plaque formation in an ICPA assay is dependent upon successful viral attachment, internalization and replication in the first population of infected cells, the cells that are then seeded atop a secondary monolayer. Abrogation of any step in the viral replication cycle in the initially infected cell will result in a failure to form plaques after infection of the secondary cell monolayer, including initial viral attachment to the receptor of the seed cell. To determine if Zn-inhibitory activity is dependent upon the availability of the virus-receptor interface, I devised an ICPA assay wherein transient Zn exposure occurred after theoretical virus-cell receptor binding,

but before virus internalization. Due to prior studies on time dependence, I was able to conclude that non-cytotoxic transient exposure would be sufficient to inhibit HRV1A, if such inhibition can occur after receptor binding, without putting the health of the cells at risk. I hypothesized that a decrease in plaques after this transient ZnG treatment of virions already theoretically bound to the LDLR receptor would indicate that interaction with the virus-cell receptor interface was not required for Zn-based inhibition of HRV1A. If access to the virus-cell receptor interface was required for Zn+ inhibition, this would result in a failure of ZnG to reduce the number of plaques on the secondary cell monolayer when applied after receptor binding of the first population of cells has already occurred. Prevention of virion internalization was performed by maintaining the virus-cell inoculate at 4C, a condition previously shown to allow receptor binding while being highly inhibitory towards the endocytic process (4). Under these conditions, HRV1A virions can interact and bind their cognate receptor while remaining on the surface of the cell rather than being immediately internalized, and therefore plaques will only be seen on the secondary monolayer if the Zn treated HRV was able to remain infectious and attached to the receptor on its seeding cell from the first monolayer (Diagram 3.4). A poliovirus control, and plaque assays using the supernatants, were used to confirm that this experimental process was not too harsh, causing HRVs to detach from the cell receptor.

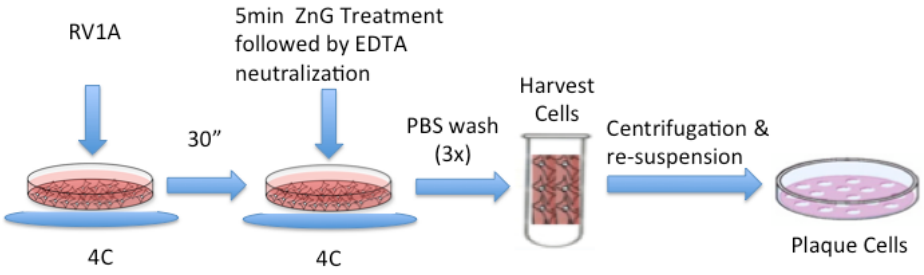

Diagram 3.4 The ICPA assay
A confluent monolayer of HeLa cells is inoculated with HRV and held at 4C for 30 minutes with gentle agitation. The monolayer is transiently exposed to ZnG for 5 min, followed by EDTA to chelate excess Zn. After undergoing washes, the cells are mechanically harvested, gently isolated via centrifugation and then re-suspended and diluted in PBS and plated upon another confluent monolayer of HeLa cells. Plaques resulting from this process are indicative of successful attachment of the HRV to its cellular receptor on the first monolayer of cells and sustained receptor attachment and infectivity of the HRV after Zn exposure.

The following figures are the result of an ICPA wherein a monolayer of HeLa cells was infected with HRV1A while held at 4C to prevent endocytosis. After sufficient incubation to allow viral binding of the receptor, ZnG was added at inhibitory concentrations for 5 min at 4C; a duration and temperature that I had previously shown to be amenable to Zn+ inhibition of HRVs (Figure 3.15). EDTA was then used to chelate excess Zn from solution, a procedure I had previously determined was not capable of reversing Zn-based HRV inhibition (Figure 3.13). Following transient ZnG exposure, this monolayer was harvested, gently washed and re-suspended in ZnG-free PBS, also at 4C. Serial dilutions of the resulting HRV1A- infected HeLa cells where then applied to a new HeLa cell monolayer and subjected to identical HRV1A plaquing conditions as shown in Diagram 3.1. The resulting decrease in plaques indicates that Zn- mediated inhibition of HRV1A was still able to occur after binding of HRV1A to the LDLR receptor. This finding demonstrates that disruption of the virus-cell receptor interaction is not topographically required for the mechanistic action of Zn-based HRV inhibition, as exclusion of Zn from this interface using pre-bound virions resulted in a decrease in plaque formation on parr

with that seen in traditional plaque assays. Therefore, the HRV1A - LDLR receptor interaction is not likely to play a mechanistic role in the Zn-based inhibition of HRV1A.

To eliminate the possibility that Zn treatment in this assay was simply removing infectious HRV1A from its receptor, thus preventing down-stream ICPA plaques, the Supernatants (SN) from the first inoculation were harvested and also assayed for infectivity and comparison to ICPA plaques (Figure 3.15). This assay was done with 1x and 2x comparative quantities to observe if the experimental assay was yielding logical results.

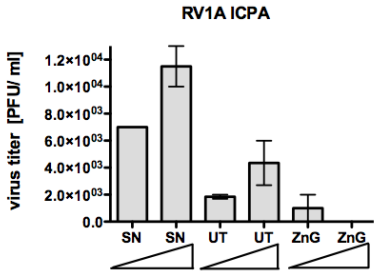

Figure 3.15 HRV1A ICPA assay
The initial inoculate from the first monolayer (SN), cells bound with untreated HRVIA (UT) and cells bound and then treated with 8mM ZnG (ZnG) were used in increasing quantities (1x, 2x) to infect the second HeLa cell monolayer of the ICPA assay. Virus titers were determined by an ICPA assay where plaques are the result of infection by a virus-harboring seed cell from the first infected monolayer.

To control for the efficacy of the ICPA assay, poliovirus (PV), which I previously demonstrated to be uninhibited by extracellular Zn compounds (Figure 3.4), was also subjected to an ICPA under identical conditions resulting in no decrease in ICPA plaque formation (Figure 3.16). Furthermore, experimentation with the centrifugal supernatants and coinciding increase in plaques seen with 2x addition of inoculate in both the control and treated groups bolsters the validity of this experimental procedure, indicating that the increase and decreases in plaque formation are not likely to be due to stochastic procedural side-effects of this assay.

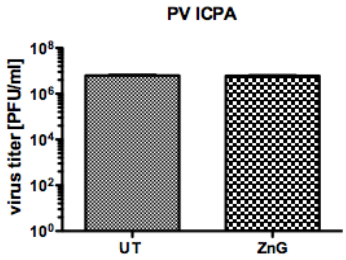

Figure 3.16 Poliovirus (PV) ICPA assay
Untreated (UT) and 8mM ZnG treated (ZnG) PV inoculated monolayers were seeded onto a second monolayer of HeLa cells. Virus titers were determined by an ICPA assay where plaques are the result of infection by a virus-harboring seed cells form the first infected monolayer

To lend credence to the literature-supported, assumption that holding the first HRV -inoculated HeLa cell monolayer at 4C effectively prevents endocytosis, the amount of infectious center plaques with and without ZnG treatment was observed as a function of time. HRV-inoculated monolayers were held at 4C for 20 and 40 min, and the amount of infectious center plaques in the second monolayer resulting from harvested cells, and the residual viral supernatant from the first infection, were observed. With no significant difference in plaque number seen between the 20 and 40 min 4C incubation groups, it is unlikely that duration of time at 4C is able to skew the results of this experiment to HRV1A internalization.

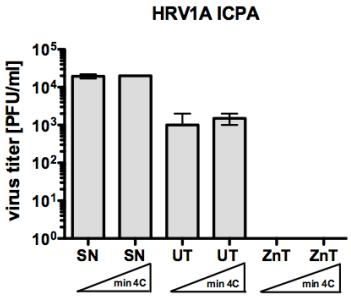

Figure 3.17 ICPA and 4C incubation
The supernatant from the initial monolayer inoculation (SN), untreated HRV1A- cells (UT) and 8mM ZnG treated HRV1A -cells (ZnT) were used to infect a second HeLa monolayer after 20 or 40 min incubation at 4C prior to Zn treatment. Virus titers were determined by an ICPA assay where plaques are the result of infection by a virus-harboring seed cell from the first infected monolayer.

Zn-treated HRV1A is still able to interact with the LDLR receptor

HRVs interact with their cellular receptor via contacts on the five-fold axis of the viral capsid which is composed of aggregates of viral capsid proteins that form the building blocks of the icosahedron (4). Therefore, binding of HRV1A to the LDLR receptor necessitates that the repeating protomer units of the viral capsid remain intact for the topography-dependent interaction with the cellular receptor to occur. To determine if Zn disrupts the non-covalent interaction that maintains these promoter units, I devised a competition-based assay wherein Zn-treated HRV1A was tested for the ability to interact with the LDLR receptor. Because Zn-treated HRV1A does not result in a successful infectious cycle and therefore does not result in plaque formation, I hypothesized that increasing quantities of Zn-treated HRV1A mixed in solution with a constant amount of untreated HRV1A would result in a decrease in total plaques observed if the Zn-treated HRV1A are capable of occupying the finite number LDLR binding sites within the HeLa cell monolayer (Diagram 3.5). EDTA was used to remove excess Zn from solution to prevent inactivation of the untreated HRV1A after my prior experimentation demonstrated it's ability to chelate excess Zn without reversing inhibition (Figure 3.18).

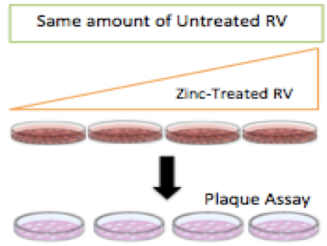

Diagram 3.5 The competition assay
Holding the amount of untreated, infectious HRV capable of plaques constant, uninfectious Zn treated HRV is titrated into aliquots of untreated HRV after chelation of excess Zn using EDTA. The untreated and Zn-treated virus mixture is then used to inoculate a confluent monolayer of HeLa cells at an MOI > 15. Plaques were visualized after application of a semi-solid agarose overlay, incubation, cell fixation and crystal violet staining. A decrease in plaques is indicative of un-infectious HRV competing with infectious HRV for receptor binding sites.

The results of this assay demonstrated that Zn-treated HRV1A is still able to interact with the LDLR receptor, leading to a decrease in the number of untreated, infectious HRV1A that can bind a receptor to gain cell entry, and hence a decrease in the number of plaques formed as increasing amounts of Zn-treated HRV1A are titrated into the mixture. This finding implies that Zn does not sufficiently disrupt the viral capsid, specifically at the 5-fold axis, allowing Zn inactivated HRV1A to occupy the limited supply of LDLR binding sites, despite its inability to initiate a successful infectious cycle.

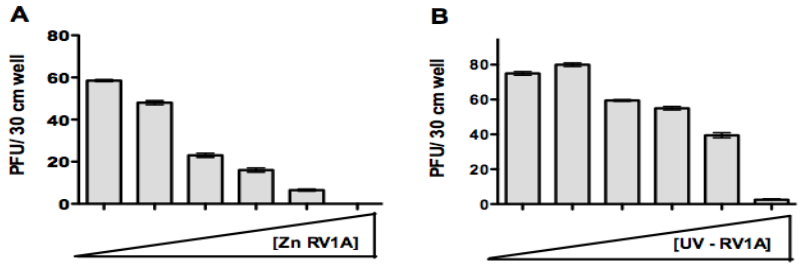

Figure 3.18 Effect of Zn+-treated HRV on virus binding to cells
Increasing amounts of Zn-inactivated HRV1A (A) or UV-inactivated HRV1A (B) were mixed with a fixed amount of untreated HRV1A and given access to bind to the LDLR receptor. After washing, the number of bound virus particles was determined by plaque assay on monolayers of HeLa cells.

To control for the validity of this assay, UV-inactivated HRV1A was used as a control. UV-light damage to viral RNA, and the resulting abrogation of infectivity is well documented (4). This viral RNA damage occurs while presumably leaving the viral capsid largely intact. After determining the conditions under which 100% inactivation of HRV1A could be achieved (Figure 3.19), this process was used to make an inactivated HRV1A control that demonstrated the efficacy of this assay. The possible variation in competitive ability of some UV-treated HRV1A aliquots is presumably due to the possible damage to the viral capsid proteins that may occur at UV-light dosages high enough to completely abrogate the infectivity of the viral population.

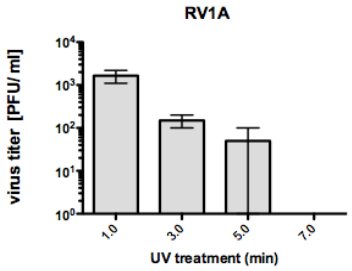

Figure 3.19 Effect of UV-treatment on HRV1A infectivity
Stocks of HRV1A were spread into a thin-aqueous layer on a 10cm petri plate and subjected to increasing amounts of UV light. Virus titer was determined by plaque assay on a monolayer of HeLa cells.

HRV1A capsid proteins do not appear altered after Zn

Without heat and reducing agents to completely eliminate protein to protein interaction and tertiary structure, native gels allow for the visualization and characterization of protein complexes as they migrate through a porous matrix. The metastability of the viral capsid necessitates the use of non-ionic bonds to aggregate the individual viral proteins into repeating protomers that comprise the complete capsid (Diagram 3.6). To investigate the stability of these non-ionic associations between viral capsid proteins and protomers, Zn treated and untreated

sucrose gradient purified HRV1A were subjected to native protein gel analysis using a variety of conditions in an attempt to preserve natural capsid protein interactions. Using both coomassie-blue and silver stain, the migration of the viral capsid proteins and their interaction after ZnG treatment could be visualized. While the unavailability of HRV1A - specific antibodies precluded the positive identification of each protein complex, the seemingly identical migration of viral capsid proteins in the untreated and ZnG treated groups as visualized with a sensitive silver-staining procedure, suggests that Zn+ treatment does not profoundly disrupt the interaction of viral capsid proteins at a level that can be observed using native gel electrophoresis. This result bolsters the conclusion of the Zn-treated HRV1A competition assay that indicates that the Zn-treated capsid must remain intact, at least at the protomer level, to successfully compete with untreated HRV1A for LDLR binding sites (Figure 3.20) Because smaller molecular weight products cannot be seen in the Zn-treated lanes as one would expect if polypeptide interactions were being disrupted to result in smaller aggregates, the dampening of signal in Zn-treated lanes is most likely due to the interaction of Zn in the sample with the Silver stain. Notably, while not shown here, the coomassie stained gels did not exhibit this decrease in band darkness in the Zn-treated lanes, supporting the notoin that the band signal is predicated on the interaction of Zn in the sample with the staining agent. While less sensitive, the coomassie stained gels also revealed no difference in band pattern and migration between the Zn treated and untreated groups.

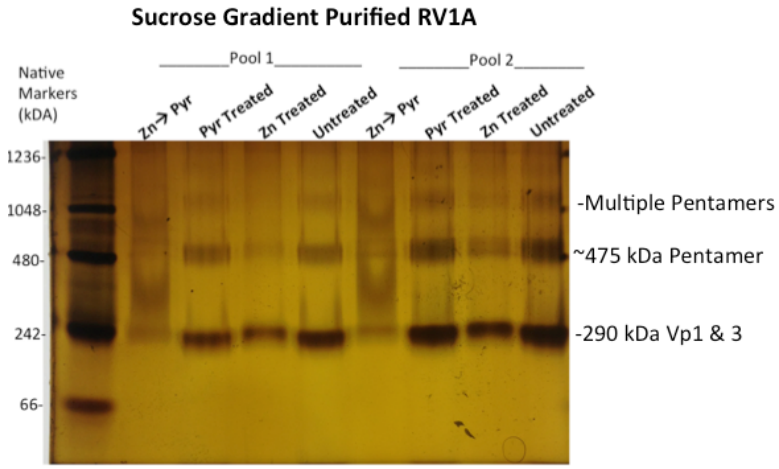

Figure 3.20 HRV1A native gel after Zn treatment.
Sucrose Gradient HRV1A from two different, but theoretically equivalent fractions, were subjected to Native Gel electrophoresis for the conditions given (12% Native PAGE, 4C, 150V, 1hr) with and without 8mM ZnCl (Zn) treatment, and with Pyrithione (Pyr) treatment alone or in conjunction with ZnG (Zn —> Pyr). A Native gel marker on the left most lane gives an approximate indication of protein complex size. A non-specific Silver Staining protocol was used to visualize all proteins, viral and non-viral, in the original sample. The viral structure whose identity is postulated (but not confirmed) for each band is given at the far right.

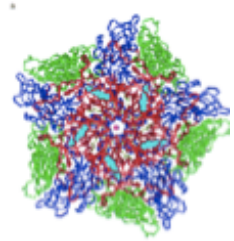

Diagram 3.6 The 475 kDa Pentamer of HRV1A
The HRV1A capsid is composed of 4 proteins whose formation of repeating units results in the formation of the holistic viral capsid. A principle unit of this structure on which receptor-binding interactions takes place is the viral protomer, composed of 5 of each of the viral capsid proteins. VP4 resides internal to the capsid structure and is not shown in the diagram.

Primary HRV1A viral proteins are not altered by Zn treatment

Previous studies investigating an anti-picornaviral mechanism of Zn activity observed disruption and possibly modulation of the picornaviral polyprotein in the presence of high intracellular concentrations of Zn. To determine if Zn might have a likewise detrimental effect on the capsid

proteins that originated from the polyprotein, I sought to visualize viral capsid proteins with and without Zn treatment to rule out possible Zn- mitigated damage that might cause visible cleavage or dissolution. Denaturing PAGE analysis with coomassie-blue (not shown) and silver-staining of sucrose gradient purified untreated and ZnG treated HRV1A revealed that untreated and ZnG treated HRV1A capsid proteins can be found to sediment in the same sucrose gradient fractions, bolstering prior observations which indicate that degradation of viral proteins is not the mechanism of extracellular Zn inhibition of HRVs. Without the availability of an HRV1A-specific antibody for each viral protein, the positive identification of each viral protein could not be made. However, the totality of the uniform lack of change seen between the untreated and Zn treated samples is visible.

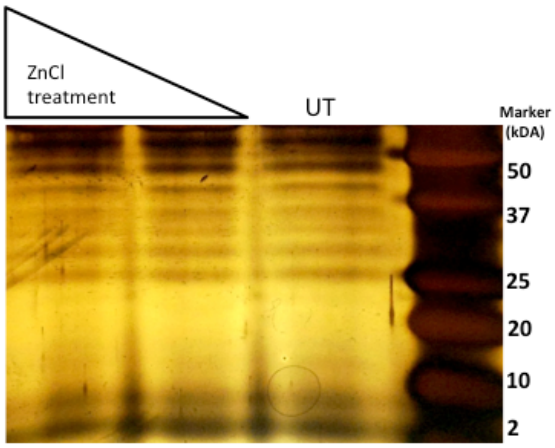

Figure 3.21 SDS-PAGE does not reveal Zn-mediated capsid protein degradation.
Untreated (U) and 5mM and 10mM Zn Chloride treated (ZnCl) aliquots of sucrose gradient purified HRV1A were subjected to 12% SDS PAGE at approximate 90-120V for 1-1.5 hrs. A standard protein size marker is shown in the right-most lane of the figure.
(VP1 = 32kDA, VP2 = 29kDA, VP3 = 26 kDA , VP4 = 7.5 kDA, Protomer = 94.5)

The presence of sucrose can prevent Zn-mediated inhibition of HRVIA

While experimenting with sucrose gradient purified HRV1A, a decrease in the degree inhibition was observed when direct aliquots of sucrose gradient purified HRV1A were subjected to Zn treatment. However, after dialysis to remove the sucrose from the purified viral fraction, Zn sensitivity was restored (data not shown). Consultation with literature implied that the chemical make-up of sucrose could lend it the ability to chelate 2+ cations . This potential finding is interesting given the historical use of sucrose and related sugars used in Zn lozenges in an effort to make them more palatable, and thereby increase trial enrollee compliance. Directly assaying non-sucrose exposed stocks of HRV1A sera for Zn sensitivity in conjunction with sucrose-purified HRV1A in which the sucrose had not been dialyzed from the sample, reinforced this finding. A lower titer sucrose gradient purified fraction of HRV1A was used for this investigation in an effort to conserve higher-titer sucrose gradient purified fractions for more critical experiments that necessitated them (Figure 3.22).

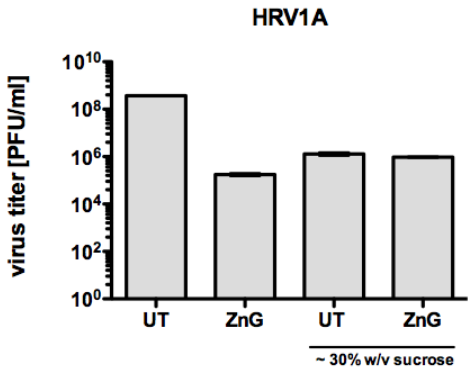

Figure 3.23 Sucrose dampens Zn inhibition of HRV1A.
Untreated (UT) and Zn Gluconate treated (ZnG) treated HRV1A with without the presence of approximate 30% sucrose were compared. Viral titers were determined by plaque assay on a confluent monolayer of HeLa cells.

RNA analysis of Zn-treated HRV1A

The HRV infectious cycle necessitates that the viral RNA genome be delivered to the cell cytoplasm intact. Prior studies with cesium have indicated that the capsid structure of HRVs is more permeable than that of PV (4). I sought to determine if Zn treatment resulted in damage to the HRV1A genome through possible Zn-penetration of the viral capsid structure, or Zn mediated partial-dissolution of the capsid structure which might make viral RNA susceptible to Rnases. Aliquots of centrifugation-purified HRV1A were subjected to Zn treatment, followed by incubation with Rnase 1 whose activity is not hindered by the presence of metal cations. RNA was isolated via Trizol extraction and resuspended in Rnase-free water prior to inspection. The amount of untreated RNA detected decreased dramatically after Rnase 1 exposure. While the total amount of RNA in the Zn-treated group was significantly less than that seen in the untreated Rnase-free fraction, the decrease in RNA present after Rnase1 exposure did not vary as greatly for the Zn-treated groups (Figure 3.23). This experiment revealed that less total RNA can be

found after Zn-treatment, and that remaining RNA might be less susceptible to the activity of RNAse 1. Alternatively, while RNAse 1 is alleged to be impervious to the presence of metal cations, it is possible that the Zn in solution hindered its catalytic activity despite reassurances to the contrary by the manufacturer.

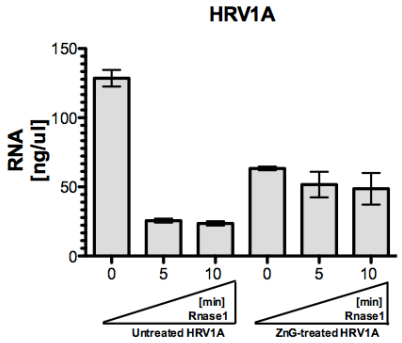

Figure 3.23 Total RNA after Zn Treatment and effect of exposure to Rnase1.
100 ul aliquots of untreated and 10 mM ZnG treated HRV1A was exposed to 100 units of Rnase for 5 to 10 minutes prior to Trizol extraction and examination using a spectrophotometer to assay for total RNA.

Decreased quantities of HRV1A RNA after Zn treatment

Centrifugation of virus particles on a sucrose gradient, wherein they settle according to their buoyant density, is a common means of purification of virus particles, separating the virions from other components of the sera milieu. During centrifugation, HRV1A characteristically sediments in sucrose gradient fractions that correspond to approximately 30-35% sucrose (w/v). Through careful fractionation of the sucrose gradient column, aliquots of highly purified and concentrated virus can be obtained. The presence and amount of infectious virus in each fraction can be determined by plaque assay. Sucrose gradient centrifugation of untreated and Zn-treated HRV1A, followed by a downstream plaque assay to determine the amount of virus in each fraction, or every

other fraction, was performed. The resulting curve demonstrated the fractions with peak infectivity, as well as the predictable absence of infectious virus in abundance in the corresponding Zn-treated sucrose fractions. While initially just used as a method to obtain purified virus for other experiments, to probe for the presence of viral RNA in these fractions, 250 ul aliquots from each fraction were subjected to Trizol extraction, reverse transcription using random hexamers and then PCR using HRV1A-specific primers . The resulting PCR product was visualized on an ethidium bromide (ETBR) agarose gel (Figure 3.24 B). This process was performed on the fractions of peak infectivity of the both the untreated and Zn-treated sucrose gradient centrifugation-purified sample sets, as well as every other fraction in higher and lower fractions in the Zn treated group to probe for possible sedimentation differences. Subject to identical extraction and PCR conditions, this result indicates that while less HRV1A genomic RNA is detected, the RNA is present in the same fractions as that seen with untreated HRV1A RNA. This nearly identical RNA sedimentation profile implies that Zn-treated RNA sediments in same fractions as RNA whose capsid structure had not been subject to Zn-onslaught. Given the relationship between molecular weight of a structure and its sedimentation profile, this result implies that the remaining RNA detected was within or associated with a whole or partial viral capsid structure, like that of untreated RNA. This result bolsters the notion that the viral capsid structure is not severely disrupted by Zn exposure and that Zn-treatment facilitates the degradation of viral RNA. However, it is also possible that the vestige of RNA observed here is merely that belonging to virus particles that were not severely impacted by Zn treatment due to insufficient exposure.

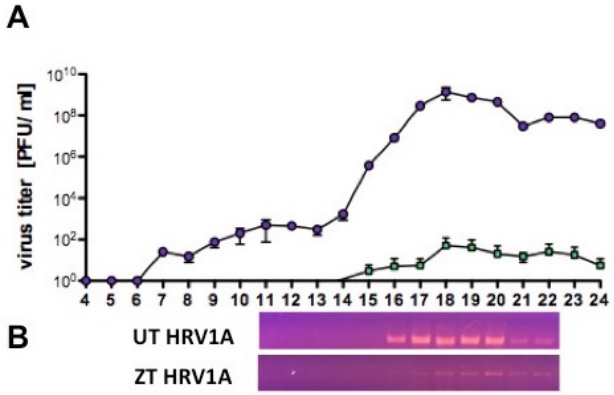

Figure 3.24 Sucrose gradient analysis of HRV after Zn+ treatment
Approximately 2 x 10 ^8 PFU of HRV1A were either untreated, or incubated with 10 mM ZnG, and then fractionated on a 5-45% (w/v) sucrose gradient. Infectivity in each fraction was determined by plaque assay on monolayers of HeLa cells. The gradient shown in (A) is from untreated HRV1A (purple) and Zn-treated HRVIA (green). Viral RNA in sucrose gradient fractions was assayed by gel electrophoresis (B) after reverse-transcription and PCR with HRV1A-specific primers. UT, untreated; ZT, ZnG treated. Titers in each fraction were determined by plaque assay on monolayers of Hela cells.

Northern blot visualization of HRV1A RNA

To visualize the impact of ZnG treatment on HRV1A genomic RNA, Northern Blot analysis using an HRV1A - specific digoxigenin probe was conducted. The HRV1A digoxigenin probe was synthesized using combinations of the HRV1A- primers and random hexamers in combination with an HRV1A DNA template. After subjection to agarose gel electrophoresis, the viral and control RNA synthesized using T7 polymerase and the pACYC177-Xmal-T7-WT-RV1A-Xho1 plasmid were transferred onto a positively charged membrane and probed for the presence of viral RNA. In addition to disappearance of full-length HRV1A genomic RNA as compared to the synthetic control (Figure 3.25), northern blot analysis using different conditions and probes of different lengths consistently revealed that ZnG treated HRV1A resulted in lower

molecular weight RNA binding targets, and a visible general decrease in signal. Furthermore, extensive Rnase inhibition prior to Zn treatment or no treatment, demonstrates that his degradation cannot be attributable to possible Rnases that might have contaminated the experimental process despite usage of DepC water and cleansing of the workspace and experimental tools with RNAse away (Figure 2.1.15.2). Given the differential migration pattern of ZnG treated HRV1A RNA, or its absence all together, the aggregate result of these northern blots suggests that ZnG treatment of HRV1A results in degradation of viral genomic RNA (Figure 3.26 and 3.27).

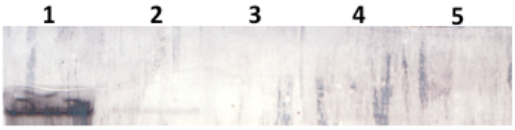

Figure 3.25 Northern blot hybridization of full-length genome.
Approximately 1 x 10 ^7 PFU of HRV1A were either untreated (2) or ZnG treated (5) and compared to a full-length synthetic RNA clone generated using T7 polymerase and PACY1A plasmid (1) after being probed with a ~ 500bp HRV1A specific digoxigenin labeled probe.

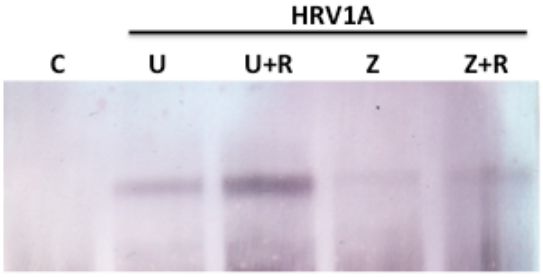

Figure 3.26 Northern blot hybridization analysis of RNA (1)
Approximately 4 x 10^6 PFU of HRV1A were either untreated, or incubated with 10 mM ZnG, and then viral RNA was extracted, fractionated by agarose gel electrophoresis, and transferred to a membrane for hybridization with a HRV specific DNA probe. C, cellular RNA; U, viral RNA from untreated sample; U+R, viral RNA from untreated sample in the presence of RNAsin; Z, viral RNA from ZnG treated sample; Z+R, viral RNA from ZnG treated sample in the presence of RNAsin.

Figure 3.27 Northern blot hybridization of RNA (2)
Approximately 6 x 10 ^5 PFU or HRV1A were treated with 10mM Zn (ZT) or left untreated (UT), and then the viral RNA was extracted using Trizol, fractionated by gel electrophoresis and then transferred to a nylon membrane and probed using a digoxigenin probe made with random hexamers using the an almost full-length amplicon of HRV1A derived from the pACYC177-Xmal-T7-WT-RV1A-Xho1 plasmid.

Zn resistant HRV1A phenotype

To determine the attributes of HRV1A that make it susceptible to inhibition with Zn compounds, I decided to cultivate and characterize Zn-resistant HRV1A for comparison. Due to the lack of a proof-reading mechanism, the RNA polymerase of picornaviruses is highly error prone, producing considerable genetic diversity within the populations (75). This creation of genetic heterogeneity within the HRV1A population results in both a high probability of drug-resistant HRV1A selection, and also necessitates the isolation of a single progenitor virion to prevent heterogeneity within the viral population that might make the establishment of a consensus sequence that is representative of the "average' genome impossible. While single-plaque purification of surviving HRV1A after ZnG treatment was unsuccessful due to the insufficient number of virus particles for downstream passages and sequencing, an analogous scheme for mutant isolation was devised which proved to be more successful at isolation of Zn-resistant mutants in quantities amenable to downstream passages. A marked decrease in viral

fitness was evident with sustained lower-titer in Zn-resistant populations as well as a variable plaque phenotype that features mostly small, anemic plaques compared to wild-type HRV1A after an equivalent incubation period (Figure 3.28).

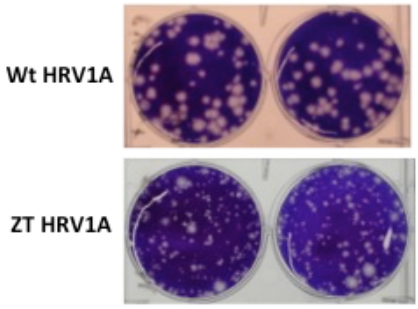

Figure 3.28 Plaque phenotype of Zn-resistant HRV.
Plaques formed by wild type HRV1A (A) or Zn-Resistant HRV1A (B) after 96 hr on confluent monolayers of HeLa cells.

Zn-resistant HRV1A isolation

As an alternative to the single-plaque isolation strategy, an alternative process illustrated in Diagram 3.6 was devised which relied on serial dilutions and CPE detection on a massive scale. In doing so, 6 HRV1A mutants were identified that demonstrated an increased resistance to inhibition by Zn compared to their wild-type counterparts, and existed in sufficient quantities that made them amenable to downstream sequencing analysis as well as having a strong consensus sequence that could be used for genotyping. However, the titers of these viral stocks were typically ~100 fold lower or more than wild type virus and retained a small plaque phenotype despite numerous passages. These observations, coupled with the general scarcity of mutant populations after ZnG treatment, emphasizes that resistance to Zn+ decreases the overall fitness of HRV1A.

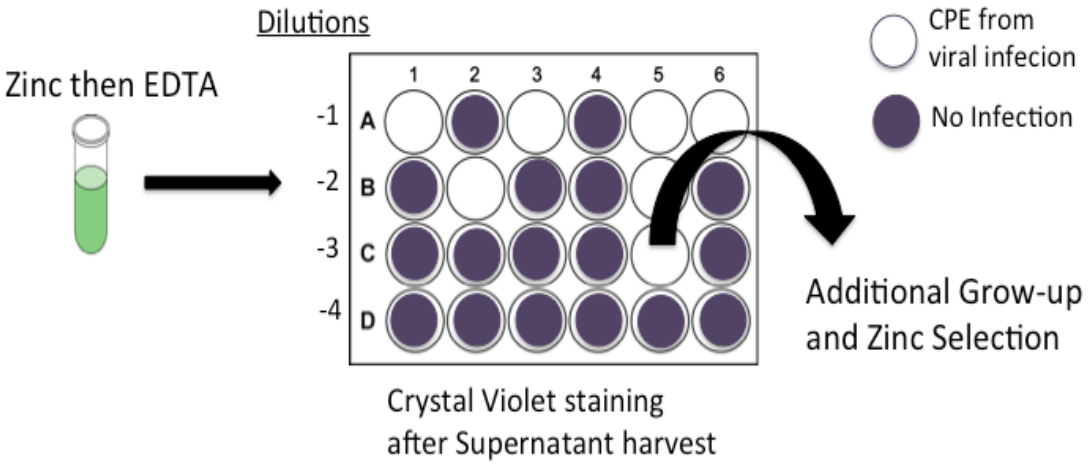

Diagram 3.6 Isolation of Zn-resistant HRV1A
Samples of Zn treated HRV1A were treated with EDTA to removed excess Zn, serially diluted and used to inoculate confluent monolayers of HeLa cells in a 24 well plate format. After 4-5 days of incubation, the supernatant of each well was harvested and each of the 24 wells were fixed and then stained with crystal violet to visualize the HeLa monolayer and detect viral CPE. The supernatant from wells in dilution sets wherein little to no CPE occurred, and could therefore plausibly be from a single virus progenitor, underwent serial passages of HeLa grow-up and Zn - treatment.

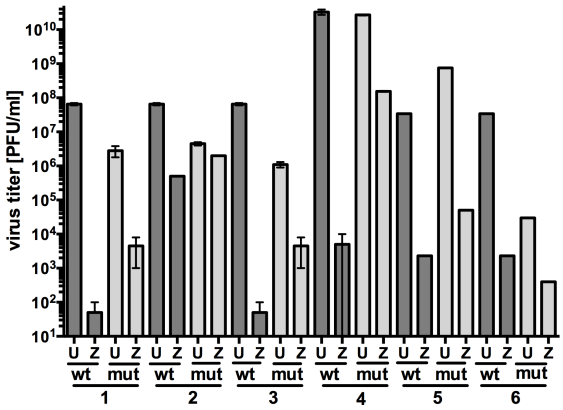

Figure 3.29 HRV1A mutants resistant to inhibition by Zn.
Stocks of wild type HRV1 (wt) or six mutants selected for resistance to Zn+ (mut 1-6) were incubated with ZnG (Z). All mutant viruses were incubated with 10 mM ZnG except for #2 which was incubated with 2 mM ZnG. Virus titers were determined by plaque assay on monolayers of HeLa cells.

Mutations found in Zn-resistant isolates

The genetic analysis of the HRV2A Zn-resistant isolates was performed using primers I designed for HRV1A. The genome of each of the 6 mutants was analyzed after RNA extraction and PCR amplification of each region. Additional mutants that demonstrated Zn-resistant were similarly isolated, but a homogenous consensus genome sequences could not be generated. Alignment of genome sequences with that of wild-type, Zn+-susceptible HRV1A revealed 3 distinct mutations in multiple isolates, both alone and in combination (Figure 3.31). These mutations were not seen in any of the wild-type control isolates that were sequenced. All three point mutations lead to amino acid changes in viral capsid protein VP1. Two changes, at residues 87 and 91, are located on the B-C loop, which forms a major antigenic region on the capsid surface. In addition, a change was identified in some isolates from Asn to Lys at residue 29 of VP1, which is located within the capsid interior Figure 3.30.

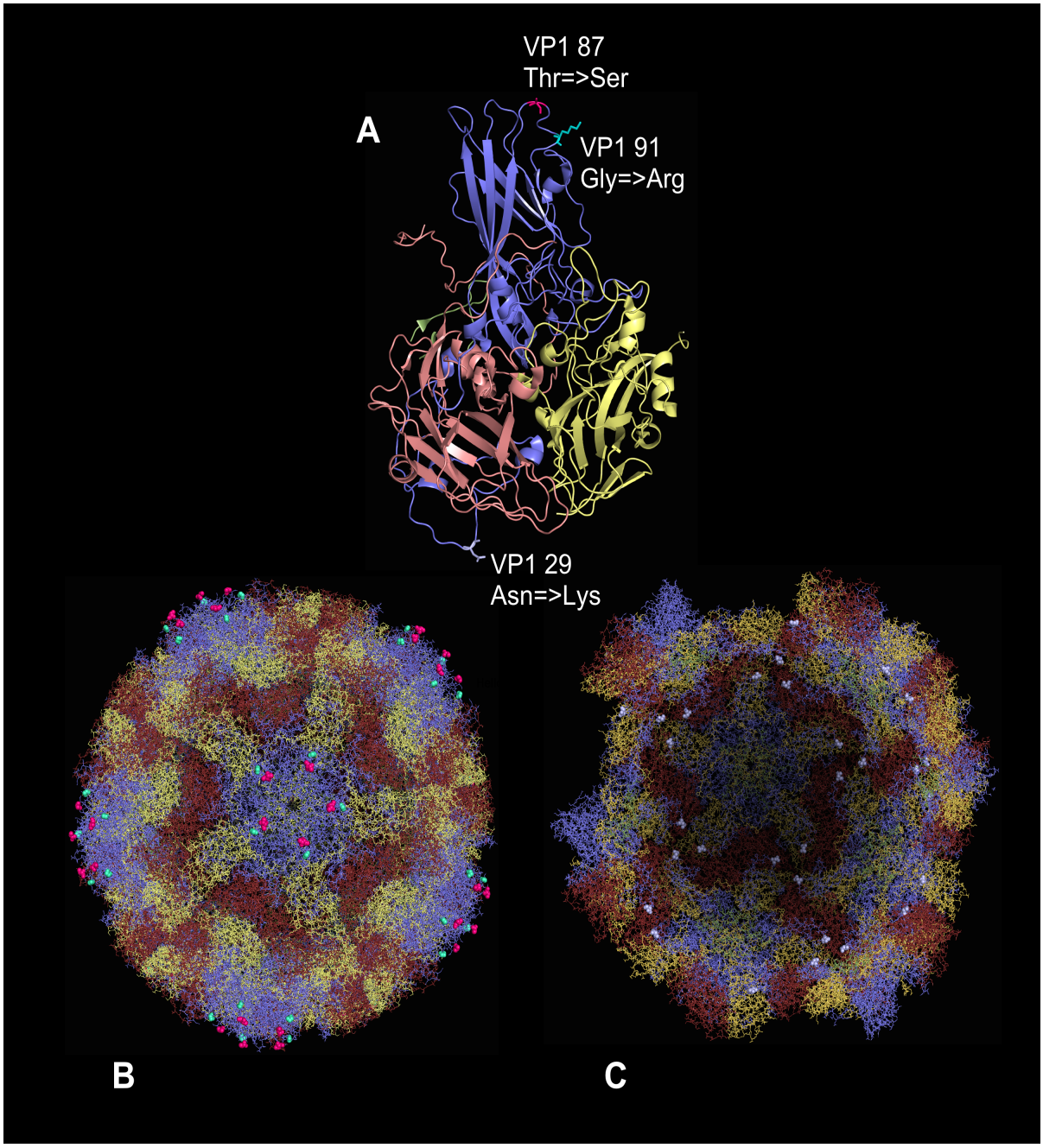

Figure 3.30 Mutations found in Zn-resistant HRV1A
Amino acid changes at VP1 residues 29, 87, and 91 are shown in the context of a protomer (A), on the surface of the full capsid (B), and on the capsid interior (C). Color key: VP1 (blue), VP2 (yellow), VP3 (red), VP4 (green). On the capsid surface amino acid 87 is shown in hot pink spheres, and amino acid 91 is colored cyan. On the capsid interior amino acid 29 is shown as grey spheres. Images were produced using MacPymol with PDB file 1r1a.pdb. Full and half capsid coordinates are from VIPERdb (viperdb.scripps.edu).

Virus	VP1 Residue 29	VP1 Residue 87	VP1 Residue 91
wiltype	**Asn**	**Thr**	**Gly**
mutant 1	*Lys*	Thr	*Arg*
mutant 2	*Lys*	Thr	*Arg*
mutant 3	Asn	*Ser*	Gly
mutant 4	Asn	*Ser*	*Arg*
mutant 5	*Lys*	*Ser*	Gly
mutant 6	Asn	Thr	*Arg*

Figure 3.31 Summation of Zn-resistant mutant findings
Residues diverging from that seen in wild-type HRV1A are demarked with a gray background.

Cloning and transfection of mutant HRV1A

Using the pACY177-Xmal-T7-WT-RV1A plasmid (Diagram 3.9), site directed mutagenesis was performed using mutagenesis sequencing primers corresponding to the VP1 region (see Materials and Methods). A diagram of the cloning scheme is shown below (Diagram 3.7 and Diagram 3.8). Confirmation of the singular successful incorporation of each mutation was determined through sequencing. Using T7 polymerase, full length RNA transcripts of each mutant virus clone were generated and used for transfection using 3 different lipofectamine-based procedures and H1- HeLa cells. While confirmation of successful transfection of each clone was performed, and some CPE resulted from passages of these viruses, their titer remained critically low, making downstream characterization impossible. Removal of Zn pressure did not result in revertants with greater titer even after 8 passages in H1 HeLa cells.

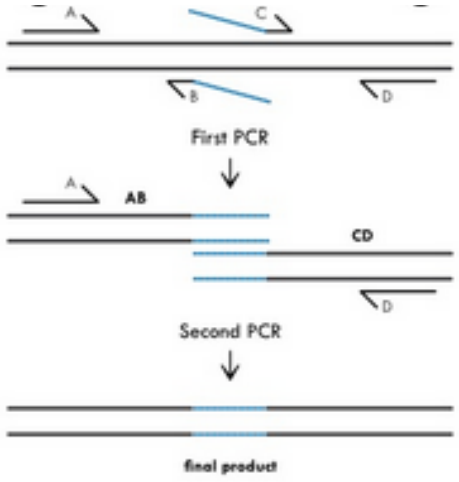

Diagram 3.7 Cloning strategy
Each of the three mutations discovered in Zn-resistant isolates were separately introduced into the pACY177-Xmal-T7-WT-RV1A plasmid using a procedure that utilized 4 primers, 2 of which were custom-designed to contain the point mutation desired. The primers used for this process and a detailed procedural description can be found in the material and methods section.

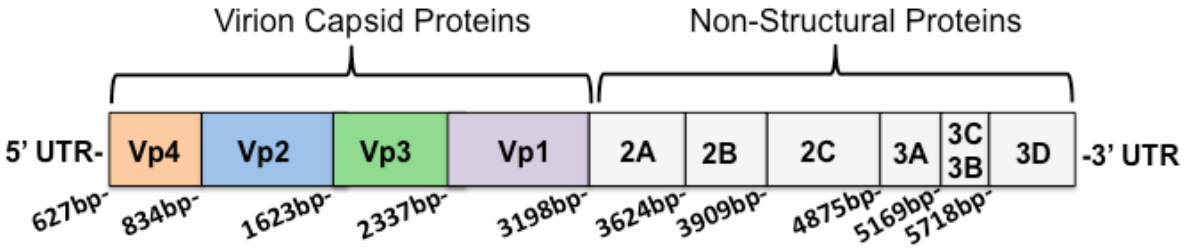

Primer set	Primer set	Primer set	Primer set	Primer set	Primer set	Primer set	Primer set	Primer set	Primer set	Primer set	Primer set	Primer set	Primer set	Primer set
1	2	3	4	5	6	7	8	9	10	11	12	13	14	15
1-510	404 -1013	939 -1475	1479 -1943	1879-2588	2406-2975	2927- 3536	3504- 4026	3952-4526	4459-5000	4891-5578	5473- 6030	5974-6548	6443-7068	6973- 7137

Diagram 3.8 Overlapping HRV1A primers
Overlapping primers, each yielding a 500-600 amplicon were designed to fully-cover the HRV1A genome. The Tm of each primer was kept in a range that allow them to be used interchangeable with other forward and reverse primers

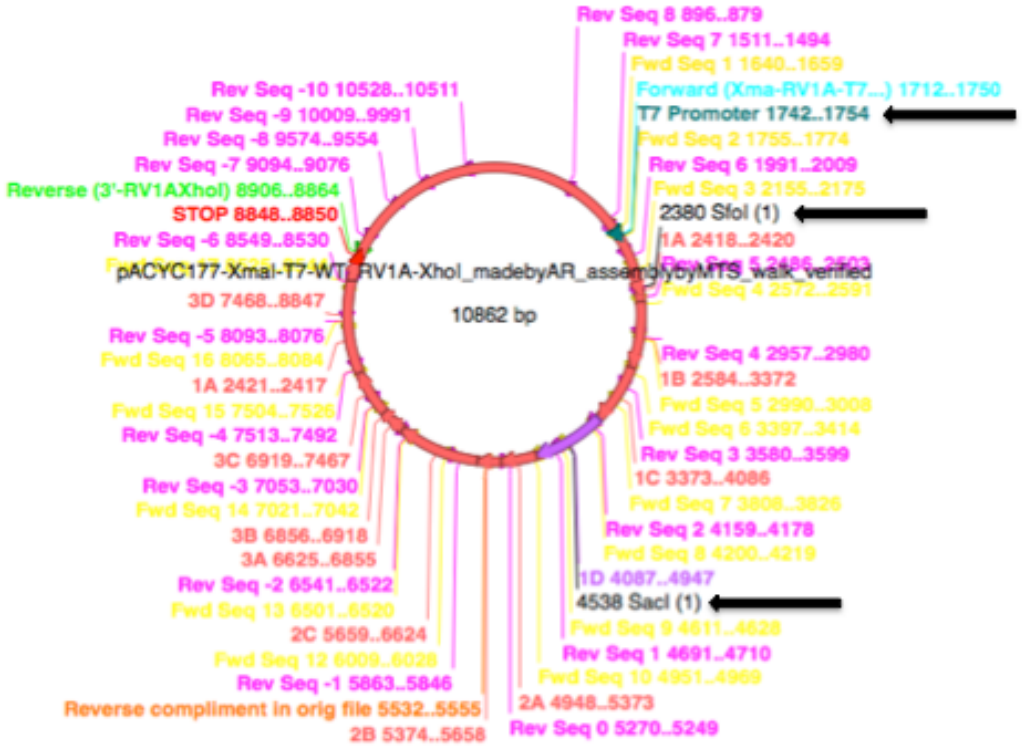

Diagram 3.9 The pACYC177-Xmal-T7-WT-RV1A-Xho1 plasmid
The pACYC177-Xmal-T7-WT-RV1A-Xho1 plasmid contains the full-length HRV1A genome as well as other features such as a T7 promoter site for full-length viral RNA synthesis. This and additional relevant features, such as the cut-sites for Sfo1 and Sac, which were used to excise and scrutinize the VP1 regions, and are de-marked by black arrows.

CHAPTER 4: PYRITHIONE, HINOKITIOL & PDTC INHIBITION OF HRV

Previous studies with picornaviruses and ionophores hinokital (HK) and pyrithione (PT) focused upon their potential antiviral utility in an intracellular environment. These studies found that in conjunction with Zn, these ionophores could impede intracellular steps in the picornaviral infectious cycle through inhibition of the picornaviral 2A protease and polyprotein processing. They further reported that "early stages" of virus infection were unaffected by these compounds. Using an approach analogous to that used with Zn compounds alone, I sought to determine the outcome of extracellular exposure of HRVs to these ionophores with and without the addition of Zn.

Extracellular exposure of HRVs to PT & HK with Zn

Extracellular exposure to HK or PT alone, at concentrations where intracellular inhibition was documented and at which extracellular Zn exposure is very inhibitory, did not decrease the titer of HRV1A . Interestingly, addition of these compounds in conjunction with ZnG lead to significant decreases in HRV1A titer, even when the amount of ZnG added was below the typical threshold wherein dramatic inhibition with Zn alone is observed (117). The decrease seen with HK and ZnG was more dramatic than that of PT and ZnG, however, the addition of Hinokital to viral serum led to the immediate formation of a dense visible precipitate whose exact chemical or biological composition could not be determined (Figure 4.1). Dissolution of HK in solutions with DMSO did not affect downstream precipitate formation. Concern that this precipitate may be preventing HRV1A infection by simply occluding receptor binding or aggregating viral particles led me to discontinue this line of experimentation as I feared that such a potentially drastically different mechanism of inhibition was beyond the scope of my research.

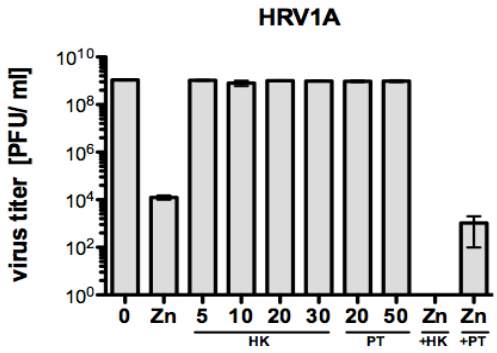

Figure 4.1 Effect of HK and PT on HRV1A
Increasing amounts of [mM] HK and PT in isolation and with 5mM ZnCl (+HK, +PT) were used to treat HRV1A and compared to untreated control HRV1A (0)

Experimentation with major group HRV16 mirrored the results seen with HRV1A. Dramatic inhibition was seen with the HK and ZnG precipitate, and HRV16 demonstrated sensitivity to PT-ZnG mixtures, even when the amount of ZnG used was below the threshold where Zn-based inhibition usually occurs (Figure 4.2). Unfortunately, experimentation with HRV39, another major group HRV, was less conclusive for PT and Zn sensitivity, but inhibition by HK & Zn was established (Figure 4.3).

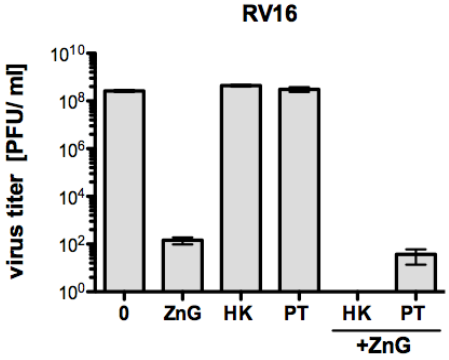

Figure 4.2 Effects of HK and PT on HRV16
20mM HK and PT were used to treat HRV16 with and without the addition of 5mM ZnG (Zn) and were compared to the untreated (0) and just Zn treated control groups. Virus titers were determined by plaque assay on monolayes of HeLa cells.

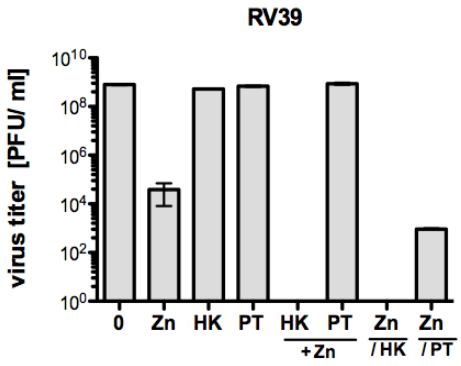

Figure 4.3 Effects of HK and PT on HRV39
20mM HK and PT were used to treat HRV39 with and without the addition of 5mM ZnG (Zn) and were compared to the untreated (0) and just Zn treated control groups. Virus titers were determined by plaque assay on monolayes of HeLa cells.

Poliovirus is not inhibited by HK or PT

Poliovirus experienced no appreciable inhibition with exposure to HK alone or in conjunction with Zn, despite formation of precipitate upon HK addition to viral serum which indicates that inhibition due to this compound is not due to universal steric hindrance to all viral - cellulr interactions. PV viral titer was also not reduced in the presence of PT or ZnG-PT mixtures. Furthermore, neither the ratio, the sequence, or order of exposure (mixing HK or PT with ZnG before PV exposure, or vice-versa) resulted in any decrease in PV titer. This observation suggests that Zn-mitigated inhibition with these compounds may also be due to an HRV-specific mechanism (Figure 4.4).

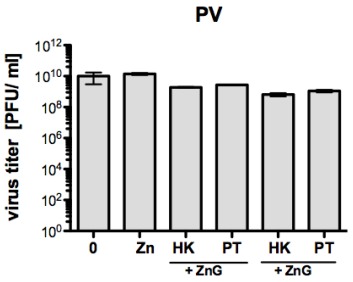

Figure 4.4 Effect of HK and PT on PV.
20mM HK and PT were used to treat PV alone or in conjunction with 10mM ZnG (+ZnG) and were compared to an untreated control (0). Virus titers were determined by plaque assay on monolayes of HeLa cells.

The ratio of PT to Zn modulates the inhibitory outcome

Interestingly, differences in ratio and sequence of exposure was observed to play a decisive role in PT & ZnG inhibition of HRV1A. The most profound inhibition of HRV1A occurred when Zn exposure occurred first, followed by the addition of PT, and the level of inhibition was substantially greater at a Zn to PT ratio of 1:2 as opposed to 1:1 or 1:3. In all instances, the degree of inhibition seen was vastly greater than that which was seen with ZnG exposure alone. Given that Zn2+ can interact with two PT molecules, this consistent ratio-based observation is not unprecedented, and suggests that 2 PT molecules binding the Zn cation plays an augmenting role in Zn-based inhibition of HRVs, or facilitates a new, more potent, mechanism of HRV inhibition, distinct from that with Zn alone (Figure 4.5).

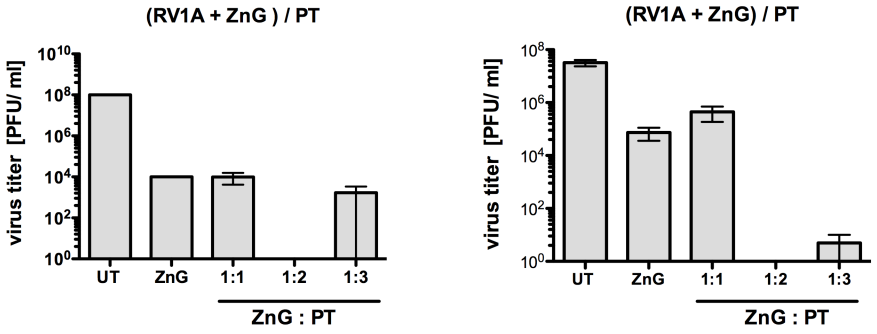

Figure 4.5 Addition of PT after ZnG treatment
HRV1A stocks were incubated for 5 min with 5uM ZnG and then PT was added in ratios 1:1, 1:2 and 1:3. These treatment groups were compared to an untreated (0) and ZnG (5um) only group prepared at equal volume under identical conditions. These mixtures were then used to inoculate a monolayer of HeLa cells and infectious titer was determined using a plaque assay.

On the other hand, when HRV1A was first exposed to PT, followed by the addition of ZnG, with the ZnG to PT ratios of 1:2 and 1:3, the viral titer of HRV1A was "rescued" or a decrease in HRV1A titer was prevented, presumably through protective chelation of Zn ions out of solution. A ZnG to PT ratio of 1:1 was unable to prevent inhibition and the decrease in titer observed was virtually identical to that of ZnG treatment alone (Figure 4.6).

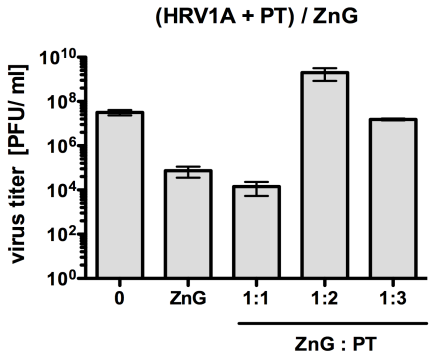

Figure 4.6 Addition of Zn after PT treatment
HRV1A stocks were incubated for 20 min with 5uM PT and then ZnG was added to achieve ZnG to PT ratios of 1:1, 1:2 and 1:3. These treatment groups were compared to an untreated (0) and ZnG (5um) only group prepared at equal volume under identical conditions. These mixtures were then used to inoculated a monolayer of HeLa cells and infectious titer was determined using a plaque assay.

Likewise, when PT and ZnG are incubated together at ZnG to PT ratios of 1:2 or 1:3 prior to HRV1A treatment, the presence of PT seems to have a protective effect, preventing Zn-based HRV1A inhibition, similar to the relationship between EDTA and PT. 1:1 mixtures of ZnG and PT incubated prior to HRV1A treatment resulted in a decrease in viral titer that was commensurate to that seen with ZnG alone, or slightly increased (Figure 4.7).

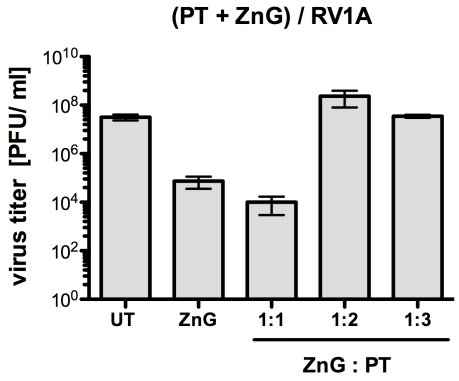

Figure 4.7 Mixing ZnG and PT prior to HRV1A exposure
HRV1A stocks were exposed to mixtures of ZnG (5mM) and PT which had undergone incubation with each other at ratios of 1:1, 1:2 and 1:3 for 20 min with gentle agitation at room temperature. These treatment groups were compared to an untreated (0) and ZnG (5um) only group prepared at equal volume under identical conditions. These mixtures were then used to inoculate a monolayer of HeLa cells and infectious titer was determined using a plaque assay.

Taken together, these experiments indicate that Zn antiviral activity is precluded by chelation with two PT molecules resulting in steric hindrance or chemical repulsion, or both, thereby preventing Zn's mechanism of action. However, studies with ZnG and PT at ratios of 1:1 and 1:3 suggests that Zn bound to one PT molecule may actually enhance this antiviral activity, given that a 1:1 addition lead to at least a mild increase in HRV1A inhibition compared to Zn alone, and 1:3 ratios of Zn and PT consistently exhibited a decrease in protective effect or titer rescue compared to 1:2 ratios (Figure 4.7).

Zn-resistant HRV1A mutants and PT

If the mechanism of inhibition of HRV1A observed with PT in conjunction with ZnG is highly similar or identical to that of Zn, Zn-resistant mutants might be expected to be resistant to this form of inhibition as well. 3 mutant isolates of unknown genotype were tested which all had demonstrated sufficient titer and decreased susceptibility to Zn in comparison to wild-type HRV1A. These 3 mutants were subjected to Zn treatment and Zn treatment followed by PT exposure. While the mutants did demonstrate a significant degree of resistance to both Zn and Zn / PT exposure, attempts to sequence these mutant populations was stymied due to non-homogenous sequences with which a consensus strand could not be generated. However, further investigation into such mutant would be a potentially compelling area of future research.

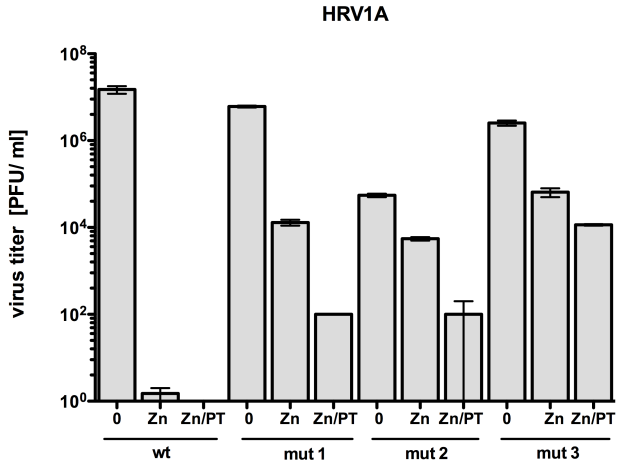

Figure 4.8 PT and ZnG-resistant mutants
Wild-type (wt) HRV1A stocks and HRV1A that was serially passaged 3-6 times after ZnG exposure and had demonstrated some degree of ZnG resistance (mut1, mut2, mut3) were subjected to (5mM) ZnG treatment followed by PT (10mM). These HRV1A treatment groups were compared to both an untreated mutant control (0) and wild-type controls that had been subjected to the same treatments under identical conditions. These mixtures were then used to inoculate a monolayer of HeLa cells and infectious titer was determined using a plaque assay.

A PDTC-Zn compound is inhibitory to HRV1A

The potential antiviral activity of Pyrrolidine Dithiocarbamate (PDTC) during intracellular stages of the picornaviral infectious cycle has been investigated, and while its precise mechanism is unknown, the presence of a 2+ cation such as Zn or Cu was determined to be essential for its intracellular viral-replication suppression activity (111). Experiments with extracellular PDTC alone, without supplementation of Zn or Cu, did not result in HRV inhibition (Figure 4.9). While this study established that a 2+ cation was essential for PDTC antiviral activity during intracellular stages of the HRV infectious cycle, they did not conduct, or did not report, findings for experimentation with extracellular PDTC treatment and 2+ cation supplementation.

Based upon these prior studies, I sought to determine if PDTC supplemented with Zn could be inhibitory to HRVs via extracellular exposure alone. Using concentrations of PDTC found to be inhibitory for intracellular processes of HRV infection, I determined that only the isolated compound formed by PDTC interaction with Zn could enact extracellular inhibition on HRV1A. PDTC alone, and ZnG used at low levels, were previously not documented to be capable of HRV inhibition, and likewise, I found that they were not capable of lowering the titer of HRV1A in my experiments. Furthermore, sequential exposure of these concentrations of PDTC and Zn to extracellular HRV1A did not result in an appreciable decrease in viral titer. Only when the precipitate formed by PDTC and Zn after incubation at 37C or higher for at least 20 minutes was harvested, re-suspended in PBS or water, then used to treat HRV1A, dramatic

reduction in viral titer was observed (Figure 4.9). Investigation into the precise parameters necessary to optimize the creation of this compound might be an interesting area of future study.

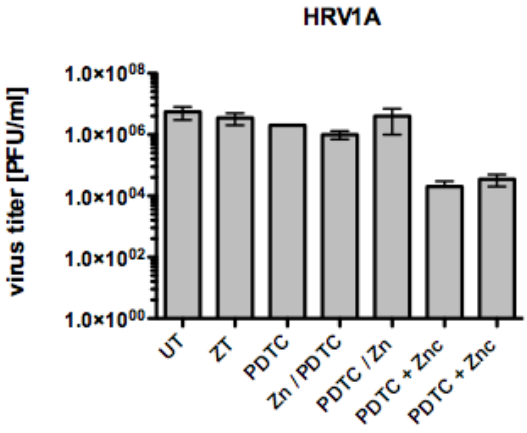

Figure 4.9 PDTC and HRV1A
30um Zn and 30umPDTC were used to treat HRV1A in isolation as well as Zn and then PDTC (Zn/PDTC) and PDTC then Zn sequentially (PDTC/Zn). Compounds generated via heated incubation of PDTC and ZnCl (PDTC + Zn) were shown to decrease the titer of HRV1A at approximately a 30uM concentration. Incubations took place at 37C with constant agitation. These mixtures were then used to inoculate a monolayer of HeLa cells and infectious titer was determined using a plaque assay.

This experimental result indicates that only the stable product of PDTC and Zn is capable of extracellular HRV1A inhibition. PDTC and Zn alone at these concentrations, or added in succession of each other, or added nearly simultaneously to solutions of HRV, are unable to render a decrease in viral titer. While chemical investigation into the precise formula of this precipitate has not been performed, prior chemical research on PDTC has concluded that it can form complexes, with Zn to PDTC ratios of 1:2. This PDTC-Zn compound has not been exhaustively characterized and other studies on its potential antiviral activity have not been conducted or reported. However, it's ability to effect antiviral activity at Zn concentrations 10-fold less concentrated than that seen with Zn alone, in combination with its documented non-toxic amenability towards medical use, should make this compound and its derivatives a

conceivably profitable area of study. While ZnG was also used in an identical set of experiments, I found that formation of the inhibitory precipitate appeared to be optimized with ZnCL, and ZnCl was used to supplement PDTC in studies looking at intracellular-based inhibition of HRVs and other viruses (Figure 4.10 and Figure 4.11). Unfortunately, testing the inhibitory potential of this compound was not performed on other picornaviruses, but I would advocate that doing so would potentially be a compelling area of future research, especially given that intracellular PDTC-based inhibition was shown to occur with other members of the picornavirus family in past studies (118).

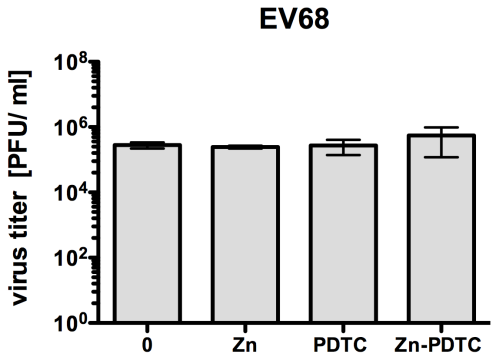

Figure 4.10 PDTC and EV68.
EV68 was treated with 30um of the Zn-PDTC compound, PDTC (PDTC) alone or Zn (Zn) alone, and compared to a untreated control (0). Incubations took place at 37C with constant agitation. These mixtures were then used to inoculated a monolayer of HeLa cells and infectious titer was determined using a plaque assay.

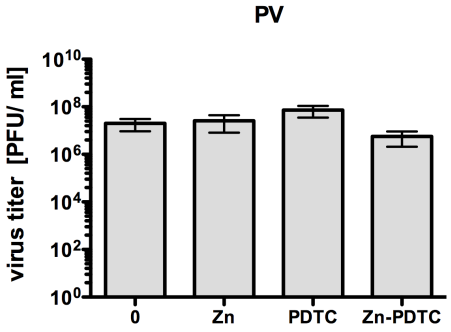

Figure 4.11 PDTC and PV
PV was treated with 30um of the Zn-PDTC compound, PDTC (PDTC) alone or Zn (Zn) alone, and compared to a untreated control (0). Incubations took place at 37C with constant agitation. These mixtures were then used to inoculate a monolayer of HeLa cells and infectious titer was determined using a plaque assay.

CHAPTER 5: DISCUSSION

Overview and Relevance of Findings

Previous studies on the mechanism of Zn+ inhibition of HRV infections were focused on events within infected cells that occur after viral entry (4). The results of these studies suggested that an intracellular interaction between Zn and the nascent capsid polyproteins might impede the HRV infectious cycle and account for successes seen in some Zn-therapeutic clinical trials. However, the cytotoxic concentrations of Zn necessary to observe this effect make it unlikely that this is the central mechanism of action, especially in the physiological context of lozenge or nasal spray use, where Zn cations would not only have to forcibly traverse the cellular plasma membrane, but also pass through protective secretions characteristic of the naso-pharyngel mucosal environment, making the bio-availability of Zn in doubt (119). Consequently, while intracellularly introduced Zn may, indeed, interrupt HRV polyprotein processing, the notion that this activity could single-handedly account for the degree of HRV inhibition necessary to yield a therapeutic benefit is unlikely. In the 1976 study led by Korant, wherein Zn based disruption and association with the nascent HRV polypeptide was observed, no other picornaviruses were investigated, making the HRV-specificity of this mechanism undetermined (106). Furthermore, in the 1974 findings by Butterworth, on which the aforementioned research was based, accumulation of nascent polypeptide precursors after a transient increase in intracellular Zn, was observed in HRV1A, PV and EMCV, with the latter two picornaviruses having never been documented to experience Zn-inhibition like that seen with HRVs (4). In addition, the Zn-based inhibition of polyprotein processing was demonstrated to be reversible, a key characteristic that differentiates this mechanism from the seemingly irreversible one investigated here (4).

Taken together, these observations imply that the inhibitory Zn interaction with the picornaviral polypeptide precursor documented in these prior two studies is not likely to be responsible for the very HRV-specific inhibition discussed here, and reported in prior investigations.

Here I have shown that extracellular exposure of HRVs to Zn, prior to contact with a susceptible and permissive cell, is sufficient to reduce viral infectivity. This inhibition might account for the reduction in duration and severity of symptoms of the common cold reported in some clinical trials in which Zn+ is provided via a lozenge or nasal-spray conduit (120).Transient exposure of extracellular virions to Zn within the respiratory tract could theoretically reduce viral infectivity, preventing infection of nearby epithelial cells, and thereby curtail the otherwise logarithmic increase in viral load during an acute HRV infection. This suppression of viral population growth may provide the advantage necessary for the immune system to more rapidly resolve these infections, or in addition to the decease in viral number, it might result in less activation of the inflammatory immune responses attributed to many of the pernicious symptoms seen in common cold sufferers (121).

Clinical trials of Zn for the common cold have had highly variable effects on symptoms and their duration (122). One explanation for this outcome could be a consequence of the unknown etiology of the virus causing the common cold, as rapid diagnostic assays were not available at the time when many of these studies were performed. It is possible that the virus triggering the symptoms in many of the study enrollees was not due to the presence of an HRV, and with the ability of other upper-respiratory viruses to be inhibited by Zn in doubt, this discrepancy could have

unwittingly contributed to a high amount of false-negative results when Zn-lozenges were tested.

An additional confounding factor may have been the formulation of the lozenge. The chelating sugars that were included in some lozenges to make them more palatable, may have dampened the ability of Zn+ to inhibit HRV infectivity. I have demonstrated that the presence of sucrose in the Zn cation milieu can result in chelation of Zn which prevents its HRV inhibitory activity in a tissue-culture assay (Figure 3.23). While relegated to a tissue culture model, this data nonetheless provides a cautionary framework when considering the formulation of future Zn-based HRV therapeutics.

Analysis of salient mechanistic findings

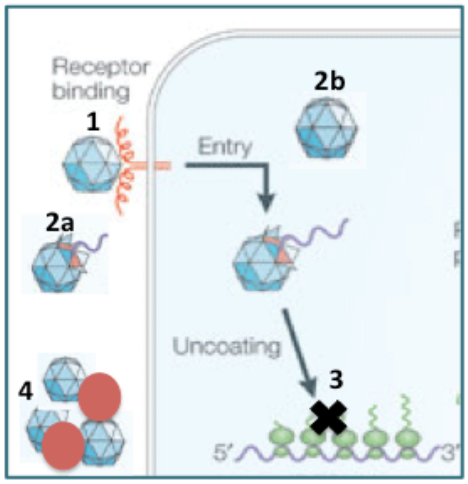

Diagram 5.1 Mechanism possibilities
1) HRV interaction with its cognate receptor. 2) Modulation of viral capsid metastability to a) dissemble the capsid outside of the host cell or b) lock the capsid structure, preventing viral genome release within the host cell cytoplasm. 3) Damage to the viral genome that prevents translation or recognition by host machinery 4) Agglutination of viral particles that decreases the efficiency of receptor binding and endocytosis.

Mechanistic hypothesis and experimental analysis

The observation that extracellular exposure to Zn results in a decrease in viral titer led me to initially postulate 4 general hypothesis to account for this mechanism through contemplation of which key steps in the viral cell-entry and replication-initiation process could potentially be disrupted by the activity of this cation (Diagram 5.1. The plaque assays used to reveal this inhibition rely upon the cytopathic virus-induced death of infected cells. While high particle to PFU ratios have been reported in picornaviruses, the production of the plaques used to calculate virus titer necessitates that the virus or viruses responsible for plaque formation be intact and capable of initiating replicative events that will produce progeny virions. Exposure to Zn results in abrogation of this ability, an irreversible loss of, plaque-production. Seeking to learn more about the mechanism of this inhibition, I initially structured my research plan around investigation of each of these 4 key routes of inhibition that might be impeded by the presence of Zn.

Zn does not interfere with receptor binding

Binding of the virus to its cognate receptor is required for endocytic access to the host cell cytoplasm and interference with this critical step in the infectious cycle has been the goal of many antiviral drugs. The ICAM1 receptor utilized by major group viruses and the LDLR receptor used by minor group viruses vary significantly in structure. The ability of Zn to inhibit both major and minor group viruses, albeit to varying degrees, was a provocative finding that implied that this inhibition might not directly involve virus-receptor interaction. However, it was not out of the realm of reason that the general

activity of a cation in surplus could be inhibitory to both major and minor HRV receptors through a general mechanism such as occluding viral-receptor contacts of negative charge at the binding interface. To explore this possibility I performed experiments wherein I transiently incubated the HELA monolayer with Zn prior to viral infection and performed PBS washes prior to HRV infection. If Zn cations were impeding virus binding through association with sites of negative charge on the cell surface, I postulated that promoting this interaction prior to application of HRV would also result in a depressed viral titer. While this experimental process did not replicate the inhibition seen with HRV-Zn exposure in isolation, I felt that this result was inconclusive as the presence and concentration of Zn after the protective washes could not be confirmed (results not shown). To more clearly determine if Zn treated virions were still capable of interacting with their receptor, I developed a "competition assay" wherein untreated, infectious virions were forced to compete with Zn-treated HRV for a limited number of receptor binding sites. Necessitating the assumption that the amount of HRV is in excess of binding sites, this assay was performed using an extremely high MOI with the proportion of Zn-treated HRVs gradually increasing in the inoculate, while the amount of untreated HRV remained constant. Theoretically, in this assay, if Zn-treated HRVs are able to bind a cellular receptor, given their inability to initiate an infectious cycle, a decrease in total plaque number will be observed as the presence of these inactivated virions occupy binding sites that might otherwise be utilized by infectious particles whose replication cycle can result in successful plaque formation (Figure 3.18). The ability of this assay to demonstrate the existence of receptor-based competition was demonstrated using UV-treated HRV virions whose RNA damage prevents the initiation of an infectious cycle,

despite the capsid remaining intact and capable of receptor binding (Figure 3.19). The decrease in plaque number seen as the amount of Zn-treated virions is increased paralleled that of UV-treated virions, indicating that Zn-treated HRVIA is still capable of interacting with its receptor.

Furthermore, in the ICPA, formation of plaques relies upon the binding of virus to the first batch of infected cells used to "seed" the second monolayer. In the ICPA I designed, holding cells at 4C was used to prevent endocytosis of virus particles after receptor binding. In this assay, plaque formation was only possible if HRV or PV was able to remain bound to its receptor for the duration of ZnG treatment, harvest and re-suspension. The dearth of plaques seen in the Zn-treated group compared to the untreated group in this assay indicate that Zn-mediated inhibition of HRV is able to occur even after binding of HRV1A to the LDLR cell receptor (Figure 3.15). This result indicates that Zn access to the geographical area that encompasses the virus-cell receptor interaction, is not necessary for inhibition to occur, and in conjunction with the competition assay, it is not likely that Zn functions by unseating virions from their receptor. Taken together, the result of these experiments allowed me to eliminate the hypothesis that Zn plays a receptor-mediated role in HRV inhibition.

Zn does not trigger extracellular capsid disassembly

Held together by non-ionic binding interactions, the capsid proteins that protect the viral genomic payload must play the dual function of safeguarding the viral genome outside of a host cell and also dissembling to release the genome once the cytoplasm of the host cell is reached. This potential energy imbued in the capsid structure that allows

for genome release is characteristic of the important “metastability” needed for the virus particle to remain infectious. Detrimental modulation of capsid metastability that results in premature genome release, or imprisonment of the viral genome after cell entry, has been the goal of numerous antiviral drugs (4). The ability of Zn to either promote capsid dissembly (Diagram 5.1, 2a) or lock the capsid structure in place (Diagram 5.1, 2b) could both account for the initial experimental outcomes I observed. However, complete capsid dis-assembly would remove the binding contacts necessary for the virus-cell receptor interaction. Therefore, the results of the competition assay made such a mechanism unlikely. Furthermore, viral capsid protein visualization through native and denaturing polyacrylamide gels implies that the interactions of Zn-treated capsids were not disrupted, and that Zn did not induced cleavage of these polypeptides (Figure 3.20 and Figure 3.21). While this result is not concrete due to the unavailability of an HRV1A-specific antibody with which to probe these proteins blots, the unchanging pattern seen in both Zn treated and untreated groups that could be observed with both a coomassie stain, and a more sensitive silver stain, implies that the totality of protein complexes, be they viral or cellular, are unchanged with Zn treatment. The possibility of Zn-treated viral capsid entry into the cell without genome release is not refutable with my experimental results. Further exploration visualizing the location of labeled virions could reveal the validity of this hypothesis, however, the small size of picornaviruses does not make them amenable to fluorphore labeling. Using radiolabeled virions, one could determine if Zn-treated virions are capable of cellular entry, however, additional experimental measures would need to be taken to determine if the capsid structure has remained intact as cell

entry with no replication is possible if the viral genome is no longer capable of being recognized and translated by host ribosomes.

Zn treatment results in degradation of viral RNA

The HRV genome consists of a single, naked strand of RNA with extensive secondary structure that forms an IRES that allows for its immediate translation upon cell entry. This RNA serves as both the template for the creation of more genomic RNA, and as an mRNA template for viral protein synthesis. To initiate a successful infectious cycle, this RNA must be recognized by host cell translation machinery and the viral proteins necessary to carry out other stages of the replication cycle must be created. Without an intact genome, the infectious cycle cannot proceed, therefore, the potential of Zn to catalyze damage to viral RNA genome was investigated (Diagram 5.1, 3). Initial tabulation of RNA quantity after isolated of HRV1A by centrifugation and Zn treatment revealed that the total amount of RNA had decreased compared to an equivalent aliquot of untreated virus (Figure 3.23). Furthermore, assaying for HRV-specific RNA in Zn-treated and untreated fractions after sucrose gradient purification revealed a decrease in detectable viral genomic material, and that the location of RNA in the centrifugal milieu did not change with Zn treatment (Figure 3.24). Additional HRV-specific probing of Northern blots after Zn treatment revealed the disappearance of full-length HRV RNA, and the general decrease in higher molecular weight viral RNA, despite the length, or the specificity of the probe used (Figure 3.25, Figure 3.26 and Figure 3.27). Rnase inhibition used in these experiments removed the possibility that this RNA degradation is the result of the presence of contaminating Rnases. These results indicate that hypothesis 3 is valid

and that RNA catalytic activity is at least partially responsible for the extracellular Zn-inhibition observed. However, the ability of Zn to promote HRV inhibition through an additional mechanism is also possible. Furthermore, the means by which the presence of Zn promotes this RNA degradation is not certain. However, the results of the competition assay, ICPA assay and the fact that remnants of viral RNA are found to sediment equivalently to untreated HRV, suggest that this process does not dramatically alter the HRV capsid structure. Without dis-assembly of the capsid, Zn mediated catalysis of genomic RNA likely occurs after entry of this cation into the capsid structure wherein it might form an RNA cleaving nuclease with interior histidine residues. Bolstering this conjecture is the documented ability of similar element, Cesium, to enter the capsid, and the presence of a pore on the capsid surface as visualized through 3 dimensional molecular imaging based upon biophysical investigations into HRV capsid structure (Figure 5.2) (4).

Zn is not inhibitory due to capsid agglutination

Zn-mediated agglutination of HRV capsids would also potentially result in the inhibition observed here. However, agglutination in this manner is unlikely to be cation-specific. The inability of other 2+ cations tested to replicate this HRV inhibition discredits this hypothesis, in addition to the unlikelihood of such aggregates remaining intact through the process of dilution, vortexing and plaque assay preparation (Figure 3.11). Furthermore, the indiscriminate formation of aggregates in HRVs alone, and not the other the picornaviruses tested to any degree, is unlikely. Given the similarity in capsid structure, at least a modest degree of agglutination would probably be seen in

different picornaviruses, even if not to the same degree of that seen in HRVS. Furthermore, cloudy precipitate, which might be indicative of aggregate formation, was never observed in any of the HRV-Zn mixtures tested.

Zn-mechanism conclusion

Taken together, the results of the northern blot analysis, competition assays and sucrose gradient fractionation suggest that the primary mechanism of Zn based inhibition of HRV1A involves the degradation of viral RNA, thereby reducing viral infectivity. Given the results of the competition assay and ICPA assay, which together imply that the interaction of the virus and its receptor is neither required for, nor disrupted, by Zn activity, I hypothesize that Zn enters the HRV1A capsid where it participates in degradation of the viral RNA while the viral capsid remains wholly or partially intact. In further support of this hypothesis, it is known that cesium, an element of similar size to Zn, can enter the HRV capsid, possibly through a pore at the 5–fold axis of symmetry (4). Given the similar size and clinical profile of these two cations, it is plausible that Zn may also enter the viral capsid in a similar fashion. However, Cesium - mediated degradation of viral RNA has not been reported. In contrast, the capsid of poliovirus is not permeable to cesium, and similarly, Zn does not inhibit the infectivity of this virus. While RNA degradation from Zn-treatment is documented, it cannot yet be disproved that additional mechanisms may be at play. It is also possible that Zn binding or entry into the viral capsid may alter the metastability of the structure, resulting in downstream difficulties with virion internalization and un-coating. However, without intact genomic RNA, such mechanistic action of Zn on HRVs would only play a secondary role in viral inhibition.

Zn-resistant HRV mutations

To understand the mechanism of Zn-mediated inhibition of HRV1A, I sought to scrutinize differences between Zn-sensitive and Zn-resistant HRV1A. While exposure to Zn is tremendously detrimental to HRVs, completely eliminating evidence of infectious virus in some experiments, infrequently, infectious HRVs can be detected after Zn treatment at more moderate concentrations. However, it was unclear if the existence of these infectious particles after ZnG is due to genetic resistance to Zn-mediated inhibition, or if insufficient Zn was available to abrogate the infectivity of every viral particle in solution, despite attempts to quantify the amount of virus particles to Zn cations in cases of 100% inhibition.

Procedure and caveats

Given the highly mutagenic-ability of RNA viruses, whose polymerase lacks proof-reading functionality, considerable genetic diversity exists in any HRV population naturally, often leading them to be described as “quasi-species”(4). While it may be responsible for the high particle to PFU ratios often reported with picornaviruses, this genetic diversity provides the evolutionary potential for the existence of virions that contain advantageous mutations that allow for survival under various conditions. Consequently, I presupposed that within a sufficiently large population, it would be statistically likely that Zn-resistant HRVs exist and might be selected for under the consistent selection pressure of Zn. However, given the cytotoxic nature of sustained Zn

exposure, relentless Zn-pressure was not possible, given that healthy HeLa cell metabolic activity is necessary to support viral replication. To prevent cell death that would limit virus production, I developed a Zn-resistant HRV cultivation strategy wherein I sequentially exposed HRV populations to Zn, removed excess Zn with EDTA prior to HeLa cell infection, and then subjected each viral harvest to an increasing amount of Zn exposure. In doing so, it was immediately apparent that resistance to Zn came at a cost of general darwinian fitness of the virus particles. In addition to a smaller plaque phenotype, Zn-resistant HRV1A titers never rivaled those of their wild-type progenitors. The reason for this stark decrease in Zn-resistant HRV1A fitness remains unexplained, but it is most likely due to disadvantageous interactions between the viral proteins which affect capsid assembly, disassembly, or selective encapsulation of viral RNA. To analyze genetic differences between wild-type and Zn-resistant HRV1A, I designed a series of over-lapping primers that collectively covered the entire HRV1A genome and whose similar Tm allows the forward and reverse members to be interchanged to adjusted amplicon size as needed. Alignment comparisons among NCBI HRVIA sequence submissions and wild-type control virus isolates subjected to the same procedure revealed genetic differences in these strains that might account for the Zn-resistance phenotype.

Summary of mutations

After cultivation, isolation and sequencing analysis of Zn-resistant HRV1A, three different amino-acid substitutions in the VP1 capsid polypeptide were found in six different Zn2+-resistant isolates. Each of these mutations was found in multiple Zn-resistant isolates, alone or in combination, and in none of the wild-type, Zn-susceptible,

control HRV1A preparations. The change in residue charge of two of the three mutations in the HRV VP1 protein found here could play a biochemical role in repelling Zn from entering the capsid while the third mutation might provide steric hindrance or stabilization of the capsid structure. In addition, it has been previously documented that interaction of Zn+ with the imidazole ring of histidine can lead to the formation of a nuclease which can catalyze degradation of RNA (4). It is plausible that a similar interaction of Zn+ with histidines in the capsid interior could precipitate the destruction of viral genomic RNA. Therefore, a mutation, which helps to exclude Zn entry into the viral capsid, might provide a protective role. While not indisputable, a mechanism such as this, which does not require extensive disruption of the viral capsid, or exit of the viral RNA from the capsid structure, is in line with the salient findings presented here. Cesium has not been documented to participate in a similar nuclease mechanism, perhaps explaining why its entry into the viral capsid is not reported to result in viral RNA degradation.

Residue 29 on VP1

The VP1 capsid protein is predominantly outward facing, but does display inward-projections into the capsid interior which may play a role in capsid stabilization, interaction with other capsid proteins, or genome interaction. In multiple Zn-resistant isolates, an amino-acid transition at the interior residue 29 on VP1 was found in conjunction with mutations on the surface-facing region of VP1. Because the amino acid alteration at position 29 was not observed independently, the possibility of this mutation playing a singular, definitive, role in Zn resistance is not concretely validated. However,

it is important to note that its representation in just 6 isolate samples may not provide the most comprehensive statistical census of its presence among Zn- resistant HRV populations. With time and additional Zn- resistant mutant isolation, it's existence in the capsid structure as a singular mutation conferring Zn-resistance would not be an unprecedented discovery given the limited scope of Zn-resistant mutants surveyed here, due to time and practicality considerations. Furthermore, only the most Zn-resistant HRVs were sequenced. It is possible that some of the intermediately resistant populations might contain this mutation. The observation of this specific residue 29 mutation in 3 out of 6 mutant VP1 proteins rendered, supports the belief that this mutation is not the result of random bottle-neck carry-over after Zn-mutation selection, as this would be statistically unlikely to have occurred in 3 of 6 separate isolation events. It is much more statistically reasonable to assume that even if not playing a direct role in in Zn-repulsion, that this mutation might play a stabilizing or supporting role for its external counterparts. This amino acid is part of the VP1 loop that projects into the capsid interior, coming into close proximity to viral genomic RNA. This geographical feature, combined with its juxtaposition to two histidine residues on residues 24 and 25 of VP1 residing near it within the capsid interior, makes the aforementioned imidazole nuclease-based catalysis of the viral RNA genome plausible for the wild-type version of HRV1A. However, the positively charged lysine in the Zn-resistant variant may also act to repel Zn from this site, preventing nuclease formation, and thereby prevent viral genomic RNA degradation.

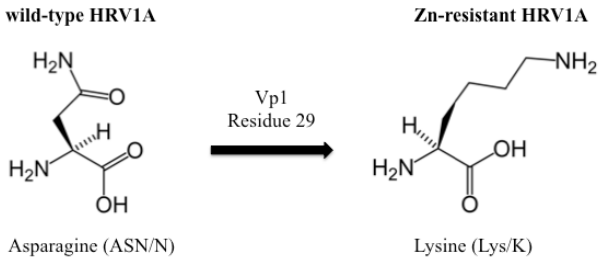

Diagram 5.2 Mutation at residue 29 in VP1.
Asparagine in wild-type HRV1A transitions into Lysine with Zn selection.

Furthermore, the presence of this positive charge within the capsid structure may function by providing an additional degree of Zn protection in the event that the exterior mutation(s) did not provide a strong enough deterrent for preventing Zn entry into the capsid. This mechanistic possibility is bolstered by the observation that three Lysine residues surround the interior side of the pore due to the repetitious nature of protomeric capsid protein interactions that comprise the icosahedron. The collective net positive charge that this mutation lends to the capsid structure through it's 60-fold repetition in the complete capsid, in conjunction with one of the other surface mutations, could result in a profound biochemical change to the capsid structure. This amino acid biochemistry change on residue 29, in combination with an additional positively charged surface residue, or in conjunction with a surface residue lending steric inhibition to capsid pore entry, might additively result in successful avoidance of Zn-catalyzed damage to viral RNA. Furthermore, the "breathing" seen in HRV capsids, wherein a transient 135S particle is formed by extrusion of VP4 and the interior N-terminus of the VP1 protein on which this mutation site resides, may put this residue in a position to more directly repel Zn (4) when projected outside the capsid structure. Alternatively, this or any of the other mutations found might play a role in prevention of 135S particle formation, and thereby possibly prevent Zn entry into the viral capsid.

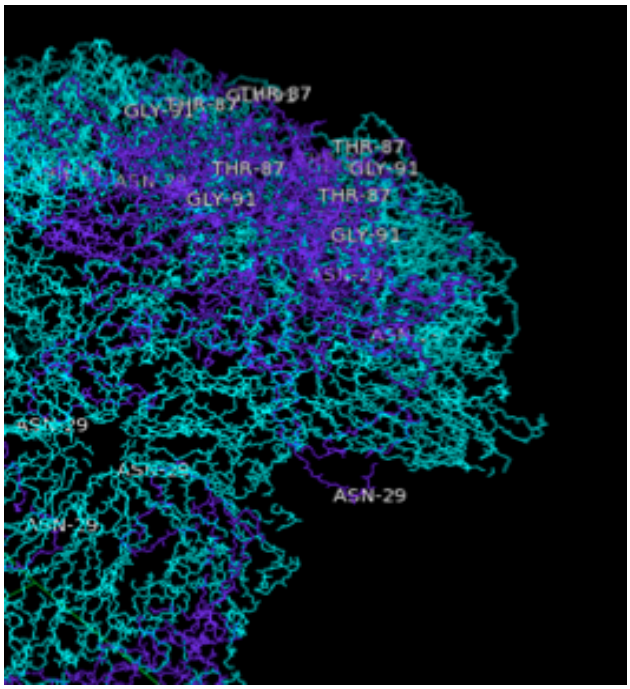

Figure 5.1 Asparagine 29 in the capsid interior.
The Asparagine 29 on HRV VP1 (purple) can be seen dipping into the capsid interior through this cut-away visualization of the capsid VP2-VP4 are shown in teal.

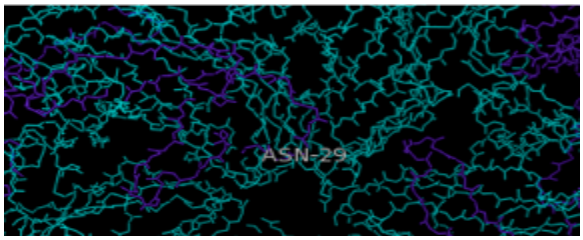

Figure 5.2 Asparagine 29 proximity to capsid pore
The Asparagine (Asp) 29 in HRV VP1 (purple) can be found in the capsid interior near the capsid pore. The repeating protein interactions that form the capsid results in three Asp 29 residues surrounding the pore entrance (labeled in white)

Residue 87 on VP1

In 3 out of the 6 Zn-resistant mutant HRV1A isolates characterized, the 87th residue of the VP1 protein transitioned from a Threonine to a Serine. This residue is found on the antigenic "B-C loop" protruding off the HRV1A surface near a clearly visible pore structure. This B-C loop has previously been described to play a role in multiple anti-picornaviral drug mechanisms. While vaguely similar in size and structure, a distinguishing characteristic that differentiates these two amino acid residues is the documented biochemical hydrophobicity displayed by the wild-type Threonine that is not seen in the Zn-resistant Serine residue. Consequently, in the aqueous solutions in which HRVs are typically found, this defining biochemical characteristic may catalyze a conformational change in the B-C loop due to the Threonine side-group's avoidance of polar solutions. This potential hydrophobicity-driven conformational change would not occur in the Zn-resistant variant where a non-hydrophobic Serine has replaced Threonine.

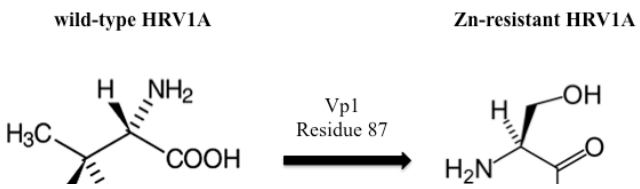

Diagram 5.3 Mutation at residue 87 in VP1.
Threonine in the wild-type HRV1A transitions into Serine after Zn selection.

Given its proximity to the pore structure, one could also postulate that such a conformational discrepancy might culminate in steric prevention of Zn access to the pore, preventing Zn entering the viral capsid. However, without detailed molecular modeling techniques coupled with biophysics experimentation to confirm conformational changes, this proposed mechanistic role is just an informed conjecture.

Residue 91 on VP1

Also in the B-C loop structure on the surface of the viral capsid, the 91st glycine residue of VP1 has been found to transition into a positively charged arginine residue in multiple Zn-resistant isolates. In addition to its positive charge, the chemical structure and large size of arginine stands in stark contrast to that of the tiny, largely non-reactive glycine.

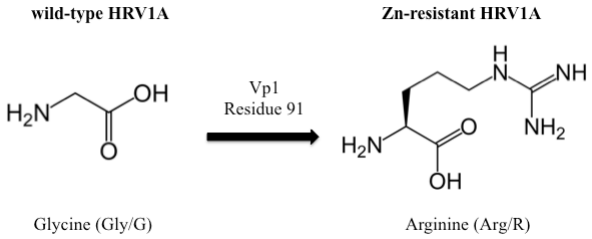

Diagram 5.4 Mutation at residue 91 in VP1.
Glycine in the wild-type HRV1A transitions to Arginine after Zn-selection.

Due to it's biochemistry, repulsion of Zn cations from the viral capsid is the most obvious potential mechanism of this mutation, especially when one considers that this mutation is replicated 60- fold around the capsid structure and lies near the pore structure on the 5-fold axis. Furthermore, this positive charge is found on the end of an elongated side group, consisting of a chain of 4 carbon atoms, which might result in pore-protecting steric hinderance, or projection of the positive charge outward in a manner that may be additionally conducive to Zn-repulsion.

In general, the conformation and flexibility of the VP1 B-C loop is known to play a role in the inhibition of picornaviruses by the antiviral compound plecornaril and other similarly structured drugs (69). Therefore, the presence of these two mutations on the B-C loop, just 3 residues adjacent to one another, and the impact such mutations might have on the conformation and flexibility of the B-loop, makes this locale an unsurprising hot-spot for Zn-resistance related mutations.

Zn-resistant HRV1A fitness cost

The decrease in fitness of the Zn-resistant isolates compared to their wild-type counterparts is staggering. In achieving a degree of resistance to Zn-catalyzed inhibition, these viruses loose efficacy in one or more stages of the viral infectious cycle, such as receptor binding, capsid un-coating, or assembly. Given that Zn-treated virions have demonstrated the ability to bind the LDLR receptor securely as demonstrated by the competition assay and the ICPA assay, it is more plausible that this decrease in fitness is due to mechanistic challenges that these biochemical or conformational changes lend to the un-coating or capsid assembly process. However, it is important to note that the B-C loop structure of VP1 contains binding contacts that interact with the ICAM-1 receptor and the B-C loop structure may also play a role in LDLR binding of minor group HRVs. Therefore, the presence of one or more mutation sites within the B-C loop might disfavor the successful virus-receptor interaction critical for virus internalization. Another possibility is that the presence of these substitutions in the singular HRV ORF decreases the efficiency of polyprotein processing and self-cleavage mechanisms that then results in a decrease in the production of cogent capsid proteins capable of assembly. Aside from plaque formation, a significant difference in cytopathic effect (CPE) between Zn-resistant and Zn-sensitive HRVs was not observed before or after fixation and staining of infected HeLa cell monolayers.

While the development of resistance is a concern for any antiviral product, the demonstrated high fitness cost that is associated with resistance to Zn+ suggests that resistant HRVs are unlikely to evolve to become the predominant endemic genotype circulating in any HRV population. Up to half a dozen serial passages were unable to

return the Zn-resistant populations isolated in this study to titers comparable to that of their wild-type predecessors. While this decrease in fitness might be attributable to a detrimental "bottle-necking" effect wherein deleterious mutations are stochastically inherited in conjunction with the beneficial Zn- resistance mutation, this is unlikely due to the lack of evidence of such mutations when genome-wide sequencing analysis was performed.

HRV inhibition mediated by Zn Ionophores

Previously, ionophores Pyrithione (PT), Hinokital (HK) and PDTC have been documented to inhibit HRV and other viruses through interaction with intracellular factors during viral replication. The presence of a Zn cation, or Copper in the case of PDTC, was shown to be required for their intracellular inhibitory activity (123). Extracellular picornavirus inhibition with Pyrithione and Hinokital has not been explored, and extracellular exposure with PDTC alone failed to inhibit HRVs (293). Here I have demonstrated that PT, HK and PDTC can inhibit HRVs through an extracellular mechanism that requires Zn. The concentrations of Zn required to see HRV inhibition in conjunction with these compounds is significantly less than that needed to see inhibition of HRVs with Zn alone. Like EDTA, these compounds have the ability to chelate Zn from solution and prevent HRV inhibition; an activity that is optimized at characteristic ratios based upon their stoichiometry of complexation with Zn cations. However, their sequential interaction with Zn and HRVs, alone or in combination, can result in protection from Zn-induced inhibition, or an escalation of loss of infectivity. It is unclear if the antirhinoviral activity of these compounds in conjunction with Zn operate by

enhancing the mechanism seen with Zn-alone, or if they facilitate a distinctive mechanism of HRV inhibition.

Hinokital - mediated Zn Inhibition

Hinokitiol, also known as Beta - thajaplicin, is a derivative of wooded plants from the Cupressacae family and has been noted for its ability to inhibit certain strains of chlamydia and streptococcus, in addition to modulating estrogen receptor signaling and inducing suppression the of the inflammatory response in vascular smooth muscle cells (124). It has also been noted for its anti-fungal properties and potential to modulate cancer-related cell-signaling pathways (125). Past research with HRVs, PV, CVB3 and mengovirus suggested that this compound, in conjunction with Zn or Cu, could impede picornaviral polyprotein processing when introduced into an infected cell (117)

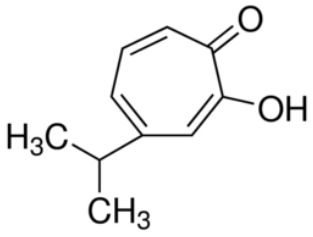

Diagram 5.5 Chemical structure of Hinokitiol

I found that Hinokitiol alone did not possess the ability to decrease HRV infectivity through extracellular exposure. However, abrogation of HRV infectivity with this compound in conjunction with Zn was dramatic to the extent that the minimum concentration required to see inhibition was not breached. However, addition of this chemical to HRV1A inoculates resulted in the immediate formation of a cloudy

precipitate that was visible throughout the solution. Hinokital solutions supplemented with DMSO did not reduce the production of this precipitate, and both ZnG and ZnCl yielded similar results (Figure 4.1). The existence of this visible precipitate created worries that it's antiviral activity was mitigated partially through aggregate formation or occlusion of access to the viral receptor. However, this HK-Zn precipitate did not inhibit PV. The inability to inhibit PV suggests that the mechanism of this compound is not attributable to generalized agglutination and indiscriminate receptor occlusion.

Pyrithione - Mediated Zn Inhibition

The Zn – Pyrithione (PT) coordination complex has been studied for its antifungal and bactericidal abilities (126). Furthermore, it's ability to ameliorate dandruff and Seborrhoeic Dermatitis have promoted its incorporation into medical and over-the-counter products (127). Virology-based research with this compound has revealed its ability to inhibit the Herpes Simplex Virus as well as coronanavirus and arterivirus through mechanisms that impede proteasome function, RNA polymerase activity and NF-kappaB activation. Past research with HRVs, PV, CVB3 and mengovirus suggested that this compound, in conjunction with Zn or Cu, could impede picornaviral polyprotein processing when introduced into an infected cell. Investigation into its possible extracellular effect on picornaviruses alone or in conjunction with Zn was not reported (117). Using concentration ranges similar to those employed for intracellular studies, I found that extracellular exposure to PT alone did not produce HRV inhibition, even at quantities that vastly exceeded that used in prior research. However, substantial inhibition of both major and minor group HRVs was observed when this chemical is used with the supplementation of Zn. In these experiments less Zn was required to elicit inhibition of HRVs

than that required for Zn-based inhibition alone. The degree of inhibition seen in experimentation with HRV1A, HRV16 and HRV39 was essentially equivalent, though not extensively scrutinized. Unlike Hinokitiol, addition of PT alone or in combination with Zn to HRVs in solution did not produce a visible precipitate and this inhibition was observed with both ZnG and ZnCl solutions.

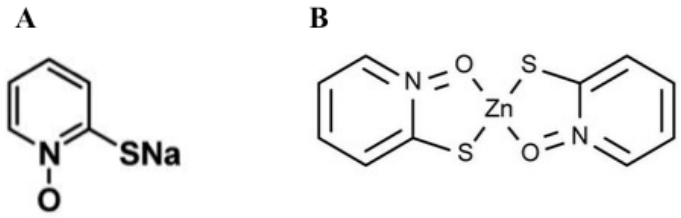

Diagram 5.6 Pyrithione and Pyrithione Zn Salts.
The structure of a single Pyrithione salt molecule (A), and two in complex with a Zn cation (B).

The relationship between PT, Zn and HRV inhibition is procedure dependent and stochiometrically modulated. PT is known to be able to chelate Zn cations at a ratio of 2:1. When PT is mixed with Zn at a ratio of 2:1 prior to HRV exposure, the effect is protective and the infectious titer of the HRV is not significantly decreased, similar to that seen in experiments with EDTA. Likewise, when PT is added to HRVs in solution, prior to ZnG supplementation, inhibition is mitigated, most noticeably at a ratio or 2:1. In both of the above scenarios, a 1:1 ratio of PT to Zn was less effective at preventing HRV inhibition, while a 3:1 ratio provided a protective effect, but one that was less defensive than a ratio of 2:1 (Figure 4.1, Figure 4.5, Figure 4.6 and Figure 4.7). However, unlike EDTA, not only did addition of PT after Zn-treated of HRV fail to reverse HRV inhibition, but it also vastly increased the scale of inhibition. This increase in inhibition appeared to be optimized at a PT to Zn ratio of 2:1 and minimized at a ratio of 1:1. A

ratio of 3:1 was capable of augmenting the amount of HRV inhibition, but not to the same degree as that seen with 2:1 ratios.

The mechanism behind this exacerbation of Zn- involved HRV inhibition after PT addition is unclear. PT may act by synergistically amplifying Zn-mediated inhibition, or by additively providing an alternative mechanism of HRV inhibition that is unique to the Zn-PT compound. The inability of PT and Zn in ratios of 1:1 or 1:3 to replicate the effect seen with ratios of 1:2 implies that characteristics specific to the di-Zn-PT complex are critical. These observations also suggest that the theoretical presence of PT molecules bound to a single Zn cation behave in a very different manner, neither facilitating, nor protecting, the HRV structure from Zn-mediated damage.

PDTC - mediated Zn Inhibition

Pyrrolidine dithiocarbamate (PDTC) has been studied for its ability to modulate physiological processes such as G1 cell cycle arrest, nitric oxide synthase production and NFkappaB activity. Furthermore, PDTC has been reported to possess bacteriacidal abilities in the presence of ZnCl (118). Recent studies on its potential antiviral properties revealed the ability to inhibit herpes simplex virus 1 and 2, enterovirus 71 and coxsackieB3 virus replication through a mechanism involving the dis-regulation of the ubiquitin-proteasome system (291). Furthermore, a study with influenza, poliovirus and HRVs cited its ability to repress viral replication through inhibition of viral polyprotein processing (123). Research targeted on HRVs documented that intracellular PDTC could impede the replication of HRV1A, 2, 14 and 16, as well as poliovirus, through interference of viral protein expression (111). Notably, the intracellular inhibitory action of PDTC in all these cases was shown to rely on the presence of metal cations such as Zn or Cu.

However, while interesting in itsown right, these documented mechanisms of PDTC inhibition are not specific to HRVs and require access to the intracellular milieu of an infected cell. While these prior studies indicated the necessity of Zn to potentiate PDTC antiviral activity, and observed that PDTC was not inhibitory to HRVs with extracellular exposure, no experimentation involving extracellular exposure of HRV to PDTC with the accompaniment of Zn has been reported.

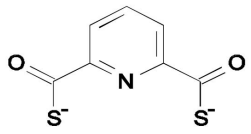

Diagrams 5.7 Pyrrolidine Dithiocarbamate (PDTC) structure.

The structure of PDTC has allowed chemists to diagram its theoretical interaction with Zn cations. Biochemically, PDTC can form aggregate complexes with Zn at a PDTC to Zn ratio of 2:1, however the prevalence of larger compounds with the same stoichiometry and their relevance to biochemical processes is not known (4). Based upon my findings with other ionophores, I sought to determine if PDTC might be able to demonstrate extracellular inhibition of HRVs when supplemented with ZnCl or ZnG. Using concentration ranges similar to that seen in intracellular studies of viral inhibition, I subjected HRVs to PDTC in combination with Zn. The concentrations of Zn used in these assays are more than ten-fold lower than those needed to see HRV-inhibition with Zn alone. The lack of HRV titer decrease I observed after treatment with PDTC alone, or Zn alone at low concentrations, was expected. Remarkably, however, inhibition of HRV1A could be demonstrated only when the precipitate from the chemical interaction of PDTC and Zn was harvested, re-suspended, and added singularly to HRVs in solution. Adding PDTC and Zn sequentially, or vice-versa, did not yield any decrease in viral

titer. Furthermore, isolation of this precipitate from its reacting solution appears necessary for optimal HRV inhibition, and the yield of this product is increased with heat. Both ZnCl and ZnG formed an identical precipitate with PDTC, however, reaction of PDTC and Zn at different ratios produced precipitates that appeared slightly different in crystalline texture when observed with microscopy after isolation and drying of the sample. Preliminary results with PV and EV68 did not demonstrate any inhibition to extracellular PDTC or to this Zn-PDTC compound, suggesting that there might be an HRV-specific mechanism at work.

This PDTC and Zn mediated extracellular inhibition of HRVs has not been published in prior literature. Given that this inhibitory activity excluded PV, it is unlikely that this mechanism functions to generally inhibit many viruses like that observed in intracellular studies. However, like PT and HK, the synergistic or additive relationship of this mechanism to that of Zn has not been determined.

Clinical relevance of Research

While acute HRV infections may not be life-threatening to the average healthy adult, they pose a great risk to the geriatric, neonatal, immune compromised, asthmatic and those suffering from cystic fibroses and other respiratory diseases (128). Furthermore, the morbidity and workforce absenteeism caused by HRV infections in healthy adults is estimated to have a profound impact on economic productivity and quality of life (4). Consequently, there is a significant medical and economic imperative to develop an efficacious therapeutic with the ability to abate the duration and severity of HRV infection symptoms in healthy adults, and to protect the vulnerable populations for whom contact with these viruses is more life threatening. Unfortunately, the widespread circulation of numerous HRV genotypes has hindered development of a vaccine, and

current antiviral compounds against HRVs have shown little therapeutic success (129). However, the poor outcome of many clinical trials, and the lack of a specific mechanism to explain the anti-rhinoviral activity of Zn, has prevented further development of Zn-based products. The insight into the mechanism of extracellular Zn inhibition of HRVs presented here might serve to focus the optimization of Zn-based therapeutics, or template the design of novel small-molecule antiviral inhibitors that may have a similar mechanism.

Future Directions

The potential to use Zn compounds or Zn Ionophores for anti-rhinoviral therapeutics had undeniable potential. However, detailed knowledge of the precise mechanism of Zn antiviral activity is necessary to optimize these products and progress forward. In this body of work I have demonstrated that there is an extracellular mechanism of Zn-based HRV inhibition that results in RNA degradation. However, the exclusivity of this mechanism is not clear and further research on additional routes of HRV infectivity abrogation should be probed, such as deeper investigation into the impact of Zn on viral capsid proteins or capsid metastability. Additional experimentation using custom-developed antibodies and electron microscopy to examine the integrity of the viral capsid after Zn treatment would be advantageous. While the small size of picornaviruses makes stable incorporation of fluorophores problematic, differential sedimentation of Zn treated and untreated radio-labeled virions may also help characterize the viral capsid after Zn treatment.

Furthermore, while this study focused upon HRV1A, more in-depth characterization of additional HRV species should be performed, including the

examination of mutant isolates. It is very likely that major group HRVs may require different mutations in the viral capsid proteins to gain Zn resistance, and comparison of these mutations to that seen in HRV1A and other minor group HRV representatives may provide more information about the mechanism at hand. Furthermore, the impact of Zn compounds on the newly characterized HRV-C species should be investigated, especially considering the clinical impact of these newly-characterized viruses. Competition and ICPA assays using a major group isolate representative might reveal if receptor binding in these HRVs appears to be likewise unaffected, or uninvolved in the inhibitory mechanism, respectively.

The promising results presented here on the use of Zn in conjunction with ionophores may only be the metaphorical tip of the iceberg when it comes to the potential use of these compounds. Showing substantial HRV1A inhibition with less Zn required, HK, PT and PDTC have demonstrated enormous potential to be used with Zn in antiviral therapeutics. PDTC has also been characterized to be physiologically amenable for possible clinical applications. High levels of Zn can be both unpalatable and detrimental to cells in the naso-pharynx. Zicam, whose Zn-based nasal spray is one the most popular over the counter treatments for the common cold, has endured lawsuits from individuals claiming to have experienced long-term detrimental side-effects with use of this product, and these claims were backed up by research on the effect of high Zn concentrations in the nasal cavity. Therefore, the ability of these ionophores to effectively inhibit HRVs in the presence of up to a ten-fold or lower Zn concentrations, might allow for the creation of safer Zn-based therapeutics. Furthermore, the current commercial use of Pyrithione in cosmetic products, and the animal research with PDTC, already demonstrates the

potential of these compounds to be clinically amenable for medical use. Experimentation with these compounds and different formulations of Zn with more representatives from the major and minor HRV groups should be conducted as well as with HRV-C. Similar steps like that shown here with ZnG and ZnCl, should be undertaken to determine if the mechanism of these compounds with Zn mirrors that of Zn alone, or acts using a different mechanism. Further characterization of the efficacy of these compounds on Zn-resistant mutants would be telling as well as the characterization of mutants arising from treatment with them alone.

CHAPTER 6: CONCLUSIONS

Extracellular Route of Zn Inhibition

Here I have demonstrated that extracellular exposure alone to ZnCL, ZnG, or Zn in conjunction with Zn ionophores, can result in a decrease in the infectivity of an HRV population. This decrease in infectivity occurs quickly, is pH-dependent, and slightly elevated at higher temperatures. This inhibition was documented with both major and minor group HRVs which interact with different receptors when gaining entry into the host. Other similar picornaviruses such as PV, EMCV, CVB3 and EV68 are not susceptible to this inhibition, and other 2+ cations like Mg+, Mn+ and Ca+ do not inhibit HRVs. This inhibition cannot be reversed by the presence of a Zn-chelating compound, but can be prevented by the presence of EDTA, Pyrithione and Sucrose.

Inhibition Characterization

This inhibition was characterized by examining the possible mechanistic routes that could accommodate the observations seen. These mechanistic routes were systematically investigated. The competition assay revealed that Zn-treated HRV1A could still interact with the LDLR receptor, a finding which indicated that Zn did not inhibit HRV1A by direct occlusion of the virus-receptor interaction. Furthermore, the results of the ICPA assay revealed that access to the virus-receptor interface was not necessary to illicit Zn-based inhibition of HRV1A, and that this inhibition can presumably still occur after the virus has formed a stable interaction with the LDLR receptor. Impeding infectivity due to virion agglutination is also unlikely, given that this inhibition was not seen with other 2+ cations which would likely have mediated the same type of non-specific mechanism, and this inhibition was not observed with other picornaviruses whose capsids share similar biochemical features. Dissolution of the virus capsid after Zn treatment,

leading to pre-mature release of the viral genome, is unlikely due to the sustained ability of the Zn-treated virion to interact with it's receptor as seen in the competition assay. The lack of migratory differences between untreated and Zn treated viral proteins on native and denaturing gels also bolsters this notion. While the failure of viral genome release after entry into the cell is not implausible given my results, the apparent degradation of the viral genome after Zn treatment makes this outcome potentially irrelevant when considering the ultimate cause of infectious failure.

Experimentally Supported Mechanism

The observations outlined in this body of work support the notion that exposure of HRVs to Zn compounds results in catalytic degradation of viral RNA. A decrease in the amount of overall-RNA and virus-specific RNA is seen after Zn treatment in both sera and sucrose gradient HRV1A fractions. This decrease in RNA after Zn treatment was observed via spectrophotometry, agarose gel visualization of HRV1A-specific PCR amplicons after reverse transcription using random hexamers, and northern blot analysis. While observation of the full-length HRV1A genome was tenuous, a profound decrease in the amount of higher-weight RNAs after Zn treatment was seen in every northern blot, irrespective of probe size and experimental conditions. Incubation of HRV1A samples with Rnase inhibitors prior to Zn treatment implies that this RNA degradation is Zn-mediated.

Zn-Resistant HRV1A Mutations

In an effort to characterize this inhibition, the genetic discrepancies between Zn-resistant and Zn-susceptible HRV1A populations were investigated. Three mutations where found in multiple Zn-resistant population isolates, alone or in combination, that could not be found in any Zn-susceptible, wild-type control isolates also sequenced. All three mutations were found in the HRV1A VP1 protein, which comprises the bulk of the capsid structure. Two of these mutations, threonine to serine on residue 87 and glycine to arginine on residue 91, were found on an outward facing structure known as the "B-C loop" whose conformation has been suspected to play a role in other anti-rhinoviral drug mechanisms. The amino acid substitution resulting from each single nucleotide point mutation might play a role in chemically repelling Zn or occluding Zn entry through the capsid pore structure. One mutation, asparagine to lysine on the interior-facing residue 29 might promote the repulsion of Zn chemically which could prevent the entry of Zn into the capsid where catalytic degradation of the viral RNA might occur. The mutation on residues 87 and 91 were found both in combination and singularly in some of the isolates sequenced, however, the mutation on residue 29 was only seen in combination with that of a surface residue. The reason for this is unclear, but may simply be the result of having sequenced an insufficient amount of samples to have discovered the existence of this mutation singularly, or might be due to the necessity of it's coupling to another mutation for stability or efficacy.

Efforts were taken to clone, transfect and propagate synthetic Zn-resistant HRV1A mutants. While the cloning strategy was a success, after transfection and numerous passages,

these viruses continually languished and failed to propagate at titers amenable for downstream experimentation. This outcome is not surprising due to the steep decrease in fitness observed in Zn-resistant viral populations. However, it may also be the case that only the mutation on residue 29 of VP1 can exist singularly, and the mutations on residues 87 and 91 must be stabilized by additional mutations to create a viable HRV1A population. The reason for this decreased fitness is unclear, but is most likely due to disruption of the capsid assembly process caused by the change in charge at these residue sites, and possibly by the change in polypeptide conformation that accompanies them which may impede the interaction of VP1 with other capsid proteins and viral genomes during the assembly process. Furthermore, due to the self-cleaving proteolytic cascade characteristic of picornaviruses, it is possible that mutations at these sites prohibits or makes this cleavage cascade less efficient.

Zn-Ionophore mediated inhibition of HRVs

In addition to Zn alone, Zn in association with Zn-binding ionophores was also shown to be inhibitory to HRVs without being inhibitory to PV. In many cases, the degree of inhibition observed was far greater than that which could be seen with the same concentration of Zn in isolation. Hinokitiol (beta thalujaplicin), pyrithione and pyrrolidine dithiocarbamate were all found to inhibit HRVs when in combination with Zn, but not in isolation. This inhibition required HRV exposure to these compounds in a sequential order, or in the case of PDTC, chemical reaction of this compound with Zn prior to HRV1A treatment. Furthermore, the ratio of the ionophore to Zn appears to modulate the level of inhibition, or prevention of inhibition, seen. The ratios observed to maximize HRV inhibition coincide with the amount of Zn cation interaction sites of each ionophore based upon chemical structures. It is unclear if this inhibition

optimizes the mechanism of that seen with Zn alone, or inhibits HRVs through a unique mechanistic pathway.

Summary of Conclusions and Implications

The ability of Zn to dampen the replication of HRVs in tissue culture was first observed over 4 decades ago. Despite ambiguity as to the inhibitory mechanism of Zn against HRVs and the questionable success of clinical trial outcomes, over-the-counter therapeutics advertised to ameliorate the symptoms of the common cold suffer have a near ubiquitous presence in pharmacies around the world. While many anecdotal reports claim that these products are effective, the lack of a scientifically-backed mechanism for their antiviral activity has prevented both their optimization and wider acceptance. While the immune system bolstering presence of Zn does not render these products harmless or useless, the potential efficacy of these products to specifically target HRVs cannot be improved upon without a deeper understanding of their precise inhibitory activity. Historically, investigations into this inhibitory mechanism were focused upon the intracellular stage of viral infection. In this body of work I took a new approach in trying to understand Zn-based inhibition of HRVs by formulating a hypothesis predicated upon extracellular-based Zn activity. After demonstrating that this hypothesis was valid, I sought to characterize this route of inhibition and understand the mechanism of Zn's rhinovirus-specific inhibitory potential. After confirming and characterizing this extracellular-based inhibition of Zn, I developed experiments to methodically hone in on the mechanism of this antiviral activity. In addition, I examined the genome of Zn-resistant HRV1A to uncover the determinants of genetic susceptibility that these viruses lack, and in doing so, understand how Zn might be interacting with the HRV1A virion. Taken together, my experimentation demonstrates that Zn catalyzes the degradation of viral RNA, thereby abrogating the infectivity of the viral population. I also demonstrated that some Zn Ionophore complexes are capable of extracellular-based inhibition of

HRVs as well, though their involvement in RNA degradation-based inhibition is unclear. While my studies do not preclude the possibility that Zn may also work to inhibit HRVs on an intracellular level, it does demonstrate and describe a mechanism of extracellular Zn-mediated inhibition of HRVs that can be used to hone the efficacy of Zn-based products intended to work as antivirals.

Works Cited

1. **Baltimore D.** 1974. The strategy of RNA viruses. Harvey Lect **70 Series:**57-74.
2. **Baltimore D.** 1980. Evolution of RNA viruses. Ann N Y Acad Sci **354:**492-497.
3. **Lauber C, Gorbalenya AE.** 2012. Toward genetics-based virus taxonomy: comparative analysis of a genetics-based classification and the taxonomy of picornaviruses. J Virol **86:**3905-3915.
4. **Anonymous.** !!! INVALID CITATION !!! .
5. **Palmenberg AC, Spiro D, Kuzmickas R, Wang S, Djikeng A, Rathe JA, Fraser-Liggett CM, Liggett SB.** 2009. Sequencing and analyses of all known human rhinovirus genomes reveal structure and evolution. Science **324:**55-59.
6. **Muehlenbachs A, Bhatnagar J, Zaki SR.** 2015. Tissue tropism, pathology and pathogenesis of enterovirus infection. J Pathol **235:**217-228.
7. **Pogue GP, Huntley CC, Hall TC.** 1994. Common replication strategies emerging from the study of diverse groups of positive-strand RNA viruses. Arch Virol Suppl **9:**181-194.
8. **Martinez-Salas E, Fernandez-Miragall O.** 2004. Picornavirus IRES: structure function relationship. Curr Pharm Des **10:**3757-3767.
9. **Flynn ME, Kaplan G, Racaniello V.** 1988. Mutational analysis of upstream AUG codons of poliovirus RNA. Journal of ,Ä¶ doi:papers2://publication/uuid/3621B77D-2405-4CB9-BCB6-80CBD813A78A.
10. **Liang RY, Li CF, Meng CC, Chen ZY, Liu GQ.** 2014. [Structure and function of 3'-untranslated region in picornavirus]. Bing Du Xue Bao **30:**463-469.
11. **Lee YF, Nomoto A, Wimmer E.** 1976. The genome of poliovirus is an exceptional eukaryotic mRNA. Prog Nucleic Acid Res Mol Biol **19:**89-96.
12. **Lyons T, Murray KE, Roberts AW, Barton DJ.** 2001. Poliovirus 5'-terminal cloverleaf RNA is required in cis for VPg uridylylation and the initiation of negative-strand RNA synthesis. J Virol **75:**10696-10708.
13. **Reddick BB, Habera LF, Law MD.** 1997. Nucleotide sequence and taxonomy of maize chlorotic dwarf virus within the family Sequiviridae. J Gen Virol **78 (Pt 5):**1165-1174.
14. **Palmenberg AC, Pallansch MA, Rueckert RR.** 1979. Protease required for processing picornaviral coat protein resides in the viral replicase gene. J Virol **32:**770-778.
15. **Wu CY, Lo CF, Huang CJ, Yu HT, Wang CH.** 2002. The complete genome sequence of Perina nuda picorna-like virus, an insect-infecting RNA virus with a genome organization similar to that of the mammalian picornaviruses. Virology **294:**312-323.
16. **Arnold GF, Resnick DA, Smith AD, Geisler SC, Holmes AK, Arnold E.** 1996. Chimeric rhinoviruses as tools for vaccine development and characterization of protein epitopes. Intervirology **39:**72-78.
17. **Martin LR, Duke GM, Osorio JE, Hall DJ, Palmenberg AC.** 1996. Mutational analysis of the mengovirus poly(C) tract and surrounding heteropolymeric sequences. J Virol **70:**2027-2031.
18. **Martinez-Salas E.** 2008. The impact of RNA structure on picornavirus IRES activity. Trends Microbiol **16:**230-237.
19. **Racaniello, R V.** 1990. Current Topics In Microbiology And Immunology: Picornaviruses doi:papers2://publication/uuid/7F1994C9-1F71-40B0-B926-3759D66729E9.

20. **Ramajayam R, Tan KP, Liang PH.** 2011. Recent development of 3C and 3CL protease inhibitors for anti-coronavirus and anti-picornavirus drug discovery. Biochem Soc Trans **39:**1371-1375.
21. **Schaffer FL, Schwerdt CE.** 1955. Crystallization of Purified Mef-1 Poliomyelitis Virus Particles. Proc Natl Acad Sci U S A **41:**1020-1023.
22. **Hogle JM, Chow M, Filman DJ.** 1985. Three-dimensional structure of poliovirus at 2.9 A resolution. Science **229:**1358-1365.
23. **Kostant B.** 1994. Structure of the truncated icosahedron (such as fullerene or viral coatings) and a 60-element conjugacy class in PSl(2, 11). Proc Natl Acad Sci U S A **91:**11714-11717.
24. **Nasz I, Adam E.** 2006. Symmetry types, systems and their multiplicity in the structure of adenovirus capsid. II. Rotational facet groups of five-, three- and two-fold symmetry axes. Acta Microbiol Immunol Hung **53:**115-133.
25. **Wang W, Lee WM, Mosser AG, Rueckert RR.** 1998. WIN 52035-dependent human rhinovirus 16: assembly deficiency caused by mutations near the canyon surface. J Virol **72:**1210-1218.
26. **Pevear DC, Fancher MJ, Felock PJ, Rossmann MG, Miller MS, Diana G, Treasurywala AM, McKinlay MA, Dutko FJ.** 1989. Conformational change in the floor of the human rhinovirus canyon blocks adsorption to HeLa cell receptors. J Virol **63:**2002-2007.
27. **Sawyer ST, Krantz SB, Goldwasser E.** 1987. Binding and receptor-mediated endocytosis of erythropoietin in Friend virus-infected erythroid cells. J Biol Chem **262:**5554-5562.
28. **Cho MW, Teterina N, Egger D, Bienz K, Ehrenfeld E.** 1994. Membrane rearrangement and vesicle induction by recombinant poliovirus 2C and 2BC in human cells. Virology **202:**129-145.
29. **Nomoto A, Lee YF, Wimmer E.** 1976. The 5' end of poliovirus mRNA is not capped with m7G(5')ppp(5')Np. Proc Natl Acad Sci U S A **73:**375-380.
30. **Towner JS, Ho TV, Semler BL.** 1996. Determinants of membrane association for poliovirus protein 3AB. J Biol Chem **271:**26810-26818.
31. **Strauss DM, Glustrom LW, Wuttke DS.** 2003. Towards an understanding of the poliovirus replication complex: the solution structure of the soluble domain of the poliovirus 3A protein. J Mol Biol **330:**225-234.
32. **Jiang H, Cho YG, Wang F.** 2000. Structural, functional, and genetic comparisons of Epstein-Barr virus nuclear antigen 3A, 3B, and 3C homologues encoded by the rhesus lymphocryptovirus. J Virol **74:**5921-5932.
33. **Jore J, De Geus B, Jackson RJ, Pouwels PH, Enger-Valk BE.** 1988. Poliovirus protein 3CD is the active protease for processing of the precursor protein P1 in vitro. J Gen Virol **69 (Pt 7):**1627-1636.
34. **Love RA, Maegley KA, Yu X, Ferre RA, Lingardo LK, Diehl W, Parge HE, Dragovich PS, Fuhrman SA.** 2004. The crystal structure of the RNA-dependent RNA polymerase from human rhinovirus: a dual function target for common cold antiviral therapy. Structure **12:**1533-1544.
35. **Aldabe R, Feduchi E, Novoa I, Carrasco L.** 1995. Expression of poliovirus 2Apro in mammalian cells: effects on translation. FEBS Lett **377:**1-5.

36. **Sieczkarski SB, Whittaker GR.** 2002. Dissecting virus entry via endocytosis. J Gen Virol **83:**1535-1545.
37. **Barton DJ, Flanegan JB.** 1993. Coupled translation and replication of poliovirus RNA in vitro: synthesis of functional 3D polymerase and infectious virus. J Virol **67:**822-831.
38. **Hayashi S, Nishimura K, Fukuchi-Shimogori T, Kashiwagi K, Igarashi K.** 2000. Increase in cap- and IRES-dependent protein synthesis by overproduction of translation initiation factor eIF4G. Biochem Biophys Res Commun **277:**117-123.
39. **Song Y, Tzima E, Ochs K, Bassili G, Trusheim H, Linder M, Preissner KT, Niepmann M.** 2005. Evidence for an RNA chaperone function of polypyrimidine tract-binding protein in picornavirus translation. RNA **11:**1809-1824.
40. **Shatsky IN, Dmitriev SE, Terenin IM, Andreev DE.** 2010. Cap- and IRES-independent scanning mechanism of translation initiation as an alternative to the concept of cellular IRESs. Mol Cells **30:**285-293.
41. **Pilipenko EV, Gmyl AP, Maslova SV, Svitkin YV, Sinyakov AN, Agol VI.** 1992. Prokaryotic-like cis elements in the cap-independent internal initiation of translation on picornavirus RNA. Cell **68:**119-131.
42. **Kean KM, Teterina N, Girard M.** 1990. Cleavage specificity of the poliovirus 3C protease is not restricted to Gln-Gly at the 3C/3D junction. J Gen Virol **71 (Pt 11):**2553-2563.
43. **Sommergruber W, Casari G, Fessl F, Seipelt J, Skern T.** 1994. The 2A proteinase of human rhinovirus is a zinc containing enzyme. Virology **204:**815-818.
44. **Reynolds C, Page G, Zhou H, Chow M.** 1991. Identification of residues in VP2 that contribute to poliovirus neutralization antigenic site 3B. Virology **184:**391-396.
45. **Arnold JJ, Cameron CE.** 2000. Poliovirus RNA-dependent RNA polymerase (3D(pol)). Assembly of stable, elongation-competent complexes by using a symmetrical primer-template substrate (sym/sub). J Biol Chem **275:**5329-5336.
46. **Hsu CH, Kingsbury DW, Murti KG.** 1979. Assembly of vesicular stomatitis virus nucleocapsids in vivo: a kinetic analysis. J Virol **32:**304-313.
47. **Andino R, Rieckhof GE, Achacoso PL, Baltimore D.** 1993. Poliovirus RNA synthesis utilizes an RNP complex formed around the 5'-end of viral RNA. EMBO J **12:**3587-3598.
48. **Chapman NM, Kim KS, Drescher KM, Oka K, Tracy S.** 2008. 5' terminal deletions in the genome of a coxsackievirus B2 strain occurred naturally in human heart. Virology **375:**480-491.
49. **Morrison JM, Racaniello VR.** 2009. Proteinase 2A(pro) Is Essential for Enterovirus Replication in Type I Interferon-Treated Cells. Journal of virology **83:**4412-4422.
50. **Ali IK, McKendrick L, Morley SJ, Jackson RJ.** 2001. Activity of the hepatitis A virus IRES requires association between the cap-binding translation initiation factor (eIF4E) and eIF4G. J Virol **75:**7854-7863.
51. **Carpentier PA, Williams BR, Miller SD.** 2007. Distinct roles of protein kinase R and toll-like receptor 3 in the activation of astrocytes by viral stimuli. Glia **55:**239-252.
52. **Castello A, Izquierdo JM, Welnowska E, Carrasco L.** 2009. RNA nuclear export is blocked by poliovirus 2A protease and is concomitant with nucleoporin cleavage. J Cell Sci **122:**3799-3809.
53. **Ben-Bassat M, Machtey I.** 1972. Picornavirus-like structures in acute dermatomyositis. Am J Clin Pathol **58:**245-249.

54. **Jennings LC, Dick EC.** 1987. Transmission and control of rhinovirus colds. European journal of epidemiology **3:**327-335.
55. **Davidson PW.** 2005. Mass tag PCR for mutliplex diagnostics patent 11119231 9780123662309.
56. **Lau SK, Yip CC, Tsoi HW, Lee RA, So LY, Lau YL, Chan KH, Woo PC, Yuen KY.** 2007. Clinical features and complete genome characterization of a distinct human rhinovirus (HRV) genetic cluster, probably representing a previously undetected HRV species, HRV-C, associated with acute respiratory illness in children. J Clin Microbiol **45:**3655-3664.
57. **Kuroda M, Niwa S, Sekizuka T, Tsukagoshi H, Yokoyama M, Ryo A, Sato H, Kiyota N, Noda M, Kozawa K, Shirabe K, Kusaka T, Shimojo N, Hasegawa S, Sugai K, Obuchi M, Tashiro M, Oishi K, Ishii H, Kimura H.** 2015. Molecular evolution of the VP1, VP2, and VP3 genes in human rhinovirus species C. Sci Rep **5:**8185.
58. **Agol VI.** 2002. [Genomic instability in picornaviruses]. Mol Biol (Mosk) **36:**286-295.
59. **Abraham G, Colonno RJ.** 1988. Characterization of human rhinoviruses displaced by an anti-receptor monoclonal antibody. J Virol **62:**2300-2306.
60. **Marlovits TC, Abrahamsberg C, Blaas D.** 1998. Very-low-density lipoprotein receptor fragment shed from HeLa cells inhibits human rhinovirus infection. J Virol **72:**10246-10250.
61. **Calvo C, Garcia ML, Pozo F, Reyes N, Perez-Brena P, Casas I.** 2009. Role of rhinovirus C in apparently life-threatening events in infants, Spain. Emerg Infect Dis **15:**1506-1508.
62. **Gern JE, Dick EC, Lee WM, Murray S, Meyer K, Handzel ZT, Busse WW.** 1996. Rhinovirus enters but does not replicate inside monocytes and airway macrophages. J Immunol **156:**621-627.
63. **Andries K, Dewindt B, Snoeks J, Wouters L, Moereels H, Lewi PJ, Janssen PA.** 1990. Two groups of rhinoviruses revealed by a panel of antiviral compounds present sequence divergence and differential pathogenicity. J Virol **64:**1117-1123.
64. **Venkataraman S, Reddy SP, Loo J, Idamakanti N, Hallenbeck PL, Reddy VS.** 2008. Crystallization and preliminary X-ray diffraction studies of Seneca Valley virus-001, a new member of the Picornaviridae family. Acta Crystallogr Sect F Struct Biol Cryst Commun **64:**293-296.
65. **Rossmann MG.** 1989. The canyon hypothesis. Viral Immunol **2:**143-161.
66. **McGregor S, Rueckert RR.** 1977. Picornaviral capsid assembly: similarity of rhinovirus and enterovirus precursor subunits. J Virol **21:**548-553.
67. **Turner RB, Dutko FJ, Goldstein NH, Lockwood G, Hayden FG.** 1993. Efficacy of oral WIN 54954 for prophylaxis of experimental rhinovirus infection. Antimicrob Agents Chemother **37:**297-300.
68. **Tsang SK, Cheh J, Isaacs L, Joseph-McCarthy D, Choi SK, Pevear DC, Whitesides GM, Hogle JM.** 2001. A structurally biased combinatorial approach for discovering new anti-picornaviral compounds. Chem Biol **8:**33-45.
69. **Florea NR, Maglio D, Nicolau DP.** 2003. Pleconaril, a novel antipicornaviral agent. Pharmacotherapy **23:**339-348.
70. **Basta HA, Ashraf S, Sgro JY, Bochkov YA, Gern JE, Palmenberg AC.** 2014. Modeling of the human rhinovirus C capsid suggests possible causes for antiviral drug resistance. Virology **448:**82-90.

71. **Kowalski H, Maurer-Fogy I, Zorn M, Mischak H, Kuechler E, Blaas D.** 1987. Cleavage site between VP1 and P2A of human rhinovirus is different in serotypes 2 and 14. J Gen Virol **68 (Pt 12):**3197-3200.
72. **Palmenberg AC.** 1987. Picornaviral processing: some new ideas. J Cell Biochem **33:**191-198.
73. **Hewat EA, Blaas D.** 2004. Cryoelectron microscopy analysis of the structural changes associated with human rhinovirus type 14 uncoating. J Virol **78:**2935-2942.
74. **Kumar M, Blaas D.** 2013. Human rhinovirus subviral a particle binds to lipid membranes over a twofold axis of icosahedral symmetry. J Virol **87:**11309-11312.
75. **Baltimore D.** 1970. RNA-dependent DNA polymerase in virions of RNA tumour viruses. Nature **226:**1209-1211.
76. **Kaminski A, Hunt SL, Patton JG, Jackson RJ.** 1995. Direct evidence that polypyrimidine tract binding protein (PTB) is essential for internal initiation of translation of encephalomyocarditis virus RNA. RNA **1:**924-938.
77. **Fujimura K, Kano F, Murata M.** 2008. Identification of PCBP2, a facilitator of IRES-mediated translation, as a novel constituent of stress granules and processing bodies. RNA **14:**425-431.
78. **Gerber K, Wimmer E, Paul AV.** 2001. Biochemical and genetic studies of the initiation of human rhinovirus 2 RNA replication: identification of a cis-replicating element in the coding sequence of 2A(pro). J Virol **75:**10979-10990.
79. **Lee WM, Monroe SS, Rueckert RR.** 1993. Role of maturation cleavage in infectivity of picornaviruses: activation of an infectosome. J Virol **67:**2110-2122.
80. **van Benten IJ, KleinJan A, Neijens HJ, Osterhaus AD, Fokkens WJ.** 2001. Prolonged nasal eosinophilia in allergic patients after common cold. Allergy **56:**949-956.
81. **Krunkosky TM, Jarrett CL.** 2006. Selective regulation of MAP kinases and chemokine expression after ligation of ICAM-1 on human airway epithelial cells. Respir Res **7:**12.
82. **Newcomb DC, Sajjan U, Nanua S, Jia Y, Goldsmith AM, Bentley JK, Hershenson MB.** 2005. Phosphatidylinositol 3-kinase is required for rhinovirus-induced airway epithelial cell interleukin-8 expression. J Biol Chem **280:**36952-36961.
83. **Griego SD, Weston CB, Adams JL, Tal-Singer R, Dillon SB.** 2000. Role of p38 mitogen-activated protein kinase in rhinovirus-induced cytokine production by bronchial epithelial cells. J Immunol **165:**5211-5220.
84. **Kawai T, Takahashi K, Sato S, Coban C, Kumar H, Kato H, Ishii KJ, Takeuchi O, Akira S.** 2005. IPS-1, an adaptor triggering RIG-I- and Mda5-mediated type I interferon induction. Nat Immunol **6:**981-988.
85. **Wang Q, Miller DJ, Bowman ER, Nagarkar DR, Schneider D, Zhao Y, Linn MJ, Goldsmith AM, Bentley JK, Sajjan US, Hershenson MB.** 2011. MDA5 and TLR3 Initiate Pro-Inflammatory Signaling Pathways Leading to Rhinovirus-Induced Airways Inflammation and Hyperresponsiveness. Plos Pathogens **7:**e1002070.
86. **Grunberg K, Kuijpers EA, de Klerk EP, de Gouw HW, Kroes AC, Dick EC, Sterk PJ.** 1997. Effects of experimental rhinovirus 16 infection on airway hyperresponsiveness to bradykinin in asthmatic subjects in vivo. Am J Respir Crit Care Med **155:**833-838.
87. **Gern JE, French DA, Grindle KA, Brockman-Schneider RA, Konno S, Busse WW.** 2003. Double-stranded RNA induces the synthesis of specific chemokines by bronchial epithelial cells. Am J Respir Cell Mol Biol **28:**731-737.

88. **Neznanov N, Chumakov KM, Neznanova L, Almasan A, Banerjee AK, Gudkov AV.** 2005. Proteolytic cleavage of the p65-RelA subunit of NF-kappaB during poliovirus infection. J Biol Chem **280:**24153-24158.
89. **Barral PM, Morrison JM, Drahos J, Gupta P, Sarkar D, Fisher PB, Racaniello VR.** 2007. MDA-5 is cleaved in poliovirus-infected cells. J Virol **81:**3677-3684.
90. **Lemanske RF, Jr., Jackson DJ, Gangnon RE, Evans MD, Li Z, Shult PA, Kirk CJ, Reisdorf E, Roberg KA, Anderson EL, Carlson-Dakes KT, Adler KJ, Gilbertson-White S, Pappas TE, Dasilva DF, Tisler CJ, Gern JE.** 2005. Rhinovirus illnesses during infancy predict subsequent childhood wheezing. J Allergy Clin Immunol **116:**571-577.
91. **Folkerts G, Busse WW, Nijkamp FP.** 1998. Virus-induced airway hyperresponsiveness and asthma. American journal of ,Ä¶ doi:papers2://publication/uuid/7B3C7E23-1065-4D40-BA7D-B8BC849D532E.
92. **Kotla S, Peng T, Bumgarner RE, Gustin KE.** 2008. Attenuation of the type I interferon response in cells infected with human rhinovirus. Virology **374:**399-410.
93. **Greenberg SB, Allen M, Wilson J, Atmar RL.** 2000. Respiratory viral infections in adults with and without chronic obstructive pulmonary disease. Am J Respir Crit Care Med **162:**167-173.
94. **Oliver BG, Lim S, Wark P, Laza-Stanca V, King N, Black JL, Burgess JK, Roth M, Johnston SL.** 2008. Rhinovirus exposure impairs immune responses to bacterial products in human alveolar macrophages. Thorax **63:**519-525.
95. **Smyth AR, Smyth RL, Tong CY, Hart CA, Heaf DP.** 1995. Effect of respiratory virus infections including rhinovirus on clinical status in cystic fibrosis. Arch Dis Child **73:**117-120.
96. **Murray CS, Simpson A, Custovic A.** 2004. Allergens, viruses, and asthma exacerbations. Proc Am Thorac Soc **1:**99-104.
97. **Gern JE, Galagan DM, Jarjour NN, Dick EC, Busse WW.** 1997. Detection of rhinovirus RNA in lower airway cells during experimentally induced infection. Am J Respir Crit Care Med **155:**1159-1161.
98. **Benoit LA, Holtzman MJ.** 2010. New immune pathways from chronic post-viral lung disease. Annals of the New York Academy of Sciences **1183:**195-210.
99. **Anttila P, Simell O, Salmela S, Vuori E.** 1984. Serum and hair zinc as predictors of clinical symptoms in acrodermatitis enteropathica. J Inherit Metab Dis **7:**46-48.
100. **Rabbani PI, Prasad AS, Tsai R, Harland BF, Fox MR.** 1987. Dietary model for production of experimental zinc deficiency in man. Am J Clin Nutr **45:**1514-1525.
101. **Beach RS, Gershwin ME, Hurley LS.** 1982. Zinc, copper, and manganese in immune function and experimental oncogenesis. Nutr Cancer **3:**172-191.
102. **Laity JH, Lee BM, Wright PE.** 2001. Zinc finger proteins: new insights into structural and functional diversity. Curr Opin Struct Biol **11:**39-46.
103. **Desjarlais JR, Berg JM.** 1993. Use of a zinc-finger consensus sequence framework and specificity rules to design specific DNA binding proteins. Proc Natl Acad Sci U S A **90:**2256-2260.
104. **Nyborg JK, Peersen OB.** 2004. That zincing feeling: the effects of EDTA on the behaviour of zinc-binding transcriptional regulators. Biochem J **381:**e3-4.
105. **Korant BD, Kauer JC, Butterworth BE.** 1974. Zinc ions inhibit replication of rhinoviruses. Nature **248:**588-590.

106. **Butterworth BE, Korant BD.** 1974. Characterization of the large picornaviral polypeptides produced in the presence of zinc ion. J Virol **14:**282-291.
107. **Korant BD, Butterworth BE.** 1976. Inhibition by zinc of rhinovirus protein cleavage: interaction of zinc with capsid polypeptides. J Virol **18:**298-306.
108. **Eby GA, Davis DR.** 1984. Reduction in duration of common colds by zinc gluconate lozenges in a double-blind study. Antimicrobial agents and ‚Ä¶ doi:papers2://publication/uuid/28C75580-6845-4034-8452-13488A01C50C.
109. **Geist FC, Bateman JA.** 1987. In vitro activity of zinc salts against human rhinoviruses. Antimicrobial agents and ‚Ä¶ doi:papers2://publication/uuid/EBE5532D-69DD-4C70-8510-6F374000C4B3.
110. **Merluzzi VJ, Cipriano D, McNeil D, Fuchs V, Supeau C, Rosenthal AS, Skiles JW.** 1989. Evaluation of zinc complexes on the replication of rhinovirus 2 in vitro. Research communications in chemical pathology and pharmacology **66:**425-440.
111. **Lanke K, Krenn BM, Melchers WJG, Seipelt J, Van Kuppeveld FJM.** 2007. PDTC inhibits picornavirus polyprotein processing and RNA replication by transporting zinc ions into cells. The Journal of general virology **88:**1206-1217.
112. **Jackson EA.** 2000. Are zinc acetate lozenges effective in decreasing the duration of symptoms of the common cold? J Fam Pract **49:**1153.
113. **Hemila H.** 2012. Zinc lozenges may shorten common cold duration. Expert Rev Respir Med **6:**253-254.
114. **Turner RB.** 2001. The treatment of rhinovirus infections: progress and potential. Antiviral research **49:**1-14.
115. **Anonymous.** 2009. Over-the-counter medications: Zicam nasal products may cause loss of sense of smell. Child Health Alert **27:**3.
116. **Godfrey JC, Godfrey NJ, Novick SG.** 1996. Zinc for treating the common cold: review of all clinical trials since 1984. Alternative therapies in health and medicine **2:**63-72.
117. **Krenn BM, Gaudernak E, Holzer B, Lanke K, Van Kuppeveld FJM, Seipelt J.** 2009. Antiviral activity of the zinc ionophores pyrithione and hinokitiol against picornavirus infections. Journal of virology **83:**58-64.
118. **Gaudernak E, Seipelt J, Triendl A, Grassauer A, Kuechler E.** 2002. Antiviral effects of pyrrolidine dithiocarbamate on human rhinoviruses. J Virol **76:**6004-6015.
119. **Calamari JE, Geist GO, Shahbazian MJ.** 1987. Evaluation of multiple component relaxation training with developmentally disabled persons. Res Dev Disabil **8:**55-70.
120. **Al-Nakib W, Higgins PG, Barrow I, Batstone G, Tyrrell DA.** 1987. Prophylaxis and treatment of rhinovirus colds with zinc gluconate lozenges. J Antimicrob Chemother **20:**893-901.
121. **Greiff L, Venge P, Andersson M, Enander I, Linden M, Myint S, Persson CG.** 2002. Effects of rhinovirus-induced common colds on granulocyte activity in allergic rhinitis. J Infect **45:**227-232.
122. **Godfrey JC, Conant Sloane B, Smith DS, Turco JH, Mercer N, Godfrey NJ.** 1992. Zinc gluconate and the common cold: a controlled clinical study. J Int Med Res **20:**234-246.
123. **Krenn BM, Holzer B, Gaudernak E, Triendl A, van Kuppeveld FJ, Seipelt J.** 2005. Inhibition of polyprotein processing and RNA replication of human rhinovirus by pyrrolidine dithiocarbamate involves metal ions. Journal of virology **79:**13892-13899.

124. **Katsura S.** 1954. [Antibacterial effect of the hinokitiol (m-isopropyltropolone)]. Zentralbl Bakteriol Orig **161:**206-211.
125. **Komaki N, Watanabe T, Ogasawara A, Sato N, Mikami T, Matsumoto T.** 2008. Antifungal mechanism of hinokitiol against Candida albicans. Biol Pharm Bull **31:**735-737.
126. **Reeder NL, Xu J, Youngquist RS, Schwartz JR, Rust RC, Saunders CW.** 2011. The antifungal mechanism of action of zinc pyrithione. Br J Dermatol **165 Suppl 2:**9-12.
127. **Kondoh Y, Takano S.** 1987. Determination of zinc pyrithione in cosmetic products by high-performance liquid chromatography with pre-labelling. J Chromatogr **408:**255-262.
128. **Avila PC, Abisheganaden JA, Wong H, Liu J, Yagi S, Schnurr D, Kishiyama JL, Boushey HA.** 2000. Effects of allergic inflammation of the nasal mucosa on the severity of rhinovirus 16 cold. J Allergy Clin Immunol **105:**923-932.
129. **Bernard A, Lacroix C, Cabiddu MG, Neyts J, Leyssen P, Pompei R.** 2015. Exploration of the anti-enterovirus activity of a series of pleconaril/pirodavir-like compounds. Antivir Chem Chemother doi:10.1177/2040206615589035.